3-1962

A Study of the Problems Involved in Measuring the Angular Momentum of Microwave Radiation

Otis Kenley Wolfe Jr.
University of Tennessee, Knoxville

To the Graduate Council:

I am submitting herewith a dissertation written by Otis Kenley Wolfe Jr. entitled "A Study of the Problems Involved in Measuring the Angular Momentum of Microwave Radiation." I have examined the final electronic copy of this dissertation for form and content and recommend that it be accepted in partial fulfillment of the requirements for the degree of Doctor of Philosophy, with a major in Physics.

W. E. Deeds, Major Professor

We have read this dissertation and recommend its acceptance:

C. J. Craven, Arthur H. Neilson, J. W. White, G. W. Hoffman, D. D. Wilson

Accepted for the Council:

Carolyn R. Hodges

Vice Provost and Dean of the Graduate School

(Original signatures are on file with official student records.)

March 10, 1962

To the Graduate Council:

I am submitting herewith a dissertation written by Otis Kenley Wolfe, Jr. entitled "A Study of the Problems Involved in Measuring the Angular Momentum of Microwave Radiation." I recommend that it be accepted in partial fulfillment of the requirements for the degree of Doctor of Philosophy, with a major in Physics.

W. E. Deeds
Major Professor

We have read this dissertation and recommend its acceptance:

C. J. Craven

Alvin H. Nielsen

J. W. White

D. W. Hoffman

D. D. Unick

Accepted for the Council:

Hilton A. Smith
Dean of the Graduate School

A STUDY OF THE PROBLEMS INVOLVED IN MEASURING THE ANGULAR MOMENTUM OF MICROWAVE RADIATION

A Dissertation

Presented to

the Graduate Council of

the University of Tennessee

In Partial Fulfillment

of the Requirements for the Degree

Doctor of Philosophy

---

by

Otis Kenley Wolfe, Jr.

March 1962

ACKNOWLEDGEMENT

The author wishes to express his appreciation of several people for their assistance in his research and dissertation.

Dr. John D. Trimmer, Head, Physics Department, University of Massachusetts, suggested the problem and supervised the research during its first stage. Dr. E. Deeds supervised the last stage of the research to its completion. Other staff members and graduate students of the Physics Department of the University of Tennessee offered many suggestions during the course of the research.

During the construction of the apparatus, valuable work and suggestions came from the personnel of the Physics Department's machine shop.

The author is indebted to his wife for her patience during the research period and for her typing of the manuscript.

Otis K. Wolfe, Jr.

TABLE OF CONTENTS

CHAPTER PAGE

LIST OF TABLES

LIST OF FIGURES

FIGURE PAGE

CHAPTER I

INTRODUCTION

Angular momentum will be defined below for material bodies and in Chapter II for electromagnetic radiation. The transfer of angular momentum from either of these to the other can conceivably be detected and measured. In this chapter there is a general discussion of the problem. Details in history and theory along with the definition of angular momentum for electromagnetic radiation will be presented in the next two chapters.

I. THE PROBLEM

A small element of mass of a material body possesses angular momentum with respect to the origin of a particular reference frame if its velocity has a component normal to a radius vector drawn from the origin to the element of mass. The definition of the angular momentum of the i-th element of mass is

$$\underline{l}_i = \underline{r}_i \times m_i \underline{v}_i \qquad (I.I.1)$$

where $\underline{l}_i$ is the angular momentum, $\underline{r}_i$ is the radius vector, m_i is the mass, and $\underline{v}_i$ is the velocity. (Underscored letters are used to indicate vector quantities.) The relationship between these quantities is shown in Figure 1

on page 3. The vector $\underline{l}_i$ is normal to a plane through $\underline{r}_i$ and $\underline{v}_i$.

Also by definition the angular momentum of the entire body with respect to the same origin is

$$\underline{L}=\sum_i \underline{l}_i \qquad \text{(I.I.2)}$$

As a special case one may have a rigid body with all of its elements moving in circles whose centers all lie on a straight line. If this line is external to the body, the body is moving in a circular orbit; if the line is internal to the body, the body is said to spin about an axis (the line).

Electromagnetic waves may also be said to possess angular momentum. If these waves do possess angular momentum and are totally absorbed by a material body, then by the law of conservation of angular momentum the absorber should receive this angular momentum and be made to spin about some axis.

It was the purpose of this research to study the problems in detecting and measuring the mechanical angular momentum imparted to an absorber by certain types of electromagnetic waves.

II. CHARGE AND CURRENT DISTRIBUTIONS

Electromagnetic radiation is emitted by accelerated charges. An arbitrary distribution of charge may vary its

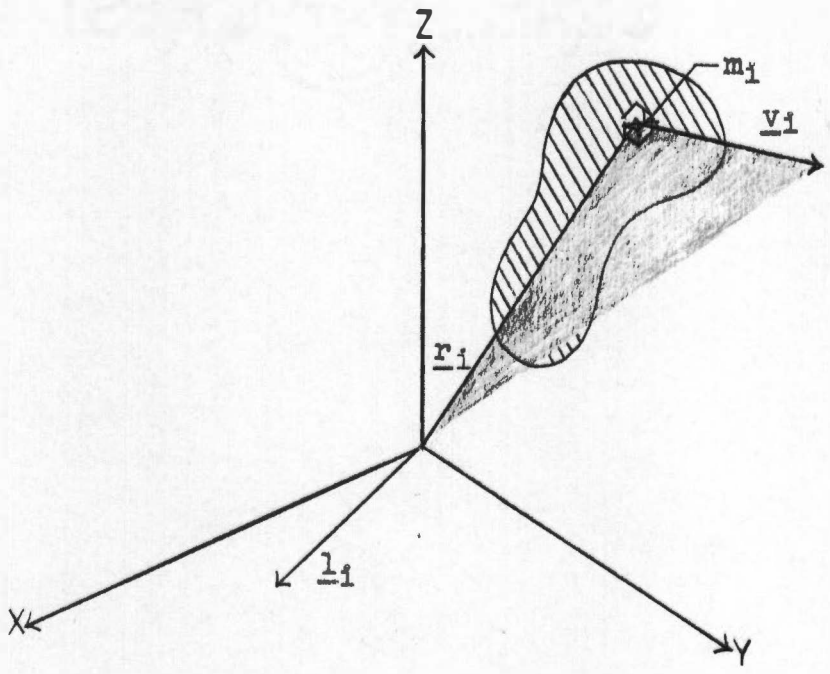

FIGURE 1

THE RELATIONSHIP BETWEEN THE RADIUS VECTOR, VELOCITY, AND ANGULAR MOMENTUM OF AN ELEMENT OF MASS IN A RIGID BODY

shape in an arbitrary manner in time. For convenience in calculating the electric and magnetic fields from such a charge distribution, the distribution of the charge in space is described in terms of multipoles; that is, the electric dipole moment, the magnetic dipole moment, the electric quadrupole moment, and higher order moments. For simplification one usually takes the time variation of these moments as sinusoidal.

As an example, the electric dipole moment $\underline{p}$ of an arbitrary distribution of charge is defined as a vector whose rectangular coordinates are

$$p_x = \int_V \rho x' \, dV', \tag{I.II.1}$$

$$p_y = \int_V \rho y' \, dV', \tag{I.II.2}$$

$$p_z = \int_V \rho z' \, dV', \tag{I.II.3}$$

where ρ is the volume charge density at the point whose coordinates are x', y', and z'.

These relationships are space relationships, and the variation in time is brought about by multiplying these expressions by the appropriate time factor. This factor is usually $\cos \omega t$ or $\sin \omega t$ as has been mentioned previously. Thus an electric dipole moment varying sinusoidally with time would be $\underline{p} \cos \omega t$ or $\underline{p} \sin \omega t$.

The magnetic dipole due to currents in the source is defined as

$$\underline{m} = \frac{1}{2}\int_V r' \times \rho \underline{v}' \, dV', \qquad \text{(I.II.4)}$$

where $\underline{v}'$ is charge velocity.

Methods of determining other moments may be found in textbooks on electromagnetism.[1]

III. WAVE POLARIZATION

The angular momentum of electromagnetic radiation may vary with the type of multipole. In addition, it is related to the polarization of the waves. If the electric intensity vector $\underline{E}$ remains fixed relative to the reference frame in which the traveling wave is observed, the wave is said to be linearly polarized. If the vector $\underline{E}$ rotates as the wave progresses, the wave is said to be elliptically polarized. Theory indicates that elliptically polarized waves should carry angular momentum while linearly polarized waves should not. This will be shown later in the theory of the electric dipole. The angular momentum is a function of the eccentricity of the ellipse described by the polarization vector $\underline{E}$.

---

[1]Julius Adams Stratton, Electromagnetic Theory (New York: McGraw-Hill Book Company, Inc., 1941), pp. 178-183.

IV. THE PRINCIPLE OF THE EXPERIMENT

If one wishes to study experimentally the radiation from a particular multipole moment, he must find a source which has a large moment of the desired multipole and negligible moments of the other multipoles.

Although a half-wave antenna (commonly referred to as a dipole) is not truly a source which emits pure electric dipole radiation, the other multipole moments are relatively small. Thus, it was of interest to see if the experimental relationship between radiated power and angular momentum is the same as that of the ideal infinitesimal dipole which has been calculated theoretically.

Research of this nature has been done with plane waves of light[2] and microwaves[3], but not with radiation of individual multipoles. The experiment actually performed concerned the electric dipole radiation.

The essentials of such an experiment are easily visualized. A transmitter generates radio frequency energy of the desired frequency. A transmission line transfers the energy from the transmitter to the antenna from which

---

[2] R. A. Beth, Phys. Rev. 50, 115 (1936)

[3] N. Carrara, Nature 164, 883 (1949)

the energy is radiated. An absorber is placed around, but not touching, the antenna. Since angular momentum is imparted to the absorber, it should turn. By knowing the mechanical constants of the absorbing system and by observing its motion, one should be able to determine the torque exerted on it by the radiation and the angular momentum carried by the radiation.

One could do this experiment for the electric dipole, magnetic dipole, electric quadrupole, magnetic quadrupole, and other multipole moments if he could produce the proper antennae and transfer energy to them.

V. ANTICIPATED DIFFICULTIES

Although simple in principle, such an experiment is difficult to perform due to the small magnitude of the torque compared to rotational disturbances encountered in the laboratory. Since an absorber has finite mass and weight, it has to be supported in some manner which will allow it to make an angular displacement which is detectable. Some conceivable devices for supporting the absorber are the elastic fiber, liquids, jets of gas, and magnetic suspension. Theoretical consideration will be given to the fiber suspension and the liquid support.

CHAPTER II

THE HISTORY OF THE CLASSICAL THEORY OF ANGULAR MOMENTUM ASSOCIATED WITH ELECTROMAGNETIC RADIATION

The first suggestion that electromagnetic radiation might carry angular momentum was made by J. H. Poynting[1] in 1909. Very few experiments which have mechanically detected angular momentum of electromagnetic radiation have been reported. A brief history of the subject and a summary of the experiments reported will be given below.[2]

I. THE STATUS OF ELECTROMAGNETIC THEORY BEFORE POYNTING'S HYPOTHESIS

By the beginning of the eighteenth century much work in optics had been performed. Some examples of the accomplishments previously made were the study of the optics of the eye, the invention of the telescope, the development of the formula for the focal length of a thin lens, the statement of the law of refraction, and the proposal of two competing theories of light, wave and corpuscular.

---

[1] J. H. Poynting, Proc. Roy. Soc. (A) 82, 565 (1909)

[2] This history summarizes the sections of the history of science which relate to electricity in Chapter I of F. K. Richtmyer and E. H. Kennard, Introduction to Modern Physics, (New York: McGraw-Hill Book Company, Inc., 1947). pp. 1-50. Other sources are also footnoted.

During the eighteenth century the research in the field of electricity was concerned primarily with electrostatics. Neither theory of the nature of light was conclusively verified by experiment.[3]

In the nineteenth century the wave theory of light gained favor as experiments performed furnished experimental evidence for its validity. Meanwhile, electric currents were being studied, electricity and magnetism were being related to each other, and the phenomenon of electromagnetic induction was discovered. In 1864 James Clerk Maxwell formulated his general equations of the electromagnetic field. He also inferred that light consisted of transverse waves in the medium through which it traveled. Electricity and light were related at this point. Mathematical theories were then developed to account for the electric and magnetic phenomena and for the principal properties of light. In 1887 Heinrich Hertz experimentally discovered waves of greater wavelength than light that were of electrical nature. The velocity of propagation of these waves proved to be the same as the velocity of light. In 1884 Poynting stated his theorem that electromagnetic energy was transferred through space or an

---

[3]Ibid., p. 30.

insulating medium outside a current-carrying wire.[4] The term "electromagnetic momentum" was apparently first used by Max Abraham to ascribe momentum to an electromagnetic field.[5] Then the proposal that angular momentum might be carried by light was made by Poynting[6] by considering the analogue of torsional waves in an elastic rod. Max Abraham[7] treated the case of two dipole moments mutually perpendicular and out of electrical phase with each other by ninety degrees. He used as the definition of angular momentum density at a point in a field $\underline{r} \times \underline{G}$, where $\underline{r}$ is the radius vector to the field point from the origin and $\underline{G}$ is the linear momentum density of the field. The result was that the ratio of the energy in the field to the angular momentum in the field was the value predicted by Poynting's mechanical analogue.

II. POYNTING'S HYPOTHESIS

From the theory of torsional waves in elastic rods Poynting predicted that circularly polarized light might

---

[4]Alfred O'Rahilly, Electromagnetics, A Discussion of Fundamentals (London: Longmans, Green and Company, 1938), p. 275.

[5]Ibid., p. 294.

[6]Poynting, loc. cit.

[7]M. Abraham, Phyzik. Z., 15, 914 (1914)

possess angular momentum. Consider a long cylindrical rod of an elastic material which is given a quick twist at one end. A torsional disturbance will travel along the length of the rod. The motion of the rod is described by the one-dimensional wave equation

$$\frac{\partial^2\theta}{\partial z^2} = \frac{1}{U_n^2}\frac{\partial^2\theta}{\partial t^2}$$

where $U_n = \sqrt{\frac{\mu}{\rho}}$ (II.II.1)

is the velocity of propagation of a torsional wave, μ is the modulus of shearing rigidity, and ρ is the mass density of the material. Figure 2 on page 12 shows such a rod with a line parallel to its axis of radial symmetry when the rod is not twisted and with the line twisted as a disturbance moves down the rod.

If one wishes to transfer energy from a rotating source to a sink he might have an arrangement such as that diagramed in Figure 3 on page 13. At the sink rotational energy is being transformed into some other form of energy. The rod will be twisted so that the line in (A) of Figure 2 on page 12 would become a spiral shown in Figure 3 on page 13.

Poynting considered the special case in which the number of rotations per second through which the rod turns is $n = \frac{U_n}{\lambda}$, where λ is the distance along the shaft in

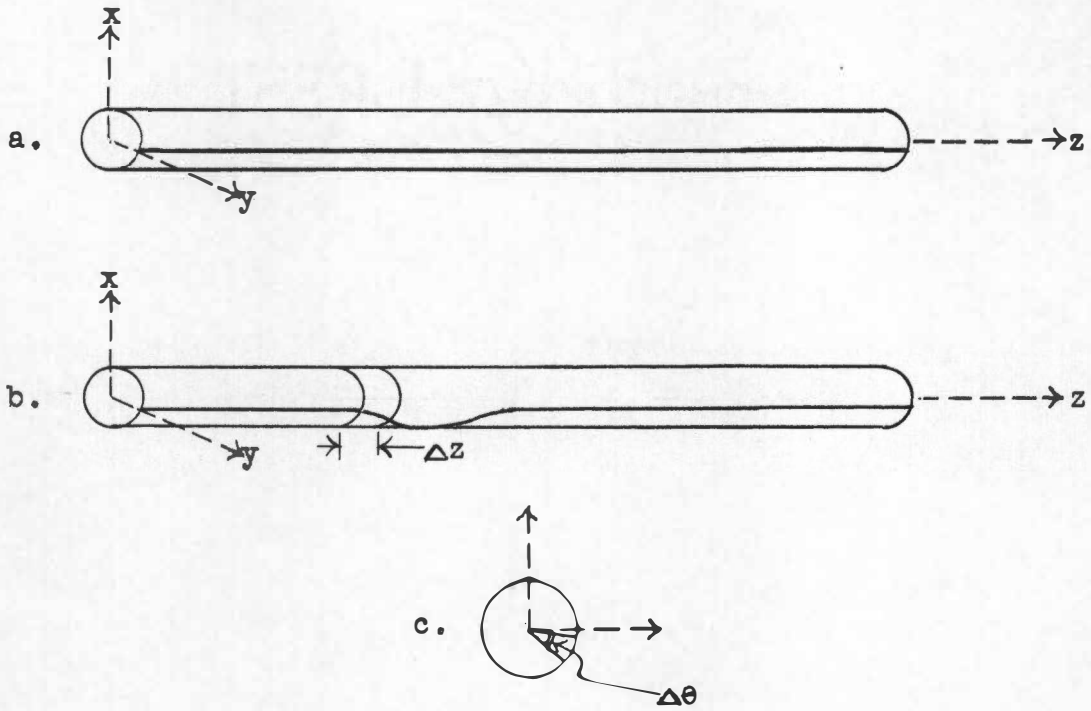

FIGURE 2

(a) A ROD WITH ALL SEGMENTS IN THEIR EQUILIBRIUM POSITIONS, (b) A ROD WITH A TORSIONAL DISTURBANCE TRAVELING ALONG ITS LENGTH, (c) THE DISPLACEMENT OF A SEGMENT OF THE ROD OF LENGTH ΔZ

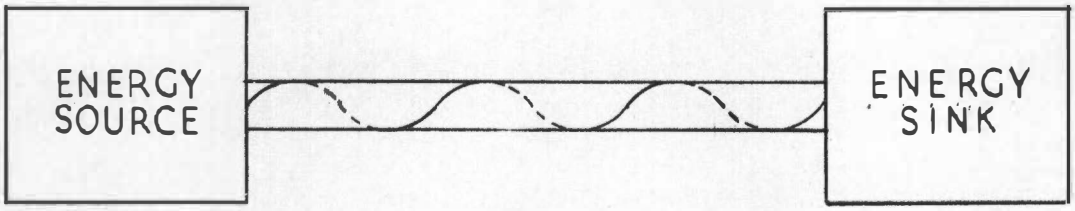

FIGURE 3

AN ELASTIC ROD TRANSFERRING ENERGY FROM
ONE POINT TO ANOTHER

which the angle of twist Θ becomes 2π radians and U_n is the natural velocity at which a wave would travel along the rod. For given N and U_n, λ is fixed. The motion in this case was regarded by Poynting as a natural wave system transmitted by the elastic forces of the material.

The elastic potential energy per unit volume of the segment of the rod of length Δz is

$$\text{P.E. per unit volume} = \frac{\frac{1}{2}k\ (\Delta\Theta)^2}{\Delta V}\ , \qquad \text{(II.II.2)}$$

where k is the torque constant for the element of length Δz.

$$k = \frac{\frac{\pi}{2}\mu r^4}{\Delta z}\ , \qquad \text{(II.II.3)}$$

where μ has been previously defined as the modulus of shearing rigidity and r is the radius of the rod. Thus

$$\text{P.E. per unit volume} = \frac{1\pi\mu r^4\ (\Delta\Theta)^2}{4\pi r^2\ (\Delta z)^2} \qquad \text{(II.II.4)}$$

$$= \frac{1\mu r^2\ (\Delta\Theta)^2}{4\quad (\Delta z)^2}\ . \qquad \text{(II.II.5)}$$

The kinetic energy per unit volume is just

$$\text{K.E. per unit volume} = \frac{\frac{1}{2}I\omega^2}{\Delta V} \qquad \text{(II.II.6)}$$

$$= \frac{1\ (\frac{1}{2}\rho\ \Delta V\ r^2)\ (\Delta\Theta)^2}{2\quad \Delta V\quad (\Delta t)^2}\ , \qquad \text{(II.II.7)}$$

where ρ has been previously defined as the mass density of the material. Now ρ and μ are related in this special case

through

$$U_n = \frac{\Delta z}{\Delta t} = \sqrt{\frac{\mu}{\rho}}\,, \qquad \text{(II.II.1)}$$

so that (II.II.5) may be put in the form

$$\text{P.E. per unit volume} = \frac{1}{4}\rho r^2 \frac{(\Delta\theta)^2}{(\Delta t)^2}\,. \qquad \text{(II.II.8)}$$

From (II.II.7) and (II.II.8) the total energy per unit volume is

$$\text{K.E. + P.E. per unit volume} = \frac{1}{2}\rho r^2 \frac{(\Delta\theta)^2}{(\Delta t)^2}\,. \qquad \text{(II.II.9)}$$

The angular momentum per unit volume is just

$$\text{L per unit volume} = \frac{I\omega}{\Delta V} \qquad \text{(II.II.10)}$$

$$= \frac{I}{\Delta V}\frac{\Delta\theta}{\Delta t} \qquad \text{(II.II.11)}$$

$$= \frac{1}{2}\rho \frac{\Delta V\, r^2}{\Delta V}\frac{\Delta\theta}{\Delta t} \qquad \text{(II.II.12)}$$

$$= \frac{1}{2}\rho r^2 \frac{\Delta\theta}{\Delta t}\,. \qquad \text{(II.II.13)}$$

The ratio of the total energy per unit volume to the angular momentum per unit volume is the ratio of (II.II.9) to (II.II.13). This is

$$\frac{\Delta\theta}{\Delta t} = \text{constant} = \frac{d\theta}{dt} = 2\pi n. \qquad \text{(II.II.14)}$$

The mechanical analogue to the frequency of an electrical oscillator is n.

In comparing this case to circularly polarized light, Poynting suggested that this relationship might hold. He also suggested an experiment which might be used to measure the angular momentum. This experimental arrangement is shown in Figure 4 on page 17.

Light is passed up through the Nicol prism N and comes out of it plane polarized. After going through p_1, a quarter wave plate, the light emerges circularly polarized and with an increase in angular momentum. The result should be a reacting torque on p_1. Quarter-wave plate q_1 causes the light to become plane polarized again. When the light passes through p_2, it should once again be converted to circularly polarized light which should exert a torque on p_2 which would add to the torque on p_1. This process would be repeated as the light passes through the rest of the plates. Poynting doubted that such a small angular momentum could be detected when he stated, "But, even with such multiplications, my present experience of light forces does not give me much hope that the effect could be detected, if it has the value suggested by the mechanical model."[8]

---

[8]Poynting, op. cit., p. 567.

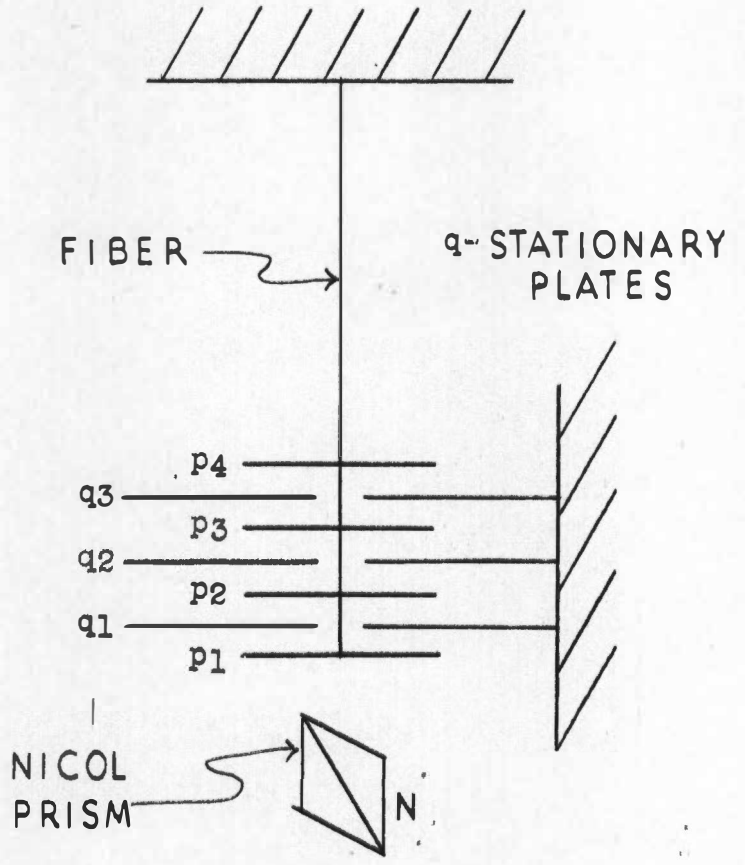

FIGURE 4

AN EXPERIMENTAL ARRANGEMENT SUGGESTED BY POYNTING FOR DETECTING ANGULAR MOMENTUM OF LIGHT

III. BETH'S EXPERIMENT

The experimental arrangement used by Beth[9] was similar to that suggested by Poynting and illustrated by Figure 4 on page 17. A diagram of the apparatus of Beth is shown in Figure 5 on page 19.

Light for this experiment came from a heated tungsten filament. It passed through lens A and a Nicol prism B from which it emerged plane polarized. The light was circularly polarized after it passed through the quarter-wave plate C, and the direction of the polarization was reversed by the half-wave plate which was suspended by a fiber. This imparted angular momentum to the half-wave plate. The light continued through the quarter-wave plate F, was reflected by an aluminum coating on the upper surface of F, and passed downward through the half-wave plate. The reversal in the direction of polarization upon passing through E was such that it added to the angular momentum of the plate imparted to it by the light in the upward direction.

The quarter-wave and half-wave plates had the proper thickness for a wavelength $\lambda = 1.2\mu$. The copper disk in the center of the fused quartz window D was to prevent the

---

[9]Beth, loc. cit.

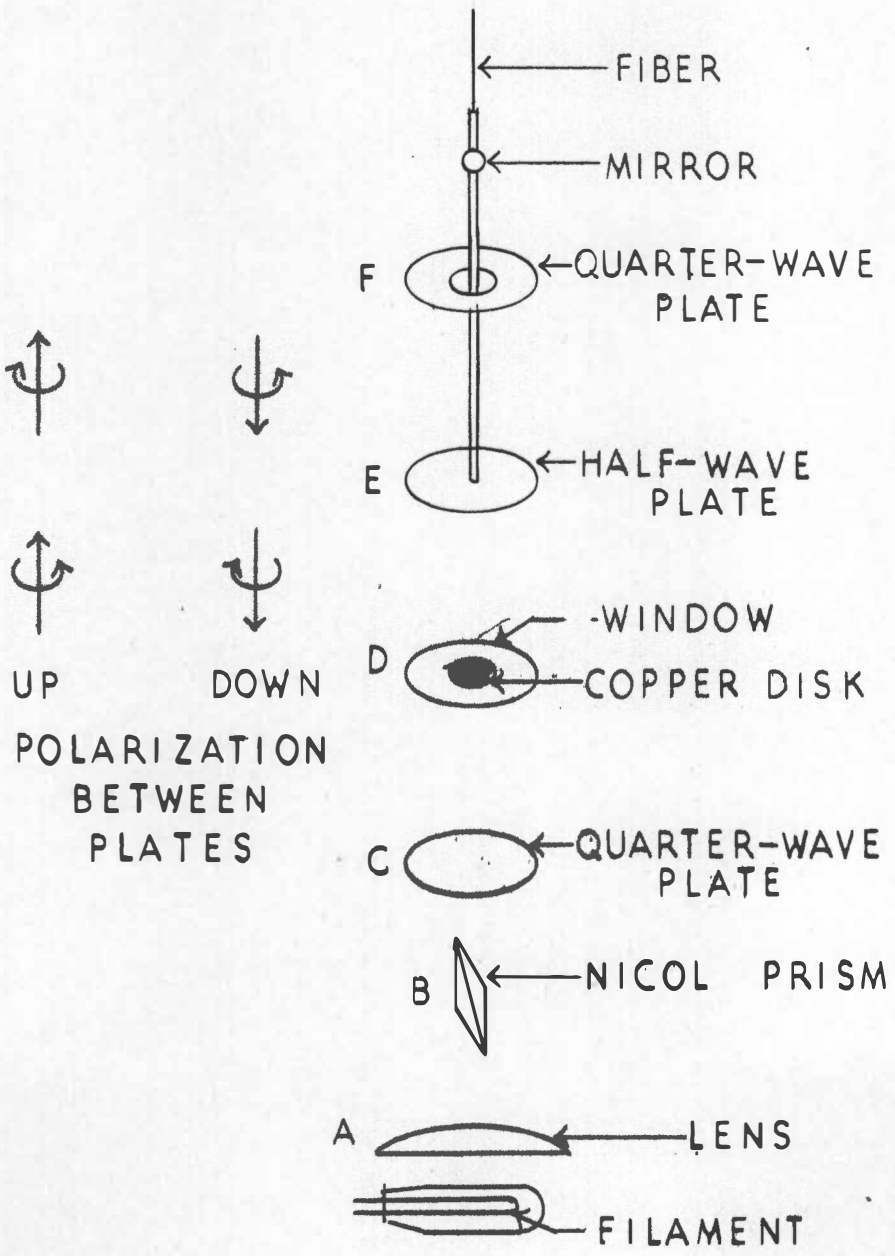

FIGURE 5

THE ESSENTIALS OF BETH'S APPARATUS

light from going up through the center hole in F and causing disturbances along the fiber.

With arrangements such as the one used by Beth and the one suggested by Poynting, one is able to obtain torques many times that which he would get with a simple absorption experiment.

Beth made measurements of the torque as a function of filament temperature and the angle between the plane of polarization of light and the axes of the plates. His measured effects agreed in sign and magnitude with theory.

IV. CARRARA'S EXPERIMENT

Carrara[10] performed experiments similar to that of Beth in a waveguide. He used circularly polarized waves of three centimeters wavelength in a waveguide. Two types of measurements were made. One was made using an absorber as a suspended system in the waveguide, and the other was made using a device which converted circular polarization to linear polarization. He reported that the effect had the expected order of magnitude.

---

[10]Carrara, loc. cit.

CHAPTER III

THE CLASSICAL THEORY OF ANGULAR MOMENTUM OF ELECTRIC DIPOLE RADIATION

In this chapter quantities such as energy, linear momentum density, angular momentum density, and angular momentum will be worked out in terms of the fields of infinitesimal electric dipoles. The units used are Gaussian.

I. AN OUTLINE OF THE CALCULATIONS

Consider the time rate of flow of electromagnetic energy in free space into a spherical shell with an inner surface of radius R_1 and an outer surface of radius R_2 as in Figure 6 on page 22. From Poynting's theorem the power is given by

$$\frac{c}{4\pi}\int_S \hat{n} \cdot (\underline{E} \times \underline{H})\, dS\,, \qquad \text{(III.I.1)}$$

where the integration is over the entire surface of the sphere of radius R_1. The energy within the shell should be

$$W = \frac{c}{4\pi}\int dt \int_S \hat{n} \cdot (\underline{E} \times \underline{H})\, dS, \qquad \text{(III.I.2)}$$

where the time integral is taken over the time it takes the radiation from the inner surface to reach the outer surface.

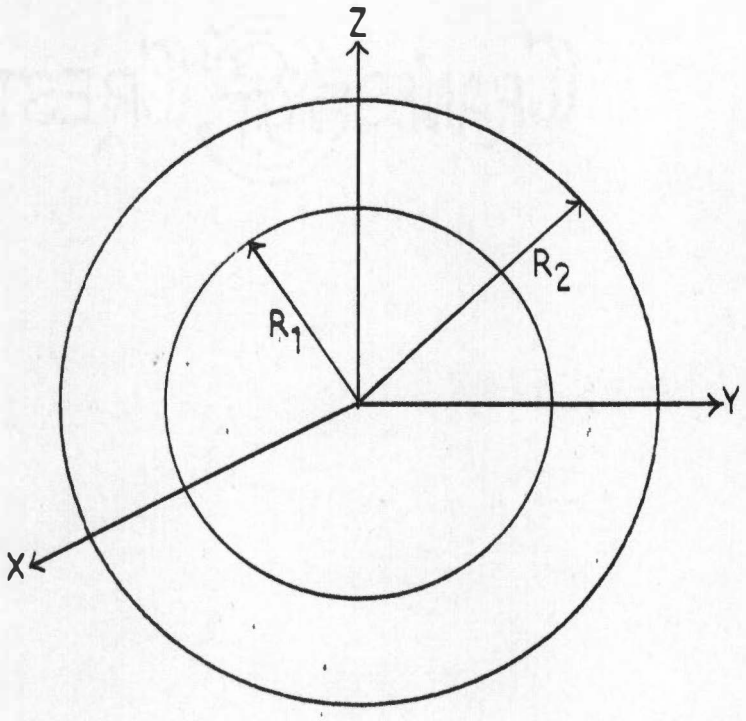

FIGURE 6

THE SPHERICAL SHELL IN WHICH THE ENERGY AND ANGULAR MOMENTUM ARE TO BE CALCULATED

This can be put in terms of the radius since $\frac{dr}{c} = dt$.

Thus

$$W = \frac{1}{4\pi} \int_V \hat{n} \cdot (\underline{E} \times \underline{H}) \, dV, \qquad \text{(III.I.3)}$$

where the volume integral is taken over the volume of the spherical shell.

The angular momentum within the shell is

$$\underline{N} = \int_V \underline{M} \, dV \quad , \qquad \text{(III.I.4)}$$

where $\underline{M}$ is the angular momentum density.

Angular momentum density is defined as

$$\underline{M} = (\underline{r} \times \underline{G}) \, , \qquad \text{(III.I.5)}$$

where r is the radius vector from the origin to the field point and $\underline{G}$ is the linear momentum density. Linear momentum density is defined as

$$\underline{G} = \frac{1}{4\pi c} (\underline{E} \times \underline{H}) \, . \qquad \text{(III.I.6)}$$

Thus $\underline{N}$ in terms of $\underline{E}$ and $\underline{H}$ is

$$\underline{N} = \hat{i} \int_V (yG_z - zG_y) \, dV + \hat{j} \int_V (zG_x - xG_z) \, dV + \hat{k} \int_V (xG_y - yG_x) \, dV \, ,$$

$$4\pi c \underline{N} = \hat{i} \int_V \left[y(E_x H_y - E_y H_x) - z(E_z H_x - E_x H_z) \right] dV + \hat{j} \int_V \left[z(E_y H_z - E_z H_y) - x(E_x H_y - E_y H_x) \right] dV + \hat{k} \int_V \left[x(E_z H_x - E_x H_z) - y(E_y H_z - E_z H_y) \right] dV \, . \qquad \text{(III.I.7)}$$

The time average of $\underline{N}$ over the time interval T $= \dfrac{\int_0^T \underline{N}\, dt}{T}$ (III.I.8)

$$= \hat{i} \frac{\int_0^T N_x\, dt}{T} + \hat{j} \frac{\int_0^T N_y\, dt}{T}$$

$$+ \hat{k} \frac{\int_0^T N_z\, dt}{T} . \qquad \text{(III.I.9)}$$

Now the components of $\underline{N}$ involve products of components of $\underline{E}$ and $\underline{H}$, each of which will be seen to contain a factor of $\sin(\omega t - \frac{r}{c})$ or $\cos(\omega t - \frac{r}{c})$. The possible combinations are $\sin^2(\omega t - \frac{r}{c})$, $\cos^2(\omega t - \frac{r}{c})$, and the product $\left[\sin(\omega t - \frac{r}{c})\right]\left[\cos(\omega t - \frac{r}{c})\right]$. The time averages of these quantities over long periods of time are

$$\overline{\sin^2(\omega t - \tfrac{r}{c})} = \tfrac{1}{2} , \qquad \text{(III.I.10)}$$

$$\overline{\cos^2(\omega t - \tfrac{r}{c})} = \tfrac{1}{2} , \qquad \text{(III.I.11)}$$

$$\overline{\left[\sin(\omega t - \tfrac{r}{c})\right]\left[\cos(\omega t - \tfrac{r}{c})\right]} = 0 . \qquad \text{(III.I.12)}$$

Thus as one calculates the time average of individual products he can omit the terms containing the factor $\left[\sin(\omega t - \frac{r}{c})\right]\left[\cos(\omega t - \frac{r}{c})\right]$.

The result which is to be obtained is the ratio of the time average of energy to the time average of angular momentum, because from this one can obtain the amount of torque exerted upon an absorber per watt of power radiated.

For a one-dimensional rigid rotator, the torque is set equal to the time rate of change of angular momentum;

$$\tau = \frac{dN}{dt} . \qquad \text{(III.I.13)}$$

By definition power is the time rate of doing work;

$$P = \frac{dW}{dt} . \qquad \text{(III.I.14)}$$

For constant τ and P,

$$\bar{P}\,\Delta t = \Delta W, \quad |\bar{\tau}|\Delta t = \Delta |N|;$$

hence

$$\frac{|\bar{\tau}|}{P} = \frac{\Delta |N|}{\Delta W} . \qquad \text{(III.I.15)}$$

It is seen that the ratio of angular momentum to energy is the same as the ratio of torque to power.

Also, in an experiment, a perfectly absorbing spherical shell is equivalent to letting the outer radius R_2 in the theoretical problem increase without limit.

II. THE ANGULAR MOMENTUM DUE TO A DIPOLE WITH MOMENT p cos ωt

For an oscillating dipole moment p cos ωt along the z-axis one obtains for the electric and magnetic fields[1] at the field point P(r, Θ, φ):

---

[1]These are standard equations. See William R. Smythe, Static and Dynamic Electricity (New York: McGraw-Hill Book Company, 1939), p. 467.

$$E_r = \frac{2p \cos\Theta}{r^3} \cos\omega(t - \tfrac{r}{c}) - \frac{2pk \cos\Theta}{r^2} \sin\omega(t - \tfrac{r}{c}) , \qquad \text{(III.II.1)}$$

$$E_\Theta = \frac{p \sin\Theta}{r^3} \cos\omega(t - \tfrac{r}{c}) - \frac{pk \sin\Theta}{r^2} \sin\omega(t - \tfrac{r}{c}) - \frac{p \sin\Theta k^2}{r} \cos\omega(t - \tfrac{r}{c}) , \qquad \text{(III.II.2)}$$

$$E_\phi = 0 , \qquad \text{(III.II.3)}$$

$$H_r = 0 , \qquad \text{(III.II.4)}$$

$$H_\Theta = 0 , \qquad \text{(III.II.5)}$$

$$H_\phi = -\frac{p \sin\Theta k^2}{r} \cos\omega(t - \tfrac{r}{c}) - \frac{p \sin\Theta k}{r^2} \sin\omega(t - \tfrac{r}{c}) , \qquad \text{(III.II.6)}$$

where $k = \frac{\omega}{c}$. The geometry is shown in Figure 7 on page 27. In the following equations, the time factor $\omega(t - \frac{r}{c})$ is used so often that it shall be represented by the symbol ψ .

The momentum per unit volume has been defined as

$$\underline{G} = \frac{\underline{E} \times \underline{H}}{4\pi c} . \qquad \text{(III.I.6)}$$

If one calculates $\underline{G}$ for the single dipole, he obtains

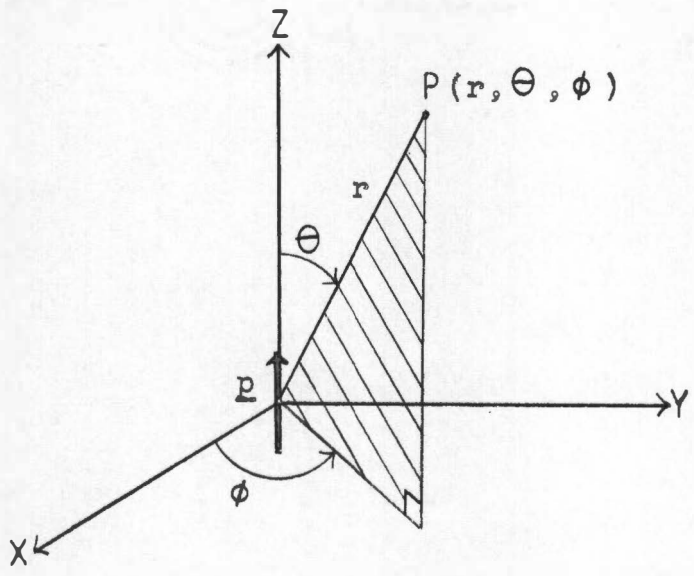

FIGURE 7

AN OSCILLATING DIPOLE ALONG THE Z-AXIS

$$\underline{G} = \frac{1}{4\pi c} \begin{vmatrix} \hat{r} & \hat{\theta} & \hat{\phi} \\ E_r & E_\theta & 0 \\ 0 & 0 & H_\phi \end{vmatrix}$$

$$= \frac{1}{4\pi c} \left[\hat{r} \, (E_\theta H_\phi) + \hat{\theta} (-E_r H_\phi) \right], \quad \text{(III.II.7)}$$

so that $\underline{G} = \hat{r} \, G_r + \hat{\theta} \, G_\theta$. (III.II.8)

The angular momentum per unit volume has been defined as $\underline{M} = \underline{r} \times \underline{G}$. (III.I.5)

In determinant form this is

$$\underline{M} = \begin{vmatrix} \hat{r} & \hat{\theta} & \hat{\phi} \\ r & 0 & 0 \\ G_r & G_\theta & 0 \end{vmatrix} \quad \text{(III.II.9)}$$

$$= \hat{\phi} \, r \, G_\theta \, . \quad \text{(III.II.10)}$$

The time average $\overline{rG_\theta}$ is shown to be zero in Appendix A on page 141, so that there is no average angular momentum radiated by a dipole moment $\underline{p} \cos \omega t$.

III. THE ENERGY IN A SPHERICAL SHELL DUE TO A DIPOLE WITH MOMENT $\underline{p} \cos \omega t$

The energy in a spherical shell is, from (III.I.3) and (III.I.6),

$$W = \frac{1}{4\pi} \int_V \hat{n} \cdot (\underline{E} \times \underline{H}) \, dV$$

$$= c \int_V \hat{n} \cdot \underline{G} \, dV. \quad \text{(III.III.1)}$$

Over the spherical surface of radius R_1,

$$\hat{n} \cdot \underline{G} = G_r,$$

so that

$$W = c\int_V G_r \, dV, \qquad \text{(III.III.2)}$$

where the integration is performed over the volume of the spherical shell. The average energy is shown in Appendix A on page 144 to be

$$\overline{W} = \frac{1}{3} p^2 k^4 (R_2 - R_1). \qquad \text{(A.13)}$$

For this single dipole the ratio of average angular momentum in the shell to the average energy is zero.

IV. THE ANGULAR MOMENTUM DUE TO TWO OSCILLATING DIPOLES AT RIGHT ANGLES TO EACH OTHER WITH A PHASE DIFFERENCE OF NINETY DEGREES

For this case one may superimpose two sets of solutions to get the electric and magnetic fields: (1) the fields of a dipole along the z-axis and (2) the field of a dipole of equal moment along the x-axis with a phase angle of a positive ninety degrees with respect to (1). The physical situation is shown in Figure 8 on page 30.

The fields of (1) have been given. To find the fields of (2), one transforms the fields of (1) to correspond to a dipole along the x-axis with a change in phase angle. This can be accomplished by first putting the components of the fields of (1) in rectangular cartesian coordinates. For brevity

$$r = \sqrt{x^2 + y^2 + z^2} \qquad \text{(III.IV.1)}$$

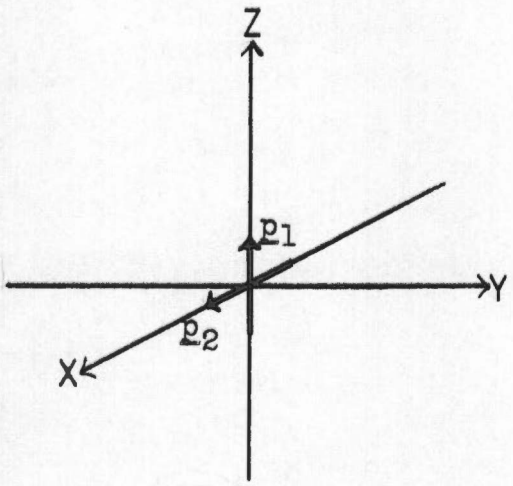

FIGURE 8

TWO DIPOLES AT RIGHT ANGLES TO EACH OTHER

will be used. Then

$$E_{1x} = \left[\frac{-pk^2zx}{r^3} + \frac{3pzx}{r^5}\right] \cos\psi + \left[\frac{-3pkzx}{r^4}\right] \sin\psi , \qquad \text{(III.IV.2)}$$

$$E_{1y} = \left[\frac{3pzy}{r5} - \frac{pk^2yz}{r^3}\right] \cos\psi + \left[\frac{-pkyz - 2pzky}{r^4}\right] \sin\psi , \qquad \text{(III.IV.3)}$$

$$E_{1z} = \left[\frac{pk^2(x^2 + y^2)}{r^3} - \frac{p(x^2 + y^2)}{r^5} + \frac{2pz^2}{r^5}\right] \cos\psi + \left[\frac{pk\,(x^2 + y^2)}{r^4} - \frac{2pkz2}{r^4}\right] \sin\psi , \qquad \text{(III.IV.4)}$$

$$H_{1x} = \left[\frac{pyk^2}{r2}\right] \cos\psi + \left[\frac{pyk}{r^3}\right] \sin\psi , \qquad \text{(III.IV.5)}$$

$$H_{1y} = \left[-\frac{pxk^2}{r2}\right] \cos\psi - \left[\frac{pxk}{r^3}\right] \sin\psi , \qquad \text{(III.IV.6)}$$

$$H_{1z} = 0 . \qquad \text{(III.IV.7)}$$

After a transformation that carries z into -x, y into y, and x into z and a change of the phase angle by ninety degrees, one obtains

$$E_{2x} = \left[\frac{2pkx^2 - pk(y^2 + z^2)}{r^4}\right] \cos\psi + \left[\frac{pk^2(y^2 + z^2)}{r^3} - \frac{p(y^2 + z^2) + 2px^2}{r^5}\right] \sin\psi, \quad \text{(III.IV.8)}$$

$$E_{2y} = \left[\frac{3pkxy}{r^4}\right] \cos\psi + \left[\frac{-pk^2yx}{r^3} + \frac{3pxy}{r^5}\right] \sin\psi, \quad \text{(III.IV.9)}$$

$$E_{2z} = \left[\frac{3pkxz}{r^4}\right] \cos\psi + \left[\frac{-pk^2xz}{r^3} + \frac{3pxz}{r^5}\right] \sin\psi, \quad \text{(III.IV.10)}$$

$$H_{2x} = 0, \quad \text{(III.IV.11)}$$

$$H_{2y} = \left[\frac{-pzk}{r^3}\right] \cos\psi + \left[\frac{pzk^2}{r^2}\right] \sin\psi, \quad \text{(III.IV.12)}$$

$$H_{2z} = \left[\frac{pyk}{r^3}\right] \cos\psi - \left[\frac{pyk^2}{r^2}\right] \sin\psi. \quad \text{(III.IV.13)}$$

For the sum of the fields one obtains

$$E_x = E_{1x} + E_{2x}$$

$$= \left[\frac{-pk^2zx}{r^3} + \frac{2pkx^2 - pk(y^2 + z^2)}{r^4} + \frac{3pzx}{r^5} \right] \cos\psi$$

$$+ \left[\frac{pk^2(y^2 + z^2)}{r^3} - \frac{3pkzx}{r^4} \right.$$

$$\left. - \frac{p(y^2 + z^2) + 2px^2}{r^5} \right] \sin\psi \,, \qquad \text{(III.IV.14)}$$

$$E_y = \left[\frac{3pkxy}{r^4} + \frac{3pzy}{r^5} - \frac{pk^2yz}{r^3} \right] \cos\psi$$

$$+ \left[\frac{-pk^2yx}{r^3} - \frac{3pzky}{r^4} + \frac{3pxy}{r^5} \right] \sin\psi \,, \qquad \text{(III.IV.15)}$$

$$E_z = \left[\frac{pk^2(x^2 + y^2)}{r^3} + \frac{3pkxz}{r^4} \right.$$

$$\left. + \frac{2pz^2 - p(x^2 + y^2)}{r^5} \right] \cos\psi$$

$$+ \left[\frac{-pk^2xz}{r^3} + \frac{pk(x^2 + y^2) - 2pkz^2}{r^4} \right.$$

$$\left. + \frac{3pxz}{r^5} \right] \sin\psi \,, \qquad \text{(III.IV.16)}$$

$$H_x = H_{1x} + H_{2x}$$

$$= \left[\frac{pk^2y}{r^2}\right] \cos\psi \left[\frac{pky}{r^3}\right] \sin\psi \,, \qquad \text{(III.IV.17)}$$

$$H_y = H_{1y} + H_{2y}$$

$$= \left[-\frac{pk^2x}{r^2} - \frac{pzk}{r^3}\right] \cos\psi$$

$$+ \left[\frac{pk^2z}{r^2} - \frac{pkx}{r^3}\right] \sin\psi \,, \qquad \text{(III.IV.18)}$$

$$H_z = H_{1z} + H_{2z}$$

$$= \left[\frac{pyk}{r^3}\right] \cos\psi + \left[\frac{-pyk^2}{r^2}\right] \sin\psi \,. \qquad \text{(III.IV.19)}$$

For the time averages one obtains

$$\overline{G_x} = \frac{1}{8\pi c} \left[\frac{p^2k^4(x^3 + 2xy^2 + xz^2)}{r^5}\right.$$

$$+ \frac{p^2k^3(2x^2z + 2y^2z + 2z^3)}{r^6}$$

$$\left. + \frac{p^2k(2x^2z + 2y^2z + 2z^3)}{r^8}\right] , \qquad \text{(III.IV.20)}$$

$$\overline{G_y} = \frac{1}{8\pi c} \left[\frac{p^2k^4(x^2y + yz^2 + 2y^3)}{r^5}\right] , \qquad \text{(III.IV.21)}$$

$$\overline{G_z} = \frac{1}{8\pi c}\left[\frac{p^2k^4z(x^2+2y^2+z^2)}{r^5} - \frac{2p^2k^3x(x^2+y^2+z^2)}{r^6} - \frac{2p^2kx(x^2+y^2+z^2)}{r^8}\right]. \qquad \text{(III.IV.22)}$$

For the time average of the components of $\underline{M}$ one obtains

$$\overline{M_x} = \frac{1}{8\pi c}\left[\frac{p^2k^3}{r^6}(-2xy)(x^2+y^2+z^2) + \frac{p^2k}{r^8}(-2xy)(x^2+y^2+z^2)\right], \qquad \text{(III.IV.23)}$$

$$\overline{M_y} = \frac{1}{8\pi c}\left[\frac{2p^2k^3}{r^2} - \frac{2p^2k^3y^2 - 2p^2k}{r^4} - \frac{2p^2ky^2}{r^6}\right], \qquad \text{(III.IV.24)}$$

$$\overline{M_z} = \frac{1}{8\pi c}\left[\frac{p^2k^3}{r^6}(-2yz)(x^2+y^2+z^2) + \frac{p^2k(-2yz)(x^2+y^2+z^2)}{r^8}\right]. \qquad \text{(III.IV.25)}$$

To get the total angular momentum in the shell one uses

$$\overline{N} = \int_V \overline{M}\, dV \qquad \text{(III.IV.26)}$$
$$= \hat{i}\int_V \overline{M_x}\, dV + \hat{j}\int_V \overline{M_y}\, dV + \hat{k}\int_V \overline{M_z}\, dV \ .$$

For

$$x = r \sin\theta \cos\phi , \tag{III.IV.27}$$

$$y = r \sin\theta \sin\phi , \tag{III.IV.28}$$

$$z = r \cos\theta , \tag{III.IV.29}$$

one obtains

$$\overline{M_x} = \frac{1}{8\pi c}\left[\frac{p^2k^3(-2r^2\sin^2\theta \sin\phi\cos\phi)}{r^4} + \frac{p^2k(-2r^2\sin\theta \sin\phi\cos\phi)}{r^6}\right], \tag{III.IV.30}$$

$$\overline{M_y} = \frac{1}{8\pi c}\left[\frac{2p^2k^3}{r^2} + \frac{2p^2k}{r^4} - \frac{2p^2k^3r^2\sin^2\theta \sin^2\phi}{r^4} - \frac{2p^2kr^2\sin^2\theta \sin^2\phi}{r^6}\right], \tag{III.IV.31}$$

$$\overline{M_z} = \frac{1}{8\pi c}\left[\frac{2p^2k^3r^2\sin\theta\cos\theta \sin\phi}{r^4} + \frac{2p^2kr^2\sin\theta\cos\theta \sin\phi}{r^6}\right]. \tag{III.IV.32}$$

Now

$$\int_V \overline{M_x}\, dV = 0, \tag{III.IV.33}$$

since

$$\int_0^{2\pi} \sin\phi \cos\phi \, d\phi = 0, \tag{III.IV.34}$$

and

$$\int_V \overline{M}_z \, dV = 0 \, , \qquad \text{(III.IV.35)}$$

since $$\int_0^{\pi} \sin\theta \cos\theta \, d\theta = 0 \, . \qquad \text{(III.IV.36)}$$

But

$$4\pi c \int_V M_y dV = \Big[4\pi p^2 k^3 (R_2 - R_1) - 4\pi p^2 k \left(\frac{1}{R_2} - \frac{1}{R_1}\right) + \frac{4}{3}\pi p^2 k^3 (R_2 - R_1) + \frac{4}{3}\pi p^2 k \left(\frac{1}{R_2} - \frac{1}{R_1}\right) \Big] \qquad \text{(III.IV.37)}$$

$$= \frac{8\pi}{3} p^2 k^3 (R_2 - R_1) + \frac{8\pi}{3} p^2 k \left(\frac{R_2 - R_1}{R_1 R_2}\right) \qquad \text{(III.IV.38)}$$

Thus

$$\overline{N} = \hat{j} \left[\frac{2p^2 k^3}{3c} (R_2 - R_1) + \frac{2p^2 k}{3c} \left(\frac{R_2 - R_1}{R_1 R_2}\right) \right] \qquad \text{(III.IV.39)}$$

This result says that with the dipoles along the x- and z-axes there should be angular momentum in the y-direction. If this radiation were to be absorbed by a

spherical shell, there should be rotation about the y-axis. If the dipoles were along the x- and y-axes, the rotation should be about the z-axis.

V. THE DISTRIBUTION OF THE ANGULAR MOMENTUM DENSITY

If one transforms the case which we have considered to the case where the dipoles are along the x- and y-axes by transforming x into x, y into -z, and z into y, then he obtains the following expressions for the components of $\underline{M}$:

$$\overline{M_x} = \frac{1}{4\pi c}\left[\frac{p^2k^3xz}{r^4} + \frac{p^2kxz}{r^6}\right], \qquad \text{(III.V.1)}$$

$$\overline{M_y} = \frac{1}{4\pi c}\left[\frac{p^2k^3yz}{r^4} + \frac{p^2kyz}{r^6}\right], \qquad \text{(III.V.2)}$$

$$\overline{M_z} = \frac{1}{4\pi c}\left[\frac{p^2k^3}{r^4}(x^2 + y^2 - z^2) + \frac{p^2k}{r^6}(x^2 - y^2 - z^2)\right]. \qquad \text{(III.V.3)}$$

Transforming these to spherical polar coordinates, one obtains simpler results:

$$\overline{M_r} = 0, \qquad \text{(III.V.4)}$$

$$\overline{M}_{\phi} = 0 \ , \tag{III.V.5}$$

$$\overline{M}_{\theta} = \frac{p^2}{4\pi c}\left[\frac{k^3}{r^2} + \frac{k}{r^4}\right]\sin\theta \ , \tag{III.V.6}$$

$$\overline{M}_{z} = -\frac{p^2}{4\pi c}\left[\frac{k^3}{r^2} + \frac{k}{r^4}\right]\sin^2\theta \ . \tag{III.V.7}$$

(III.V.7) shows the dependence of the angular momentum density upon r and θ. Figure 9 on page 40 shows the orientation of the dipoles.

VI. THE ENERGY IN THE SPHERICAL SHELL DUE TO THE TWO DIPOLES

The energy will be just twice that of a single dipole, or from (A.13) on page 145,

$$\overline{W} = \frac{2}{3}p^2k^4(R_2 - R_1) \ . \tag{III.VI.1}$$

VII. THE RATIO OF THE ANGULAR MOMENTUM IN THE SPHERICAL SHELL TO THE ENERGY DUE TO THE TWO DIPOLES

From (III.IV.39) and (III.VI.1) one obtains

$$\frac{|\overline{N}|}{\overline{W}} = \frac{\frac{2p^2k^3}{3c}(R_2 - R_1) + \frac{2p^2k}{3c}\left(\frac{R_2 - R_1}{R_1R_2}\right)}{\frac{2p^2k^4(R_2 - R_1)}{3}} \ , \tag{III.VII.1}$$

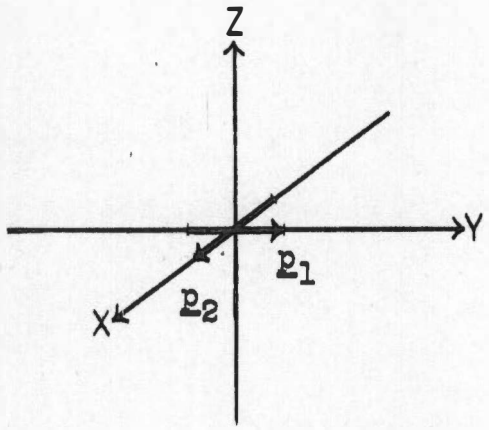

FIGURE 9

TWO ELECTRIC DIPOLES ALONG THE X- AND Y-AXES

$$\frac{|\bar{N}|}{\bar{W}} = \frac{1}{kc} + \frac{1}{k^2 c R_1 R_2} ,$$

$$= \frac{1}{\omega} + \frac{1}{\omega R_1 R_2} . \qquad \text{(III.VII.2)}$$

$$\text{As } R_2 \longrightarrow \infty , \quad \frac{|\bar{N}|}{\bar{W}} \longrightarrow \frac{1}{\omega} . \qquad \text{(III.VII.3)}$$

IX. THE CASE OF TWO EQUAL DIPOLE MOMENTS WHICH ARE MUTUALLY PERPENDICULAR AND HAVE AN ARBITRARY PHASE DIFFERENCE

A more general case than the one just treated is one in which the phase difference between the dipoles is not ninety degrees. It has been shown that for two equal dipole moments and an arbitrary phase difference the limiting ratio,

$$\frac{|\bar{N}|}{\bar{W}} = \frac{1}{\omega} , \qquad \text{(III.VII.3)}$$

becomes

$$\frac{|\bar{N}|}{\bar{W}} = \frac{\sin \phi}{\omega} , \qquad \text{(III.IX.1)}$$

where ϕ is the phase difference between the dipoles.[2]

---

[2]Arnold Sommerfeld, Atomic Structures and Spectral Lines (London: Methuen and Company, Ltd., 1923), p. 261.

In the experimental research conducted, the powers to the dipoles were equal, but the phase difference was approximately 115 degrees. Since sin ϕ varies relatively slowly with ϕ in the range near ninety degrees, this does not decrease the torque greatly. When the phase difference is 115 degrees, one would expect 0.91 times the torque obtainable with a phase difference of ninety degrees.

CHAPTER IV

THE THEORY OF A ONE-DIMENSIONAL, SYMMETRICAL, RIGID ROTATOR

Consider a rigid body which is symmetrical about an axis and pcssesses a moment of inertia I about the symmetry axis. Let the following torques act on it about the axis of symmetry: (1) a restoring torque proportional to the angular displacement from the equilibrium position and (2) a torque which is due to a viscous liquid and is directly proportional to the magnitude of the angular velocity. Torque (2) will be in the direction opposite to the angular velocity.

The linear differential equation with constant coefficients which describes the motion of such a system in terms of angular position is

$$I\frac{d^2\theta}{dt^2}+\gamma\frac{d\theta}{dt}+k\theta = 0 , \qquad \text{(IV.1)}$$

where I is the moment of inertia, γ is the torque per unit angular velocity, and k is the torque per unit angle provided by the device which furnishes the restoring torque.

The general solution to this equation is

$$\theta = A_1e^{r_1t} + A_2e^{r_2t} \qquad \text{(IV.2)}$$

for $r_1 \neq r_2$, and

$$\theta = (A_1' + A_2' t)\, e^{r_1 t} \qquad \text{(IV.3)}$$

for $r_1 = r_2$, where A_1, A_2, A_1', and A_2' are constants, and

$$r_1 = -\frac{\gamma}{2I} + \sqrt{\frac{\gamma^2}{4I^2} - \frac{k}{I}}\,, \qquad \text{(IV.4)}$$

$$r_2 = -\frac{\gamma}{2I} - \sqrt{\frac{\gamma^2}{4I^2} - \frac{k}{I}}\,.$$

Special cases of this general solution will be considered in this chapter. Cases I, II, and III are needed in connection with experimental work performed. Case IV was not treated experimentally, but it is included to determine the feasibility of performing such an experiment.

Another section is included in this chapter to show how the torque due to the viscosity of the water was estimated theoretically in designing the experiment.

II. AN EXTERNAL CONSTANT TORQUE APPLIED ABOUT THE SYMMETRY AXIS WITH $k = 0$ AND γ SUPPLIED BY A LIQUID

Consider the system illustrated in Figure 10 on page 45.

The equation of motion for this case is

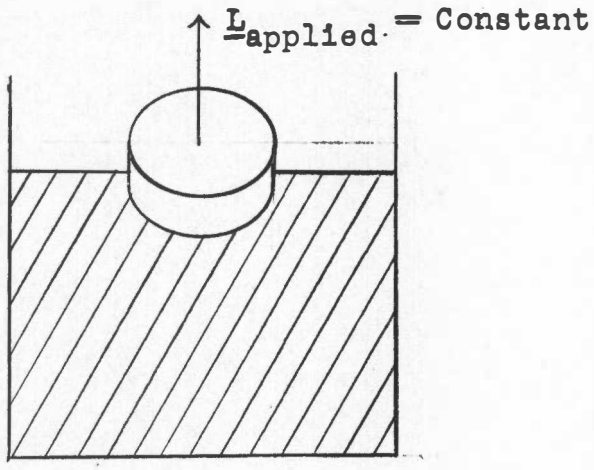

FIGURE 10

A FLOATING ROTATOR WITH A CONSTANT EXTERNAL TORQUE APPLIED

$$I \frac{d^2\theta}{dt^2} + \gamma \frac{d\theta}{dt} = B_3 \,, \qquad \text{(IV.I.1)}$$

where B_3 is the applied constant torque. The solution to the homogeneous equation (IV.1) from IV.2) becomes

$$\theta = B_1 + B_2 e^{-\frac{\gamma}{I}t} \,, \qquad \text{(IV.I.2)}$$

where the B's are constants.

One must add to (IV.I.2) a particular solution of (IV.I.1). A particular solution of (IV.I.1) is

$$\theta = B_4 + \frac{B_3 t}{\gamma} \qquad \text{(IV.I.3)}$$

Adding (IV.I.2) and (IV.I.3), one obtains

$$\theta = B_5 + \frac{B_3}{\gamma} t + B_2 e^{-\frac{\gamma}{I}t} \,. \qquad \text{(IV.I.4)}$$

Now B_3 is presumably a known torque, so this leaves B_5 to be determined from the initial angular position and velocity of the system.

The torque in the actual experiment was to be supplied by the electromagnetic radiation and was theoretically equal to

$$B_3 = \frac{P \sin\phi}{2\pi f} \,, \qquad \text{(IV.I.5)}$$

where ϕ is the phase difference between the two dipole

moments. For $\theta=\theta_0$ and $\frac{d\theta}{dt} = 0$ when $t = 0$, (IV.I.4) becomes

$$\theta = (\theta_0 - \frac{IB_3}{\gamma^2}) + \frac{B_3}{\gamma} t + \frac{IB_3}{\gamma^2} e^{-\frac{\gamma}{I}t}. \qquad \text{(IV.I.6)}$$

II. THE ROTATOR WITH NO EXTERNAL TORQUE, AN INITIAL ANGULAR DISPLACEMENT, ZERO INITIAL ANGULAR VELOCITY, $k \neq 0$, AND γ SUPPLIED BY A LIQUID

This system is illustrated in Figure 11 on page 48.

For this case, one has only the homogeneous equation (IV.1). The solution (IV.2) has been given, and it is a matter of evaluating two constants. From (IV.2)

$$\theta = c_1 e^{r_1 t} + c_2 e^{r_2 t} \quad , \; r_1 \neq r_2 \; .$$

For $\theta=\theta_0$ and $\frac{d\theta}{dt} = 0$ when $t = 0$ one obtains

$$\theta = \theta_0 \left[\frac{r_2}{r_2 - r_1} e^{r_1 t} - \frac{r_1}{r_2 - r_1} e^{r_2 t} \right] . \text{(IV.II.1)}$$

The best form of this equation depends upon the character of r_1 and r_2 in the exponential functions of time.

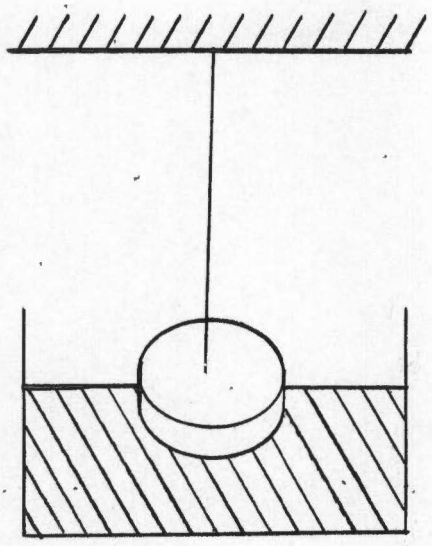

FIGURE 11

A FLOATING ROTATOR WITH A FIXED FIBER

III. THE ROTATOR WITH AN EXTERNAL TORQUE SUPPLIED BY A FIBER WITH ITS UPPER END ROTATED AT A CONSTANT ANGULAR VELOCITY AND $\gamma \neq 0$

This system with the appropriate angles is diagramed in Figure 12 on page 50. When $\theta_2 = \theta$, there is no torque exerted by the fiber on the rotator.

The equation of motion of this system is

$$I \frac{d^2\theta}{dt^2} + \gamma \frac{d\theta}{dt} = (\theta_2 - \theta)k \qquad \text{(IV.III.1)}$$

This may be put in the form

$$I \frac{d^2\theta}{dt^2} + \gamma \frac{d\theta}{dt} + k\theta = k\theta_2 \ . \qquad \text{(IV.II.2)}$$

But

$$\theta_2 = \omega_2 t,$$

where ω_2 is a constant angular velocity, and (IV.III.2) becomes

$$I \frac{d^2\theta}{dt^2} + \gamma \frac{d\theta}{dt} + k\theta = (k\omega_2)t. \qquad \text{(IV.III.3)}$$

The general solution to the homogeneous equation is

$$\theta = D_1 e^{r_1 t} + D_2 e^{r_2 t},$$

and a particular solution of (IV.III.3) is

$$\theta = -\frac{\gamma\omega_2}{k} + \omega_2 t \ .$$

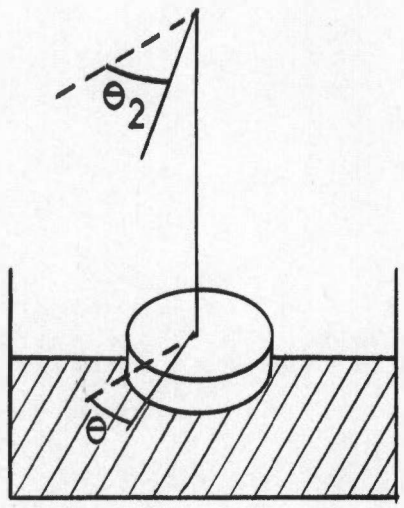

FIGURE 12

A FLOATING ROTATOR WITH A FIBER
WHOSE UPPER END IS ROTATED

The general solution to (IV.III.3) is

$$\theta = D_1 e^{r_1 t} + D_2 e^{r_2 t} - \frac{\gamma \omega_2}{k} + \omega_2 t \, . \qquad \text{(IV.III.4)}$$

For $\theta = 0$ and $\frac{d\theta}{dt} = 0$ when $t = 0$,

$$D_1 = \frac{(r_2 \gamma + k)\omega_2}{k(r_2 - r_1)} \, , \qquad \text{(IV.III.5)}$$

$$D_2 = \frac{-(r_1 \gamma + k)\omega_2}{k(r_2 - r_1)} \, . \qquad \text{(IV.III.6)}$$

IV. SINUSOIDAL FORCING APPLIED AT THE RESONANT FREQUENCY BY ELECTROMAGNETIC RADIATION, $\gamma \neq 0$, AND $k \neq 0$

Such a system is diagramed in Figure 13 on page 52.

For this system, the equation of motion is

$$I \frac{d^2\theta}{dt^2} + \gamma \frac{d\theta}{dt} + k\theta = E_0 \sin \alpha t \, . \qquad \text{(IV.IV.1)}$$

Consider only the steady state part of the solution of (IV.V.1). This is

$$\theta = \frac{E_0}{\sqrt{(k - I\alpha^2)^2 + (\gamma\alpha)^2}} \cos(\alpha t - \xi), \qquad \text{(IV.IV.2)}$$

where

$$\xi = \arcsin \frac{(k - I\alpha^2)}{(k - I\alpha^2)^2 + (\gamma\alpha)^2 \, \frac{1}{2}} \, . \qquad \text{(IV.IV.3)}$$

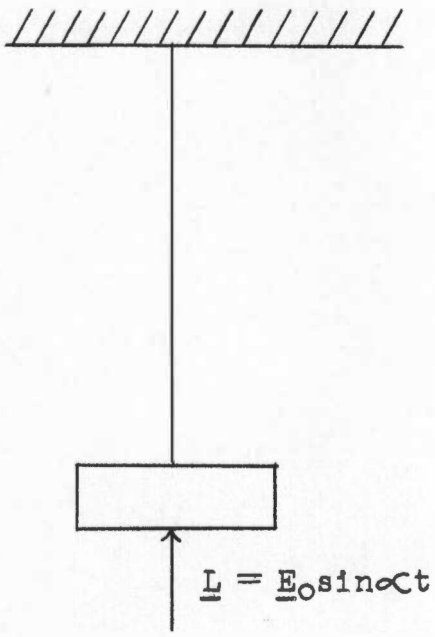

FIGURE 13

A SUSPENDED SYSTEM WITH SINUSOIDAL FORCING

For fixed values of k, I, and γ, θ_{max} will occur for the resonant condition

$$k - I\alpha^2 = 0 \text{ .} \qquad \text{(IV.IV.4)}$$

The angular frequency for which this will occur is

$$\alpha = \sqrt{\frac{k}{I}} \text{ .} \qquad \text{(IV.IV.5)}$$

From (IV.IV.2),

$$\theta_{max} = \frac{E_0}{\gamma}\sqrt{\frac{I}{k}} \text{ .} \qquad \text{(IV.IV.6)}$$

V. AN ESTIMATE OF THE TORQUE ON THE EXPERIMENTAL ROTATOR DUE TO THE VISCOSITY OF WATER

The greatest part of the torque on the rotator shown in Figure 14 on page 54 is on the side of the float. Assuming that this is a cylinder with a radius of seven inches and a length of five inches, one can estimate the torque from

$$L = \left[\frac{4\pi\mu_v \ell a^2 b^2}{(b^2 - a^2)}\right]\omega \qquad \text{(IV.V.1)}$$

$$= \gamma\omega \text{ ,} \qquad \text{(IV.V.2)}$$

where μ_v is the coefficient of viscosity of water, ℓ is the length of the cylinder, a is the radius of the inner

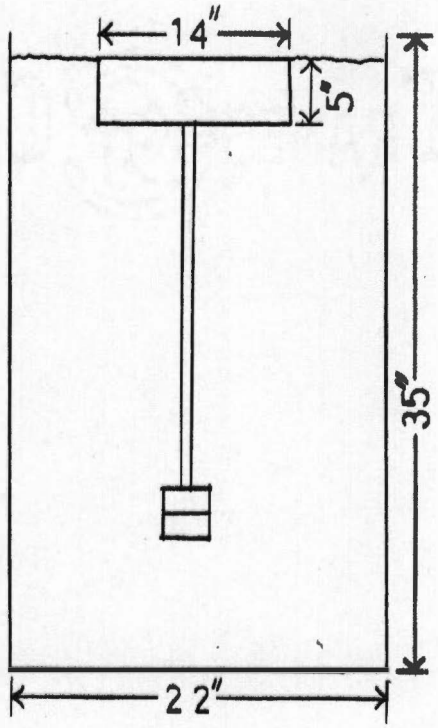

FIGURE 14

AN EXPERIMENTAL ROTATOR

cylinder, and b is the radius of the outer cylinder.[1]

For a coefficient of viscosity of 0.010 poise for water at a temperature of twenty degrees Centigrade and the dimensions for a and b as shown in Figure 14 on page 54, a value of 8.6×10^{-5}n m sec is obtained for γ.

---

[1]Leigh Page, Introduction to Theoretical Physics (New York: D. Van Nostrand Company, Inc., 1949), p. 262.

CHAPTER V

THE BASIC EXPERIMENT

The basic experiment is described in this chapter. More detailed drawings and photographs of specific parts of the apparatus will be given in Chapter VI, and specific testing procedures will be given in Chapter VII.

I. THE APPARATUS

The essentials of the apparatus for performing the basic experiment are shown in Figure 15 on page 57. Omitted from this simplified diagram of the apparatus are the supporting framework for the tank and the air-shield about the floating apparatus.

The absorbing spherical shell is mounted on top of a circular piece of plywood which also carries a scale around its periphery. The hollow float supports the plywood, scale, and sphere. An aluminum rod runs to the bottom of the tank. An iron needle in the end of the rod is attracted by a magnet in the bottom of the tank and keeps the floating apparatus centered in the water tank.

II. THE EXPERIMENTAL TRIAL

In an experimental trial data were taken for four and one-half days without energy radiated from the antenna

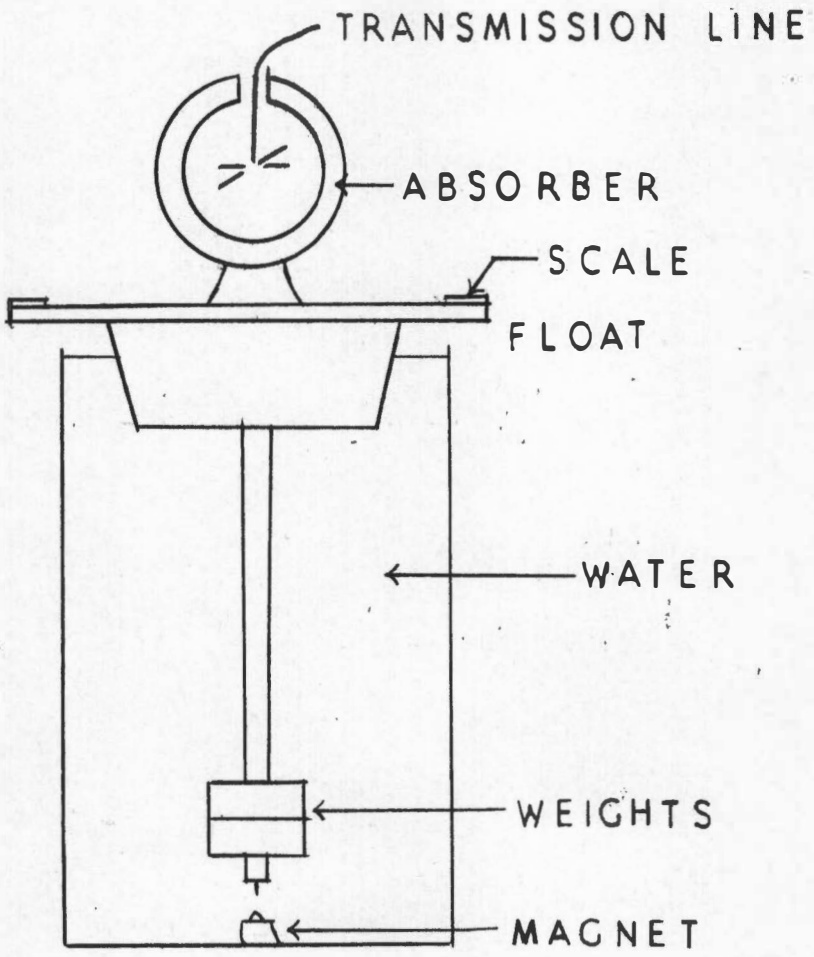

FIGURE 15

THE BASIC APPARATUS

to observe the rotational disturbances. The transmitter was then turned on. The observed angular position of the floating apparatus versus the time it plotted in Figure 16 on page 59. Also plotted is a theoretical curve of the predicted motion by the general solution to the equation

$$I \frac{d^2\theta}{dt^2} + \gamma \frac{d\theta}{dt} = \frac{P \sin\phi}{2\pi f} \qquad \text{(V.II.1)}$$

with $\frac{d\theta}{dt} = 0$ and $\theta_0 = 0$ when the transmitter was turned on. I is the moment of inertia of the floating apparatus, γ is the theoretically estimated viscous torque coefficient, P is the power radiated, ϕ is the phase angle between the dipole moments of the two half-wave dipoles, and f is the frequency of the radiation.

It may be seen that the actual rotation due to the electromagnetic waves is negligible compared to that predicted. Since experiments have been performed which have detected the angular momentum of microwave radiation, one would suspect that there are experimental difficulties present in this experiment.

As one looks at the experiment and at the factors involved in the theory, he sees that there are but few basic quantities involved. First, consider the radiation. Power meters kept in the transmission lines indicated that energy was going right up to the dipoles. At the dipoles

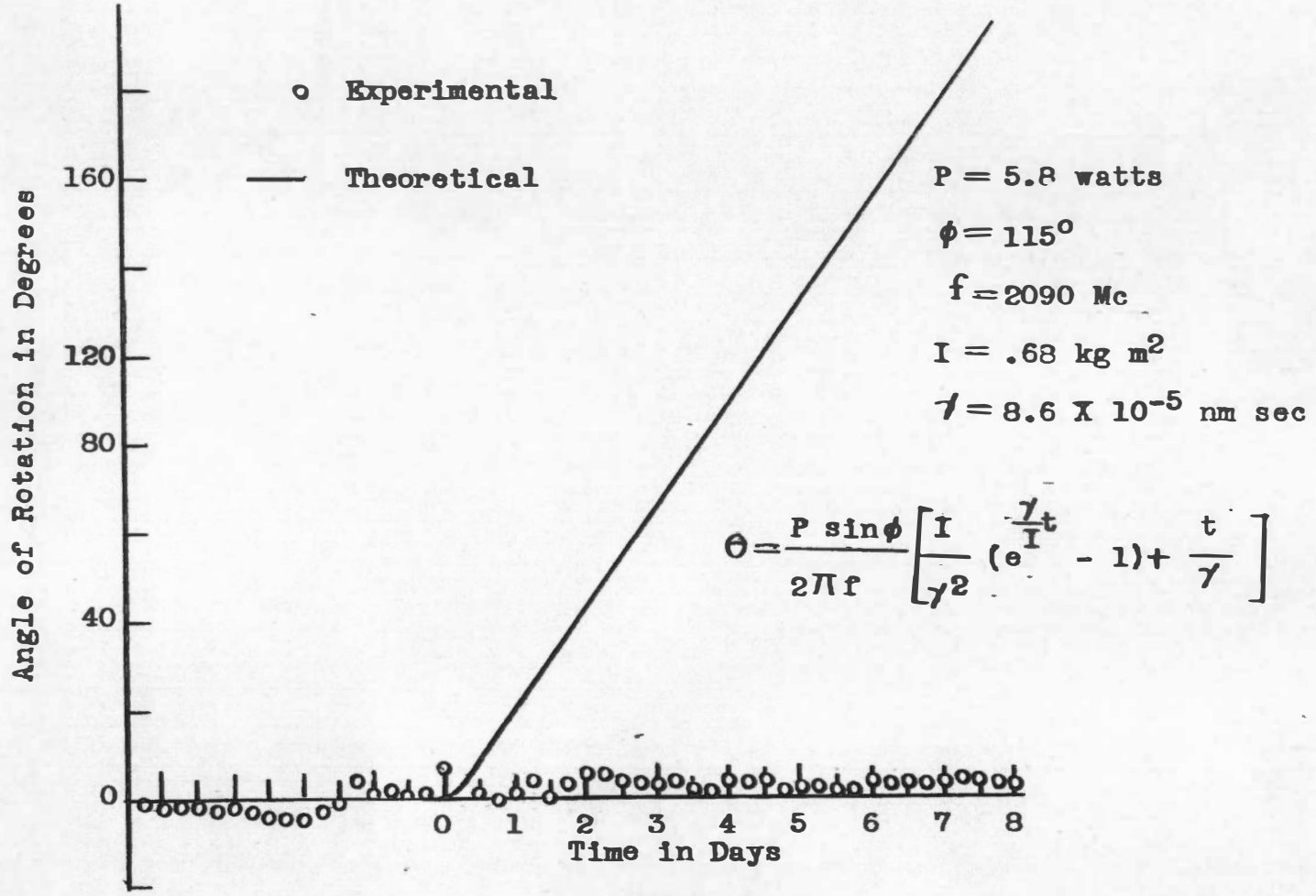

FIGURE 16

THE OBSERVED AND THEORETICAL MOTIONS OF THE FLOATING APPARATUS WITH THE TRANSMITTER OPERATING

faulty connections could have absorbed the energy, and it could have gone into heat. But, this is doubtful. Although no absolute measurement of power was made in space, there were indications that the dipoles were radiating.

Secondly, consider the absorption. The manufacturer of the absorber claims that it is ninety-five per cent efficient at the frequency used.

Finally, consider the opposing torque of the liquid in which the rotating apparatus rested. The viscosity of water should be well-known by now. But, as will be shown in Chapter VII, erratic results were obtained when trying to determine a factor in which viscosity is the main effect. This leads the author to speculate that there was some surface effect, due either to the pure water itself or impurities on the surface of the water, which was very much greater for small shearing stresses than the viscosity itself.

CHAPTER VI

APPARATUS

The experimental work has been described in general terms. In this chapter the specific pieces of equipment are described in detail.

I. THE TRANSMITTER

The Klystron Chassis and the Meter Panel

The transmitter consisted simply of a klystron which had been adjusted at the factory to the frequency at which it would deliver its maximum power. The klystron was a product of Sperry Rand Corporation, and its type number was SRL-7C. A summary of its description is given in Table I on page 147. During this experiment the operating frequency was 2,090 megacycles.

Figure 17 on page 62 shows the klystron mounted on a chassis along with its blower and controls. A schematic diagram of the klystron chassis and the meter panel is given in Figure 58 on page 149.

The electrical quantities metered were the beam voltage, the beam current, and the repeller voltage. Typical values were a beam voltage of 950 volts, a beam current of 160 milliamperes, and a repeller voltage of -680 volts. Voltages were measured with respect to the

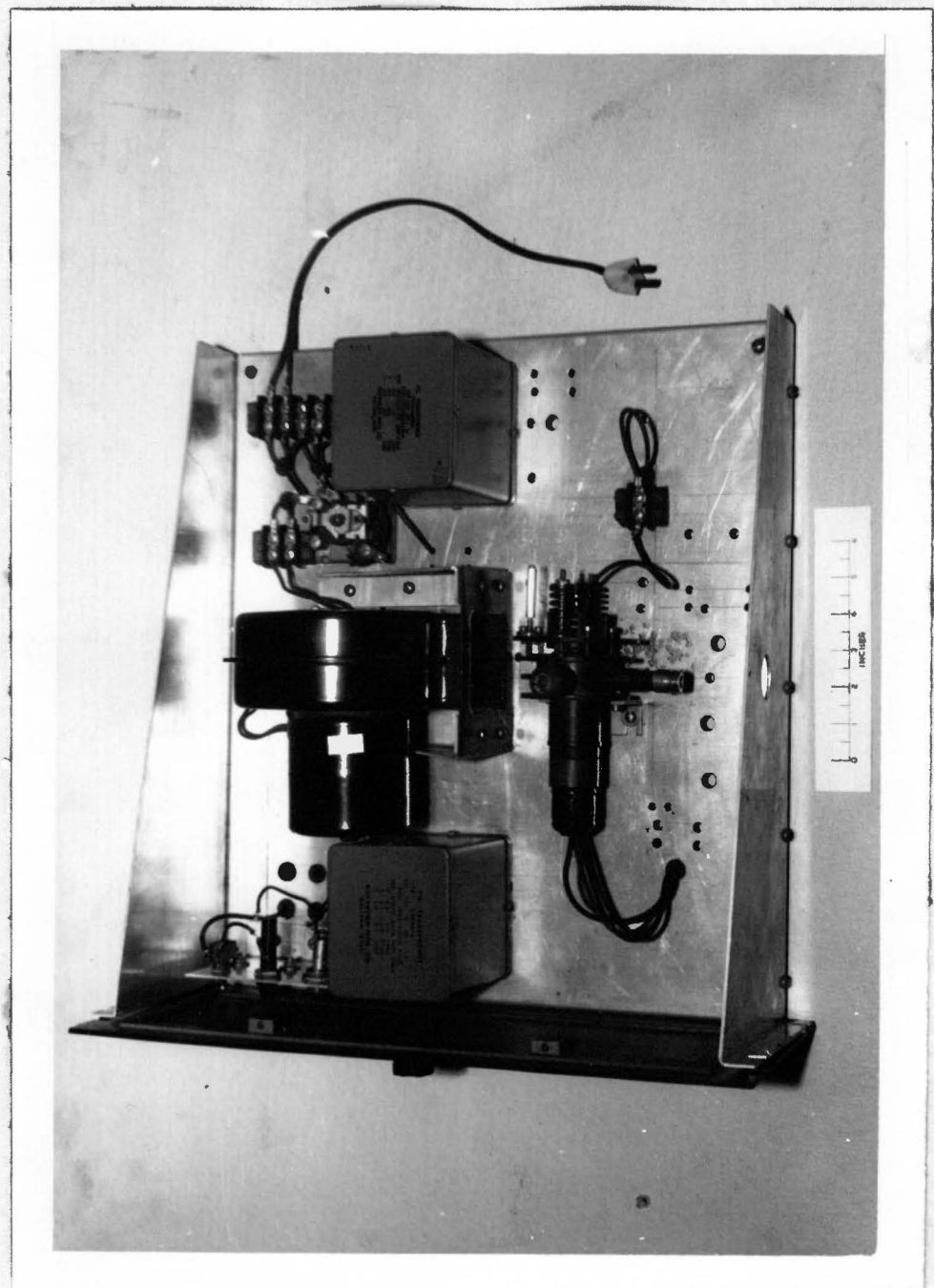

FIGURE 17

THE KLYSTRON AND ITS ASSOCIATED COMPONENTS

cathode. The specifications of the components on the chassis and meter panel are given in Table II on page 150.

The Variac Circuit

A Variac was used to control the dc output voltage of the klystron beam power supply by controlling the ac input to the primary of its plate transformer. For convenience the Variac was mounted on a standard relay rack panel with a switch, fuse, and pilot lamp. (Figure 59 on page 151 is a schematic of the circuit, and Table III on page 152 gives the specifications of the components.

The Klystron Beam Power Supply

The klystron beam power supply consists of two parts: (1) an unregulated supply and (2) an electronic regulator. Both circuits are conventional and will not be discussed in detail.

Figure 18 on page 64 shows the output dc voltage as a function of the input ac voltage and the load resistance. Figure 60 on page 153 is a schematic diagram of the unregulated supply. Table IV on page 154 gives the specifications of the components used.

The schematic diagram of the electronic regulator is shown in Figure 61 on page 155. Table V on page 156 gives the specifications of its components.

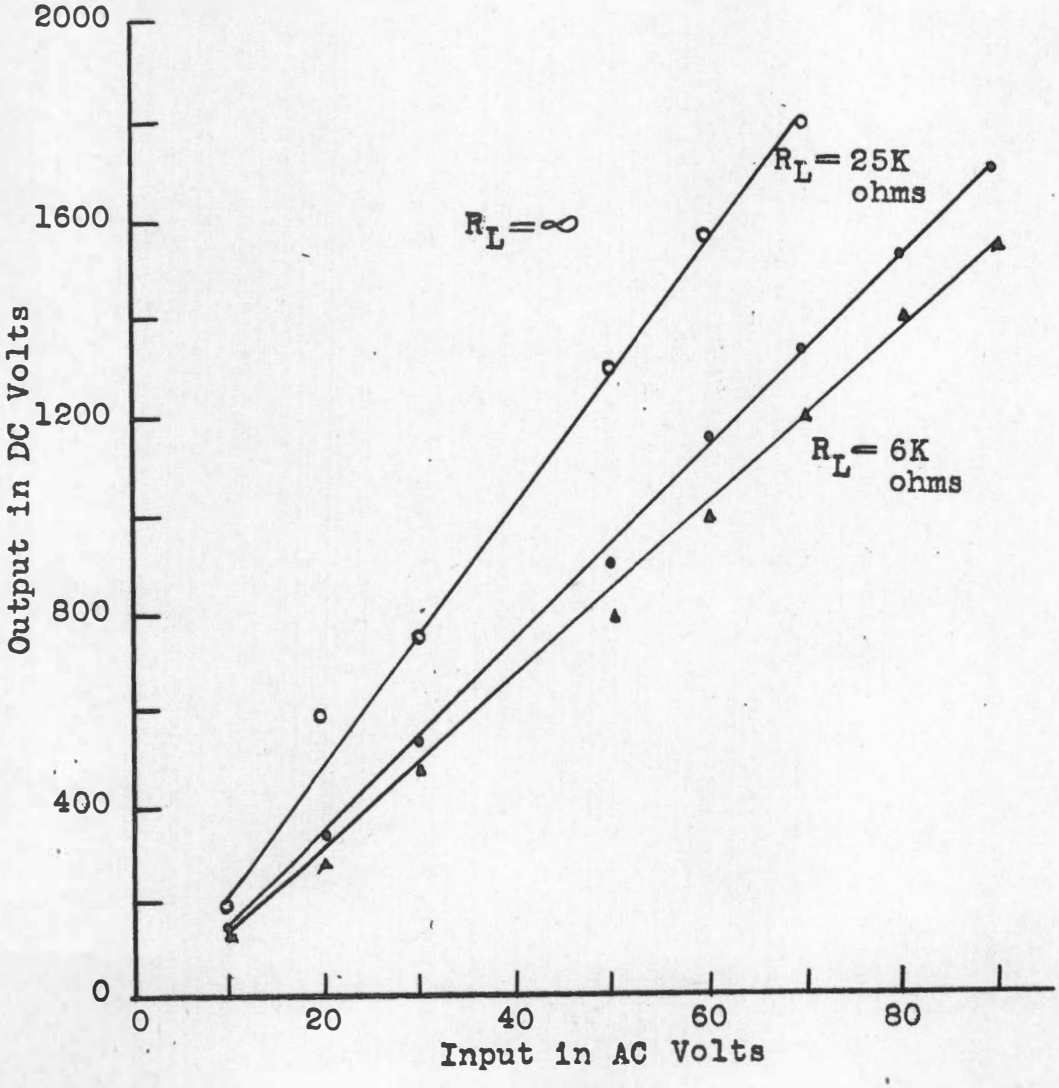

FIGURE 18

THE VARIATION OF THE OUTPUT VOLTAGE OF THE UNREGULATED POWER SUPPLY AS A FUNCTION OF THE INPUT VOLTAGE

The output voltage of the regulator as a function of the input ac voltage to the unregulated supply is shown in Figure 19 on page 66.

The Klystron Repeller Power Supply

The klystron repeller power supply is a conventional power supply with voltage regulator tubes across its output terminals. By adjusting a potentiometer across the individual voltage regulator tubes, a negative output voltage of from 450 to nine hundred volts can be obtained.

Figure 62 on page 158 is a schematic diagram of the unit, and Table VI on page 159 gives the specifications of the components. Figure 20 on page 67 shows the output dc voltage as a function of the input ac voltage.

Time Delay Circuits

The following sequence was desirable in applying ac voltages to the units in the transmitter: (1) all filaments and the klystron blower, (2) the klystron repeller supply, and (3) the beam power supply. This sequence of applications of ac to these units could be handled manually; but in the event of a power failure, it was desirable to accomplish this automatically when the power failure was remedied.

Figure 21 on page 68 shows the control circuit with the time-delay relays which were used. The time-delay

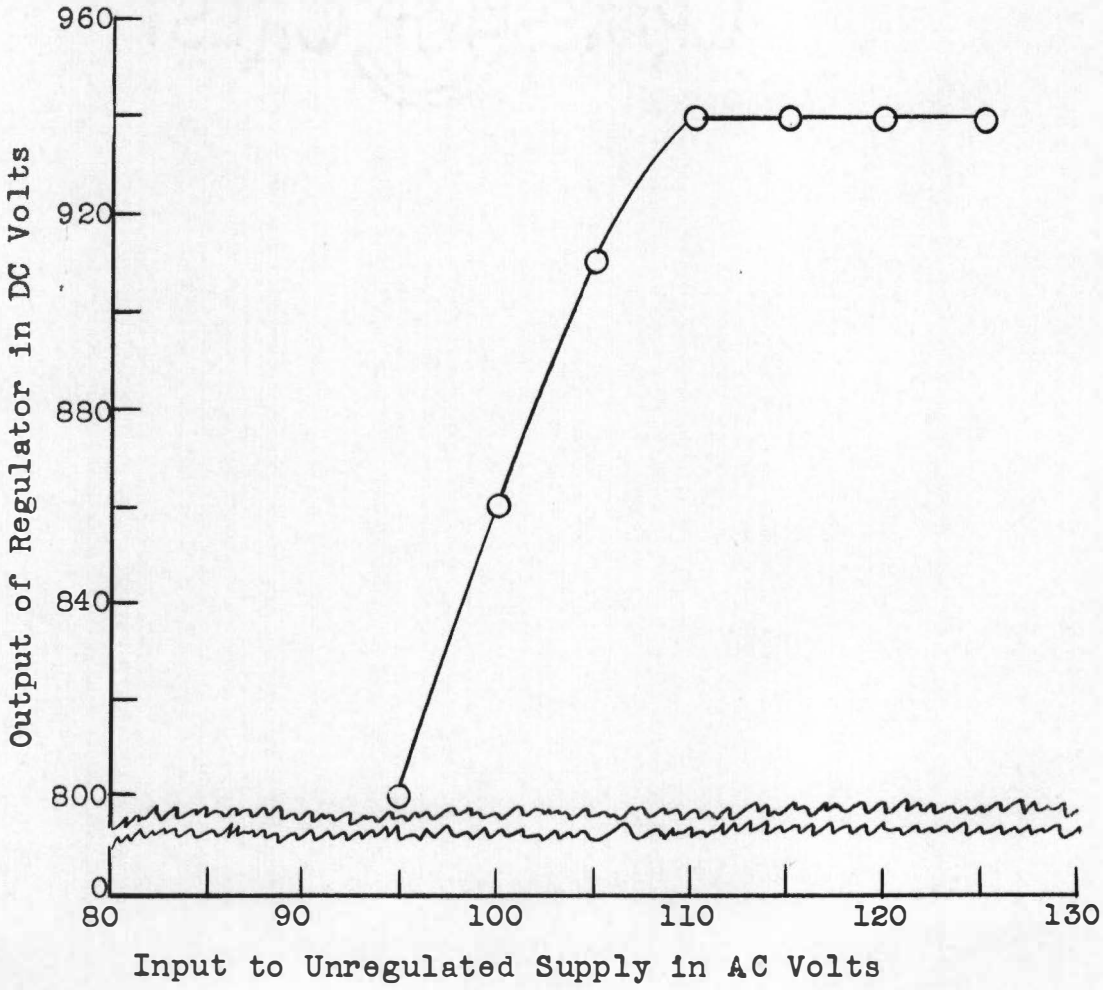

FIGURE 19

THE OUTPUT VOLTAGE OF THE REGULATOR AS
A FUNCTION OF THE INPUT VOLTAGE
TO THE UNREGULATED SUPPLY

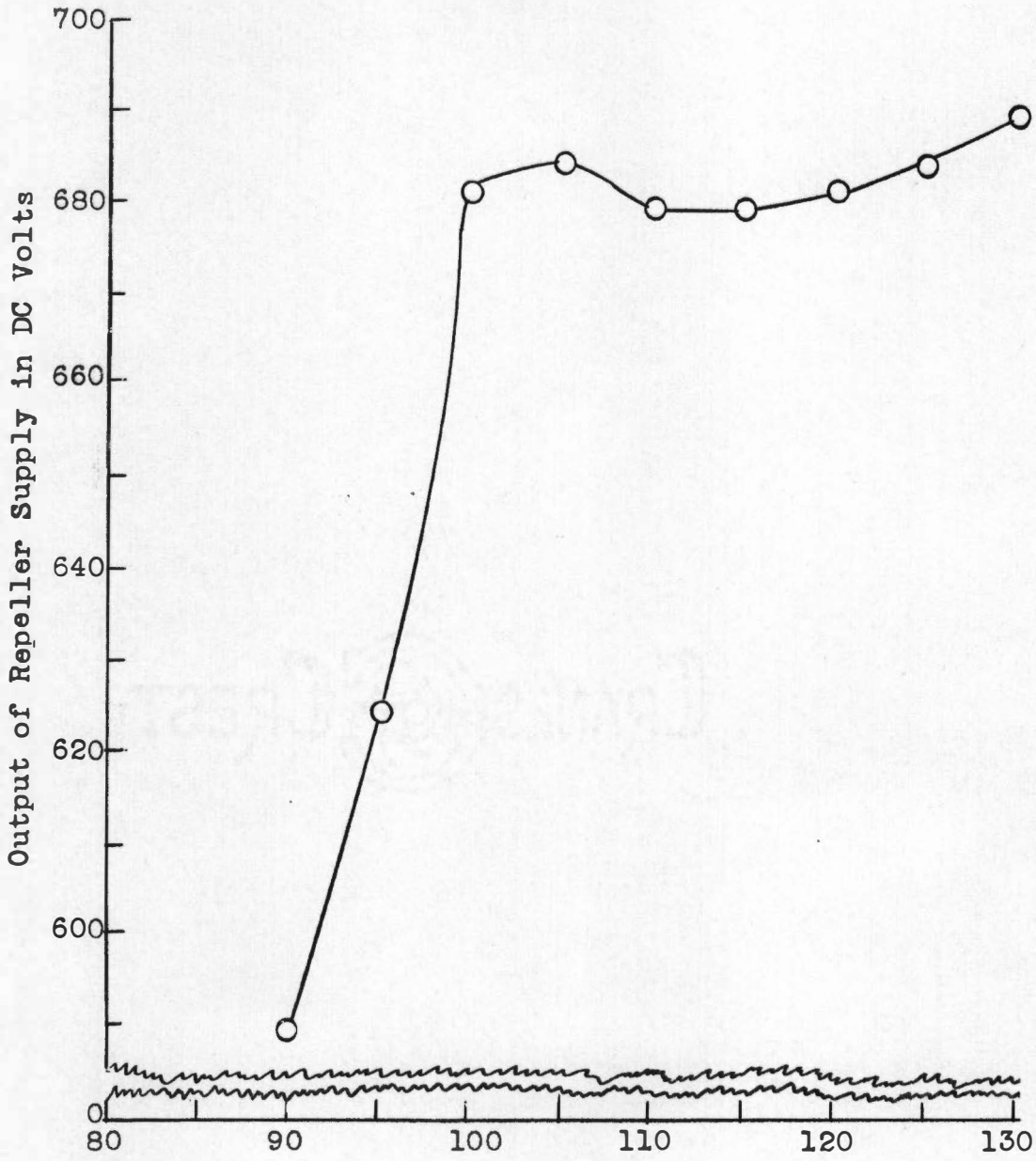

FIGURE 20

THE OUTPUT VOLTAGE OF THE REPELLER SUPPLY
AS A FUNCTION OF THE INPUT VOLTAGE

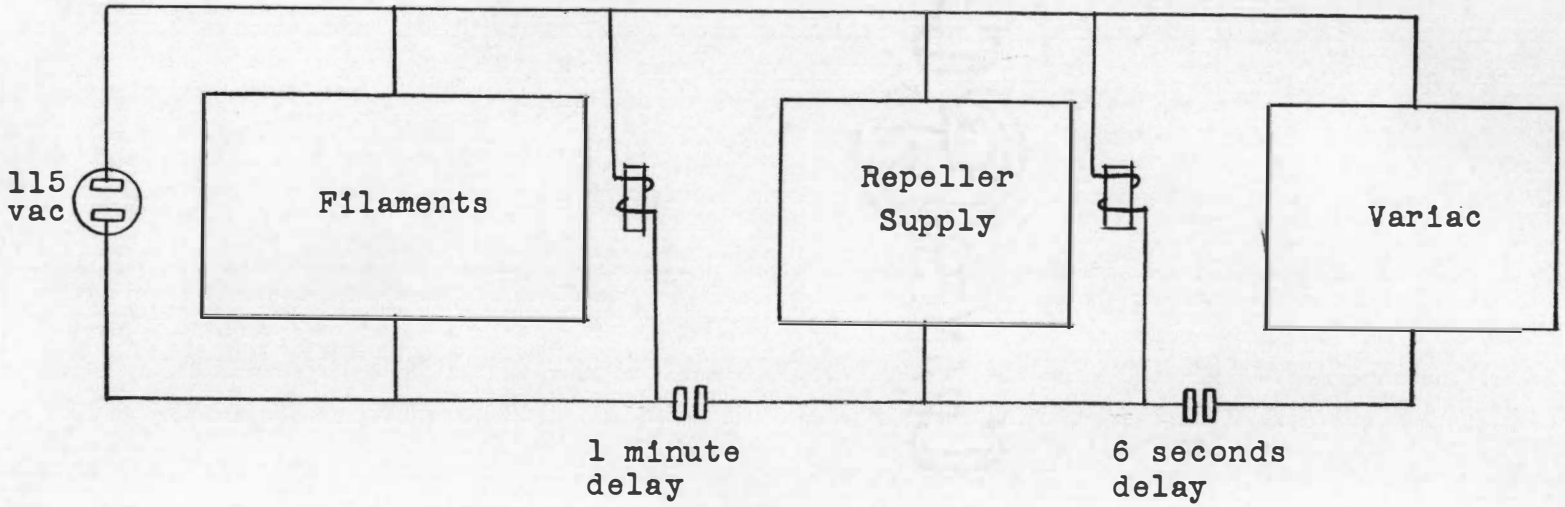

FIGURE 21

THE CONTROL CIRCUIT FOR THE TRANSMITTER

relays are Agastat Type NE-11 which can be adjusted so that their contacts close at times of from a few seconds to one and one-half minutes after their coils are energized.

The Transmitter Cabinet

The klystron and its power supplies were housed in a cabinet approximately six feet high. Figure 22 on page 70 shows this apparatus.

II. THE TRANSMISSION LINES AND ANTENNA

The Power Divider

The radio-frequency energy from the klystron was carried by RG-9A/U coaxial cable to a coaxial device known as a power divider which has one input and two output connections. Some of the total energy fed into its input comes out of each output. A Microlab Type DS-3000 power divider was used.

The Transmission Lines in General

Two transmission lines carried the energy from the power divider to two half-wave dipoles which were mutually perpendicular. By making one line longer than the other it is possible to cause a wave in it to arrive at its dipole later than the wave at the other dipole thus feeding the two dipoles out of phase. This phase difference determines the type of polarization of the emitted radiation.

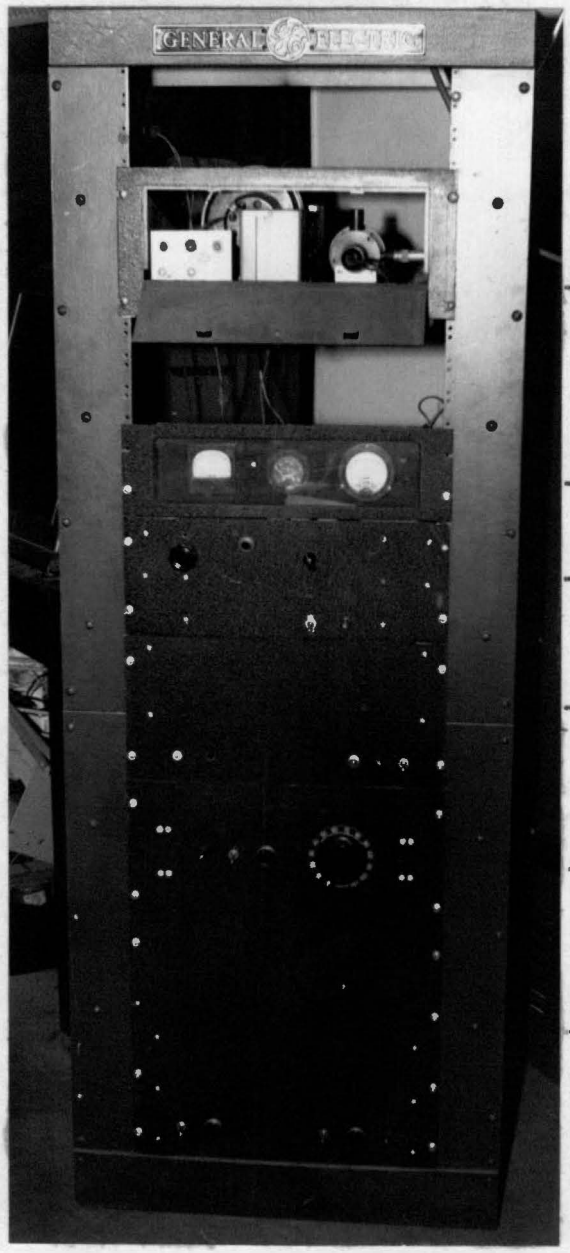

FIGURE 22

THE TRANSMITTER

Two sizes of coaxial cable were used. For transferring power with small losses RG-9A/U coaxial cable was used with Type N UG-21B/U male connectors and UG-23B/U female connectors. Small cable was needed to lead directly to the dipoles inside the absorbing spherical shell, so RG-58A/U coaxial cable was used. Short lengths were used because losses are higher in this type cable.

The Attenuators

An attenuator with an attenuation of one decibel was used in each of the two transmission lines to limit the power to a value within the range of the power meters used. Each attenuator was a Microlab Type AA-01N.

The Phase Shifters

The phase shifters were simply different lengths of RG-9A/U cable with Type N connectors on their ends. These were the portions of the two transmission lines which were made of unequal length to change the phase difference between the dipoles.

The Power Meters

The power to each dipole was measured by a Model 722N radio-frequency power meter manufactured by the M. C. Jones Electronics Company, Incorporated. These meters remain in the circuit as energy is fed through them.

The Single Stub Tuner

The Microlab Type SS-1000 single stub tuner was used to match the impedance of each small coaxial cable with its dipole to the remainder of the transmission line.

The Dipoles

The two dipoles were made of brass rod with a diameter of one-sixteenth of an inch. Each was made approximately one-half wavelength long. The dipoles and their small feed lines were attached to a wooden dowel. Figure 23 on page 73 shows the dipoles with their small coaxial cables, and Figure 24 on page 74 shows the dipoles themselves with the connections made to the cables.

Figure 25 on page 75 is a diagram of the entire antenna system.

III. THE ABSORBER AND HOUSING

The Absorbing Spherical Shell and the Float Assembly

The absorbing spherical shell consists of two thin, rigid hemispherical radomes lined with a flexible absorber. The radomes are one foot in diameter with a flange three-eighths of an inch wide around their peripheries such that the two can be fastened together easily. The absorber itself is Eccosorb Type AN 75 manufactured by Emerson and Cuming, Incorporated. This material is one inch thick,

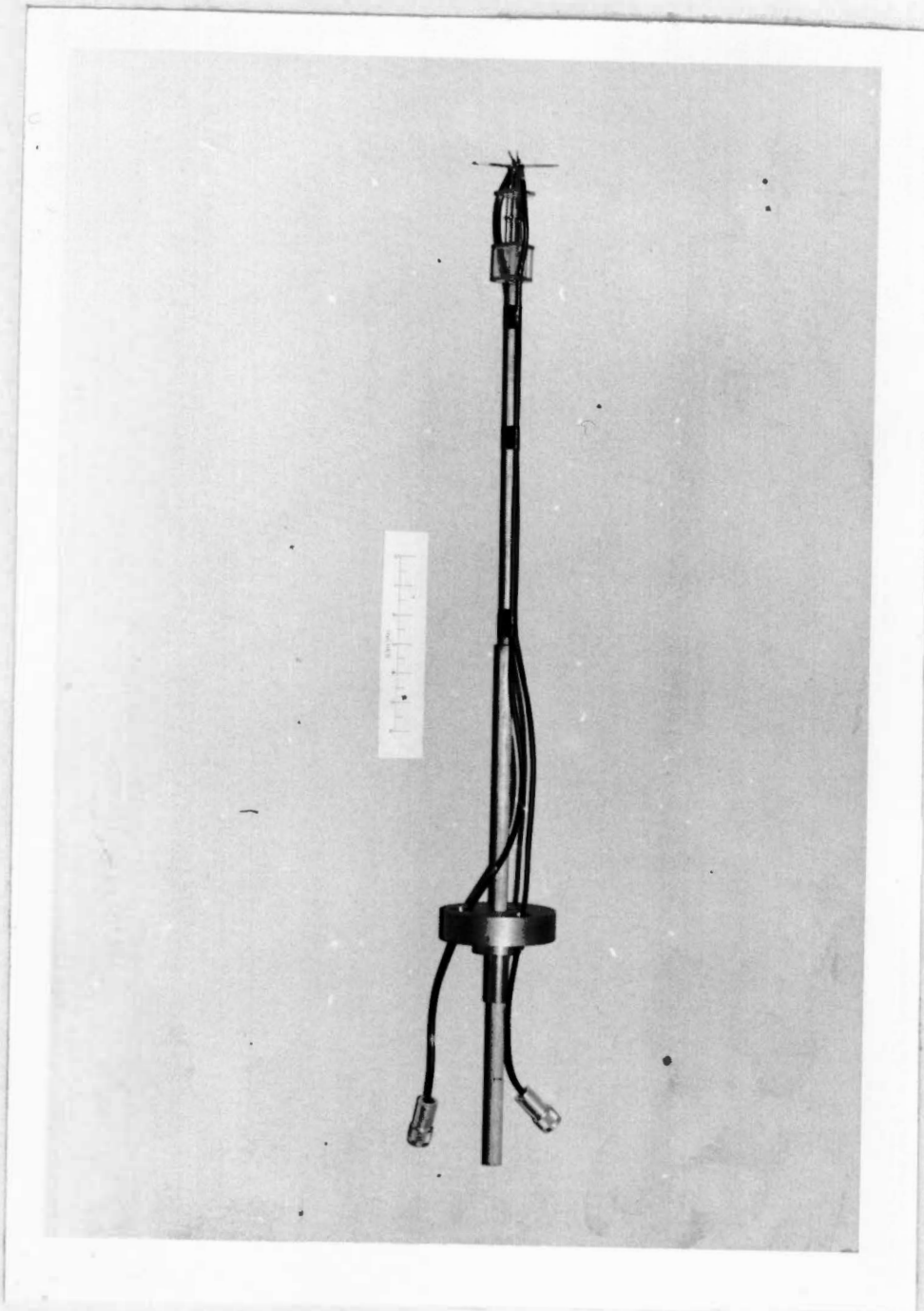

FIGURE 23

THE DIPOLES WITH SMALL TRANSMISSION LINES

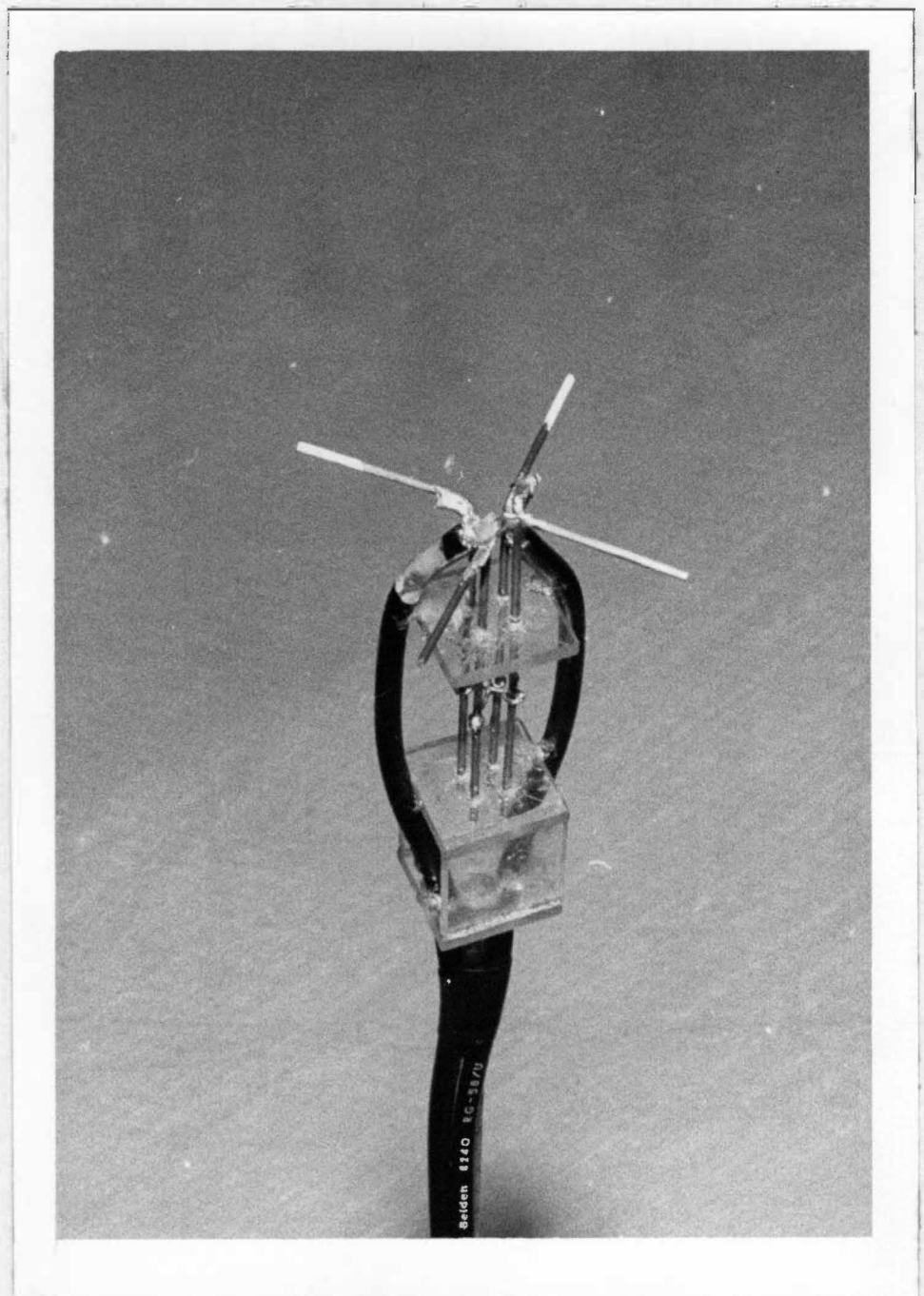

FIGURE 24

THE DIPOLES

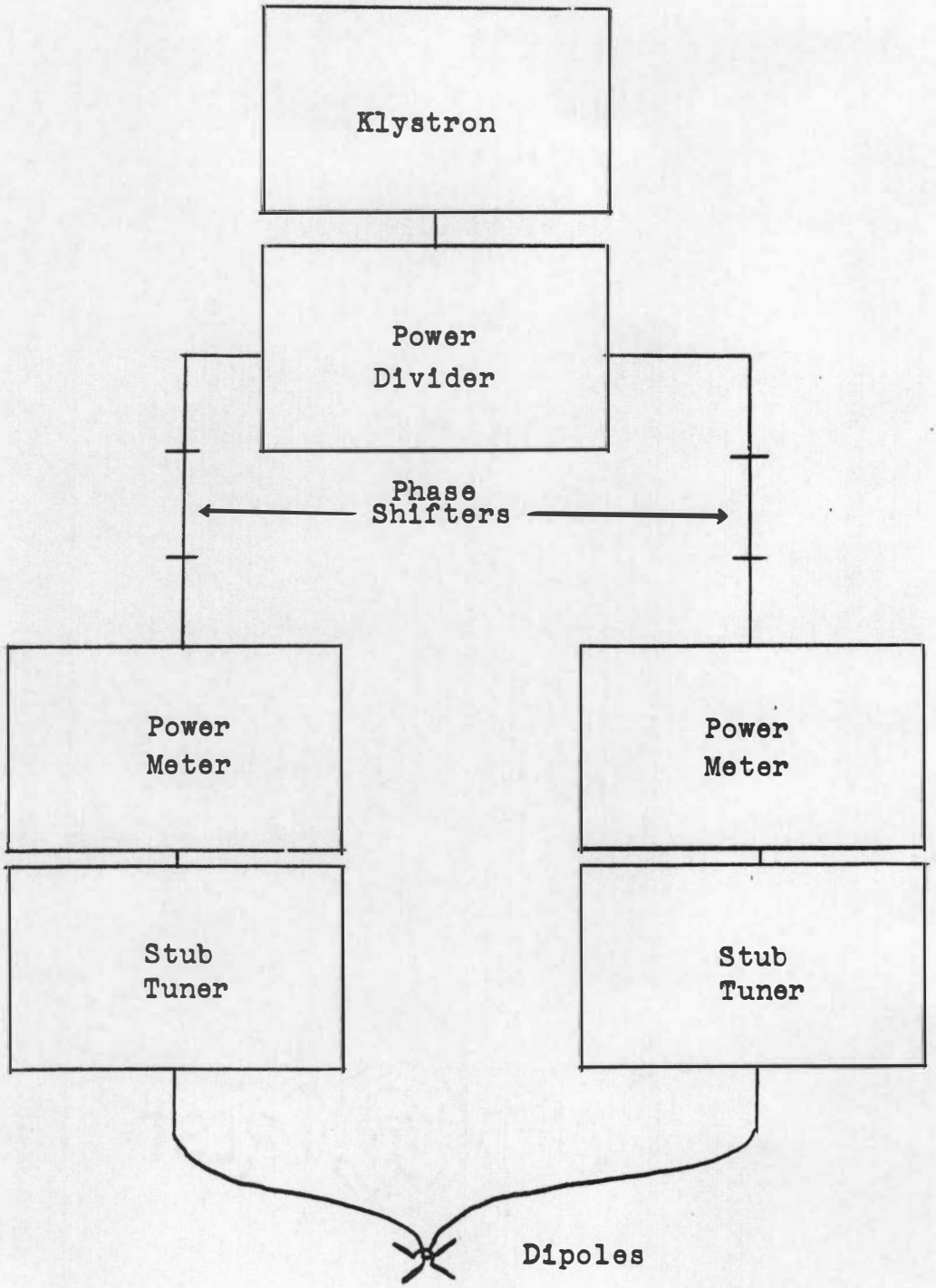

FIGURE 25

THE TRANSMISSION LINES

and the manufacturer claims an absorbing efficiency of approximately ninety-five per cent for radiation incident normally to its surface. The inside of one of the hemispheres is shown in Figure 26 on page 77.

The sphere was mounted on top of and in the center of a piece of plywood of circular shape. The plywood is three-fourths of an inch thick, and the circle has a diameter of two feet. A scale marked every ten minutes of angle was placed on the outer edge of the plywood. The sphere, its holder, and the scale may be seen in Figure 27 on page 78.

A hollow float was placed under the plywood circle. To make the assembly stable while floating, an aluminum rod with brass weights at the bottom was used. A steel needle in the end of the rod was attracted by a magnet mounted in the bottom of the water tank and kept the assembly centered in the tank. Figure 28 on page 79 shows the sphere and float assembly. Every part that touched water was coated with plastic.

The Water Tank

The water in which the sphere and its support floated was contained in a fifty-five gallon oil drum. It was coated on the inside with a Fibromid polyester resin to prevent rusting. Centered in the bottom of the tank was

FIGURE 26

A HEMISPHERICAL ABSORBER

FIGURE 27

THE SPHERE AND SCALE

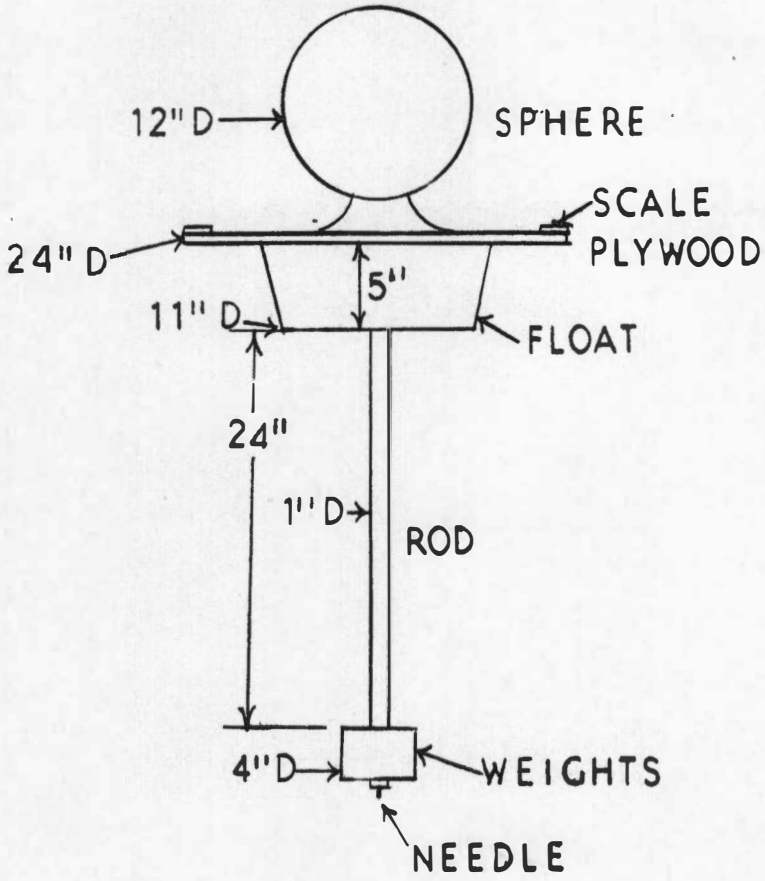

FIGURE 28

THE SPHERE AND FLOAT ASSEMBLY

a magnet. Approximately three inches of concrete was poured in the bottom of the tank to make it rigid.

The Evaporation Problem

Since some of the water evaporated during an experimental trial, it was necessary to replace this water to keep the sphere floating at the same level. This was done by allowing water to flow into the tank when the water level fell below some predetermined level. A picture of the arrangement is shown in Figure 29 on page 81.

The Housing

The details of the housing of the floating equipment are shown in Figure 30 on page 82.

The automobile tires and springs were to isolate the equipment from building vibrations. The cans of mineral oil under the legs afforded a small amount of viscous damping.

The floating apparatus may be seen in Figure 31 on page 83 in which the camera rack and light-baffles have been removed.

The Fiber-Drive Mechanism

The fiber-drive mechanism consists of a motor with its shaft connected to a Millen #1000 right angle reduction gear. The output shaft to which a fiber can be attached

FIGURE 29

THE WATER SUPPLY TO REPLENISH EVAPORATION LOSSES.

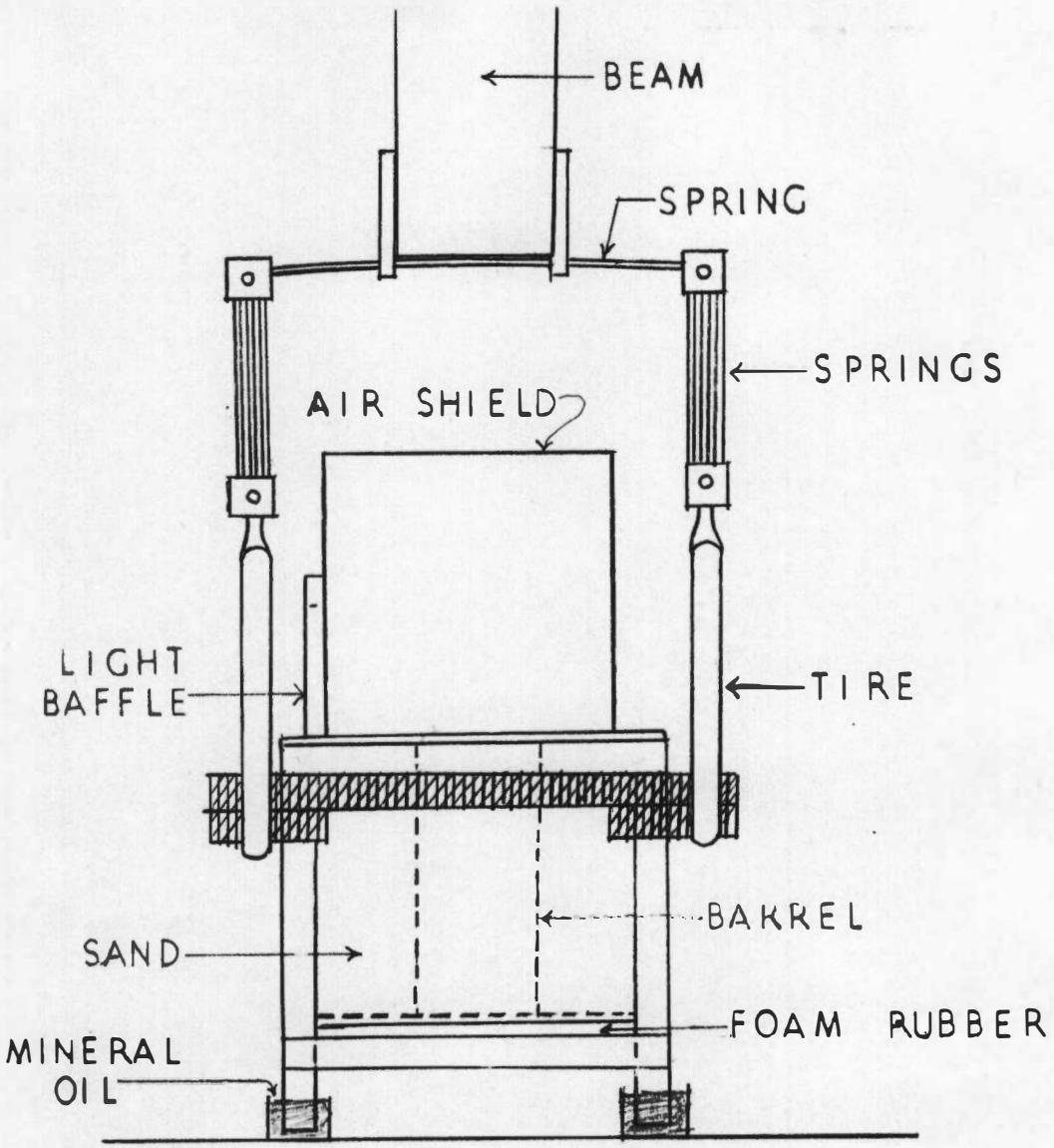

FIGURE 30

THE SUSPENDED HOUSING

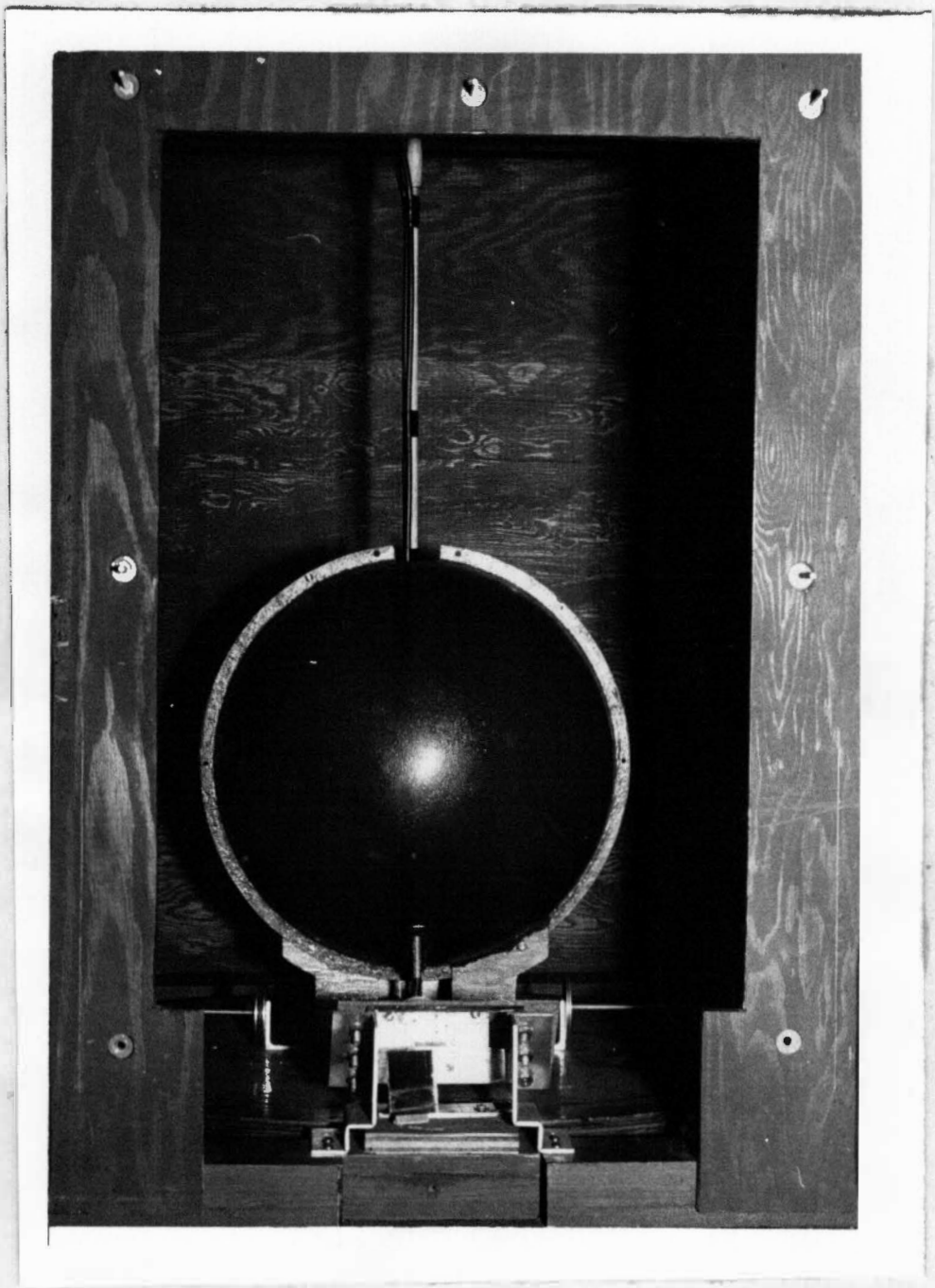

FIGURE 31

THE FLOATING APPARATUS AS SEEN WITH LIGHT BAFFLES REMOVED

turns at a rate of one revolution every sixteen days. Figure 32 on page 85 is a photograph of the unit.

IV. THE DATA RECORDING APPARATUS

Introduction

The data were photographed periodically. Figure 33 on page 86 is a picture of the camera rack with the front door of the camera compartment open.

The Timer

The purpose of the timer was to provide a momentary low resistance periodically which energized the power supply for the motor of a camera. For this research, time intervals of fifteen minutes, one hour, and three hours were used. The low resistance supplied to an external circuit is just the resistance of the contacts of a switch and wire leads. When the switch is not closed, the output resistance is very high.

Figure 63 on page 160 is a schematic diagram, and Figure 34 on page 87 is a top view of the timer. It consists of a motor with a wheel attached to its shaft. Protruding from the edge of the wheel is a short segment of a screw. As the wheel rotates, it brings the screw into contact with a lever on a microswitch S_2, and at some

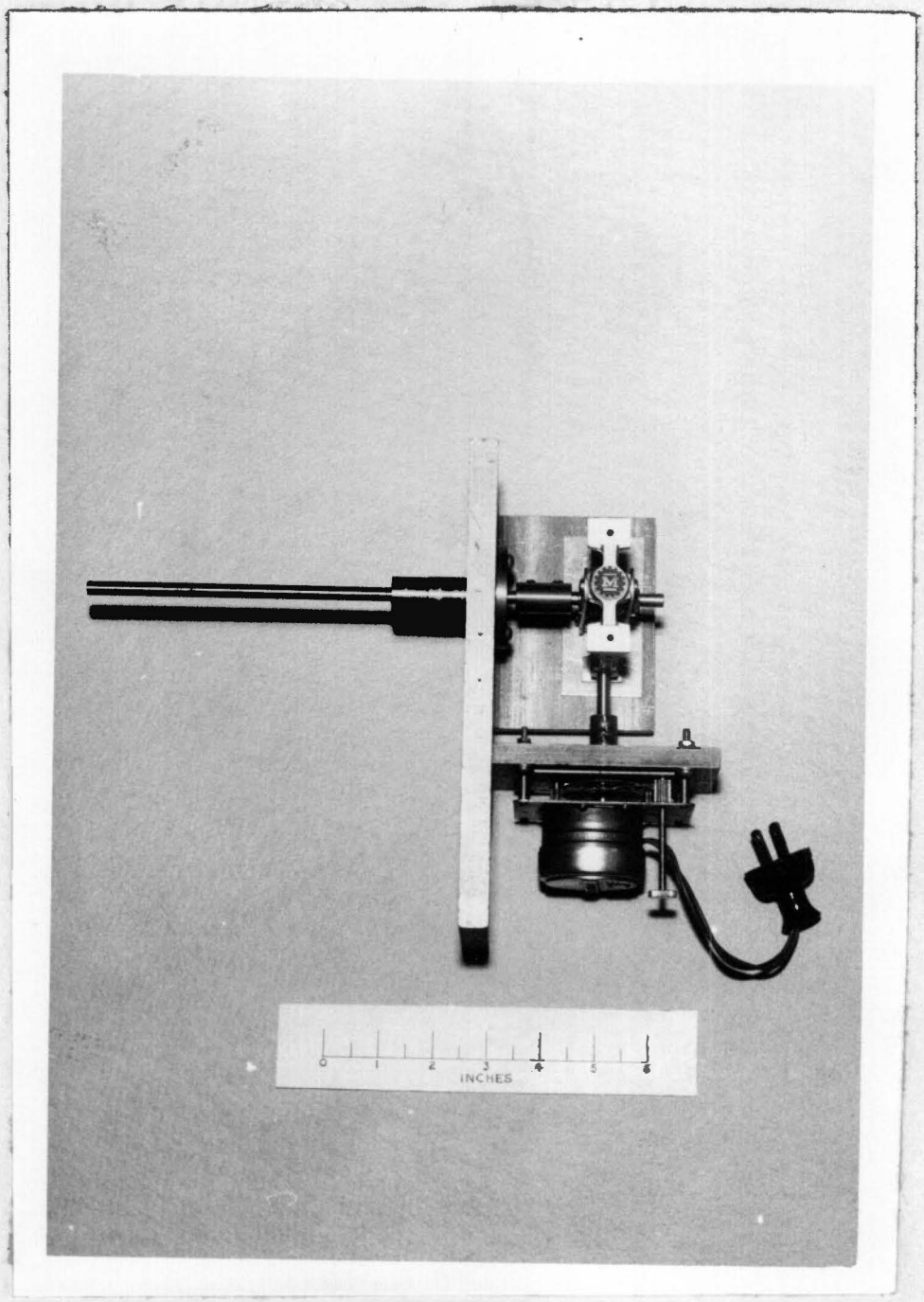

FIGURE 32

THE FIBER-DRIVE MECHANISM

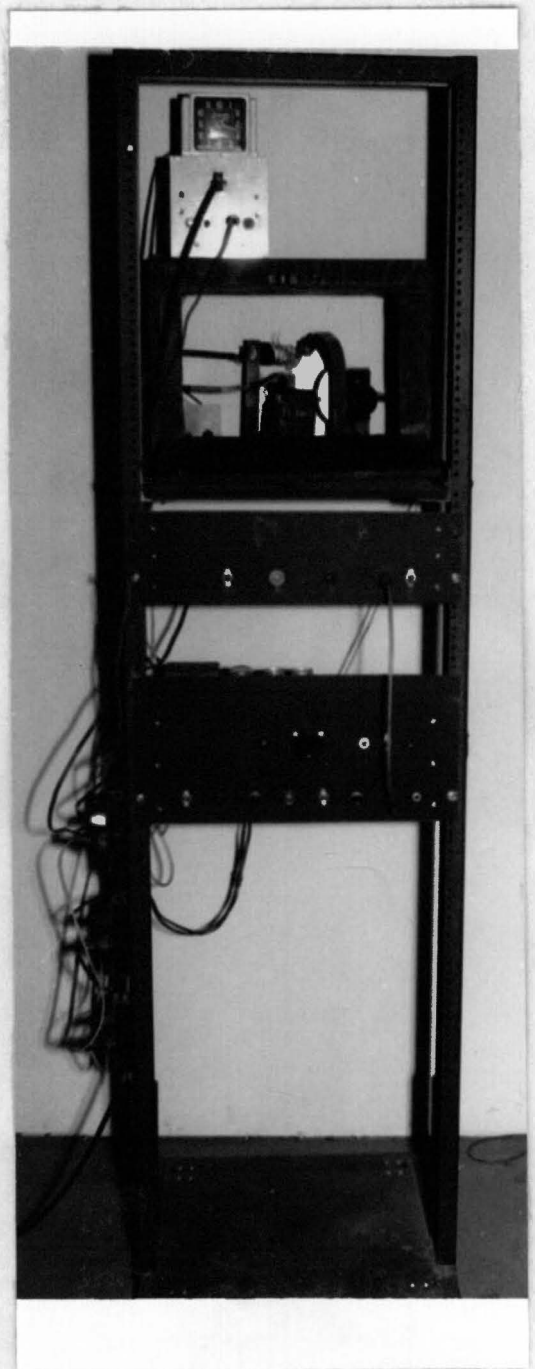

FIGURE 33

THE PHOTOGRAPHIC EQUIPMENT RACK

FIGURE 34

THE TIMER

instant the microswitch is actuated. The period of rotation was changed by changing motors.

The motors are rated at 115 volts ac and monitored by the front panel controls and indicators S_1, F_1, and PL_1.

The microswitch is indicated in Figure 63 on page 160 by S_2. Another switch S_3 is in series with the microswitch so that the motor can run continuously without actuating the microswitch if this is desired. Table VII on page 161 gives the specifications of the electrical components.

The Camera Power Supply

When the input terminals of the camera power supply are momentarily shorted (automatically by the timer or manually by a switch), power is furnished to the camera motor until a pair of contacts on the armature shaft of the motor is closed after one complete revolution of the shaft. During this one revolution one frame of film is exposed.

Using the contacts on the armature shaft to sense the position of the shaft affords a positive control over the position of the camera shutter at the end of one exposure. This allows economical use of the film since one obtains one, and only one, frame of exposed film per pulse of power. One can not apply a burst of power to the motor and allow it to run freely without making the burst long enough to get at least one frame. This usually leaves

the shutter open or results in the exposure of two or three frames of film.

A block diagram of the camera power supply is shown in Figure 35 on page 91. The general operation may be understood by starting with the input from the timer on the block diagram.

The switch in the timer discharges a capacitor in the pulse-forming network. The resulting negative pulse is amplified and inverted by an amplifier with vacuum tube V_1 in it.

The output of tube V_1 is connected to a second amplifier which has two inputs. A pulse to either of these inputs (grids of V_2) produces an output pulse which is fed to a scale-of-two circuit.

A scale-of-two circuit has two stable states. It changes states when a pulse is placed to its input. A pulse marked "on" on the block diagram changes the state of the scale-of-two circuit such that the next stage, the relay control tube V_5, is caused to conduct.

When the relay control tube conducts, the plate current exists in the relay and causes its contacts to close. These contacts are in a thyratron circuit which furnishes the motor current.

Upon being supplied with current, the motor armature rotates until contacts on the armature shaft close.

Electrical connections to these contacts come back into the camera power supply, and the closing of these contacts generates a pulse. After being reversed in polarity by V_7, the resulting pulse triggers a univibrator circuit.

A univibrator circuit generates uniform pulses of controlled length relatively independent of the shape of the input pulse. The output of the univibrator is fed into the second input of the dual-input amplifier. This pulse is marked "off" on the block diagram. Again, there is an output pulse from this amplifier which causes the scale-of-two circuit to revert to its original state. As a result the relay control tube ceases conducting, the relay contacts open, and the motor stops.

There is an additional input jack on the front panel of this unit so that negative pulses from a pulser can be fed into the amplifier tube V_1 to actuate some of the circuits. This affords a convenient means of testing the stages containing tubes V_1, V_2, V_3, V_4, and V_5.

Schematic diagrams are shown in Figures 64 and 65 on pages 162 and 163, respectively. The components are listed in Table VIII on page 164.

The Camera

A sixteen millimeter camera was used to photograph the equipment from which data were obtained. It is a modified Army surplus gun sight aiming point camera.

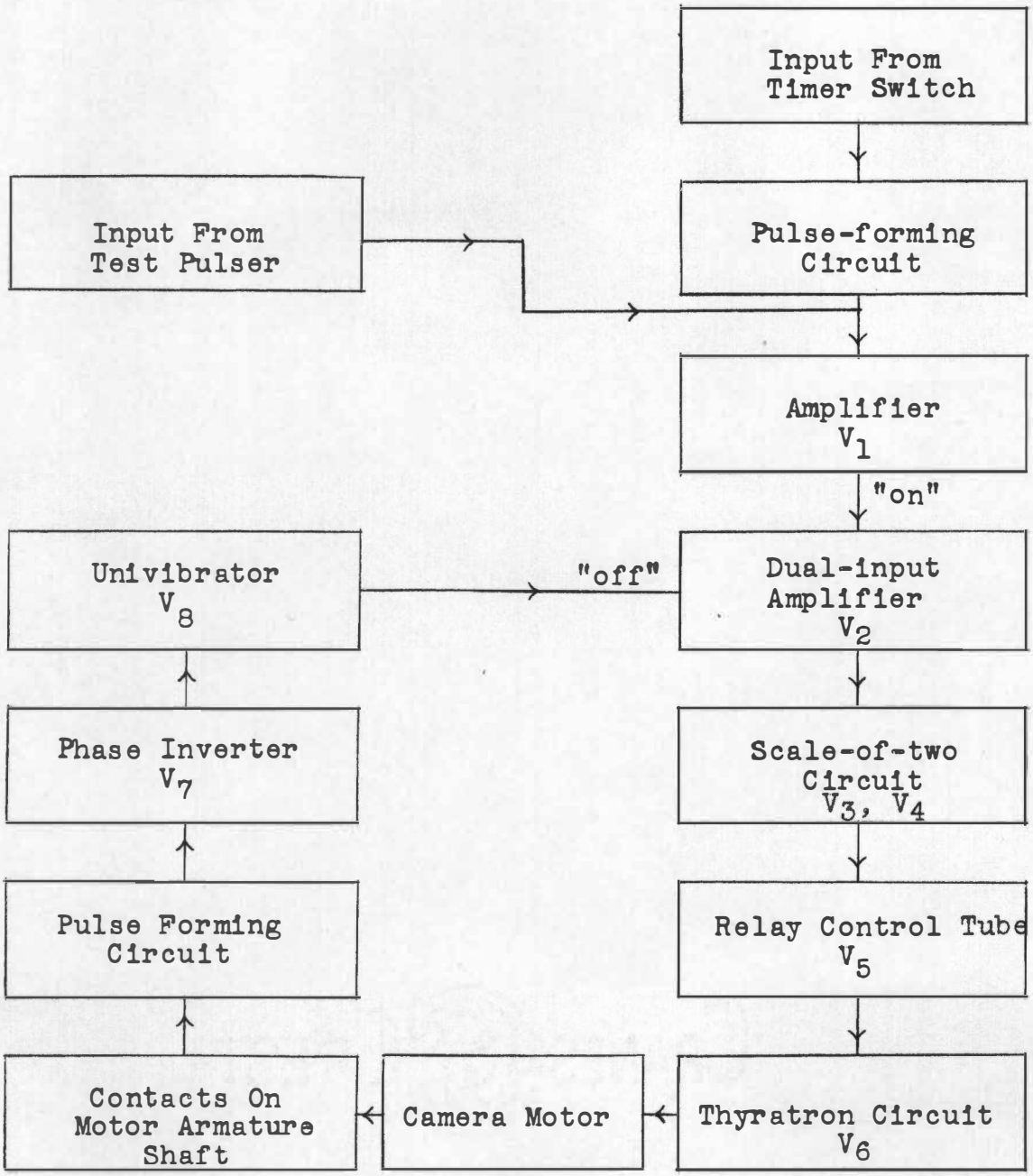

FIGURE 35

THE CAMERA POWER SUPPLY

Optically it was modified by moving the lens out from the body of the camera with a metal spacer so that it focussed at a distance of about six inches.

Mechanically it was modified by adding a brake.

Two contacts insulated from the body of the camera were added. One is a flash synchronization contact; the other is a contact to cause the power to the motor to switch off. The latter has been mentioned in connection with the camera power supply.

Figure 36 on page 93 shows the camera as modified.

The Flash Unit

Light to take the picture was provided by an electronic flash unit. Figure 66 on page 170 is a schematic diagram of the unit, and Table IX on page 171 gives the specifications of its components. The flash bulb was covered by aluminum foil which had a hole in it with a diameter of about one-half inch to emit sufficient light for illumination of the scale and a clock face.

The Clock

The clock consists of a motor with a circular scale attached to its shaft. The scale is numbered from one to sixteen around its edge. At least one of the numbers appeared in each photograph taken indicating the time at which the picture was taken. The clock face made one

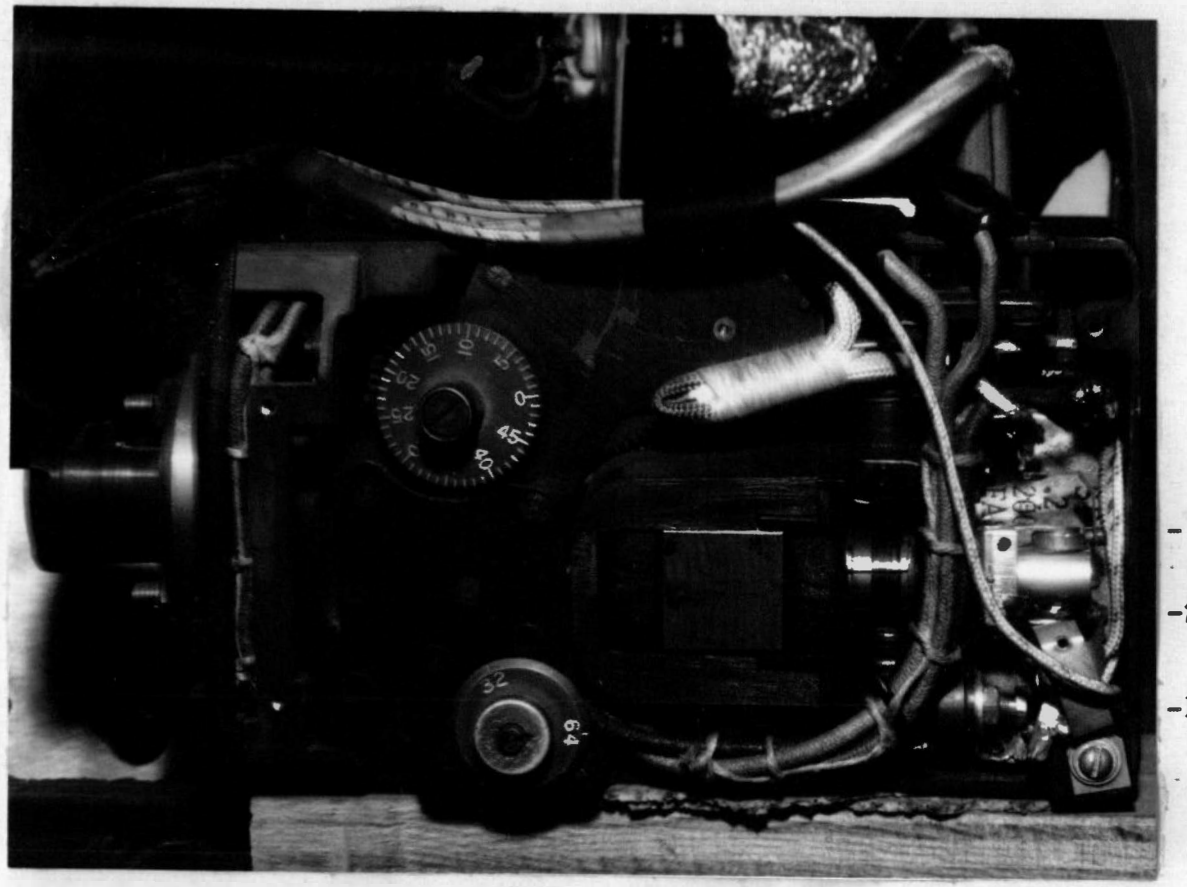

FIGURE 36

THE CAMERA

complete revolution every four hours. This clock may be seen in Figure 37 on page 96.

Optical Alignment

Figure 38 on page 97 is a diagram of the relative position of the elements required for recording the data.

Photography

Sixteen millimeter Kodak Plus-X negative-type film was used. It was purchased in one-hundred foot rolls and loaded in shorter lengths into metal magazines of the camera. It was possible to get thirty-six frames of data on one foot of film.

The film was developed in a Morse G-3 developing tank. The developer was prepared by dissolving four small packages of Kodak Microdol-X developer in one quart of water. Each package is ordinarily recommended for four ounces of solution.

The film was developed for one-half hour with an initial temperature of sixty-five degrees Fahrenheit. After rinsing with water, the film was placed in a fixer for twenty minutes. The fixer was prepared by dissolving seven tablespoons of Kodak Acid Fixer per quart of water. The film was then rinsed in water for twenty minutes and dried.

The negatives were placed in a Recordak microfilm reader, and the data recorded from the image on the machine.

Figure 39 on page 98 is a photograph made directly from the negative of one frame of data.

FIGURE 37

A REAR VIEW OF THE PHOTOGRAPHIC EQUIPMENT

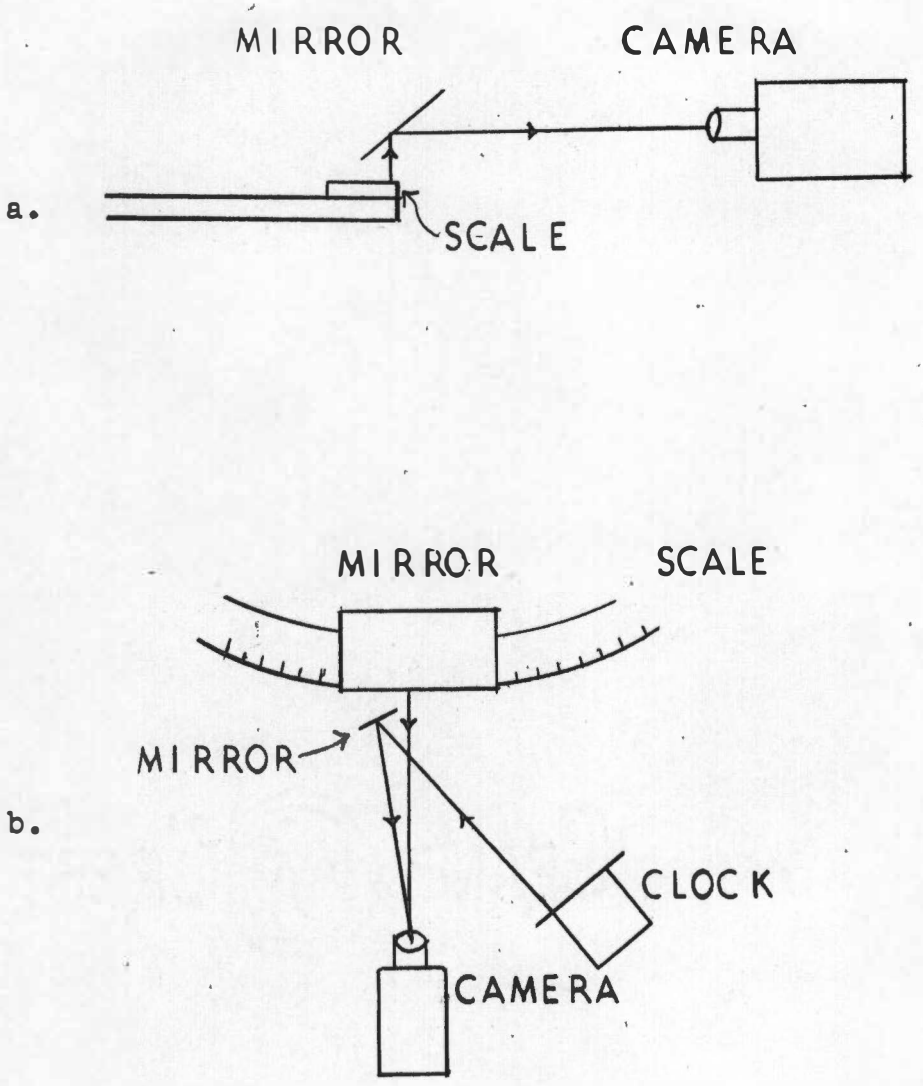

FIGURE 38

(a) AND (b), THE OPTICAL ALIGNMENT

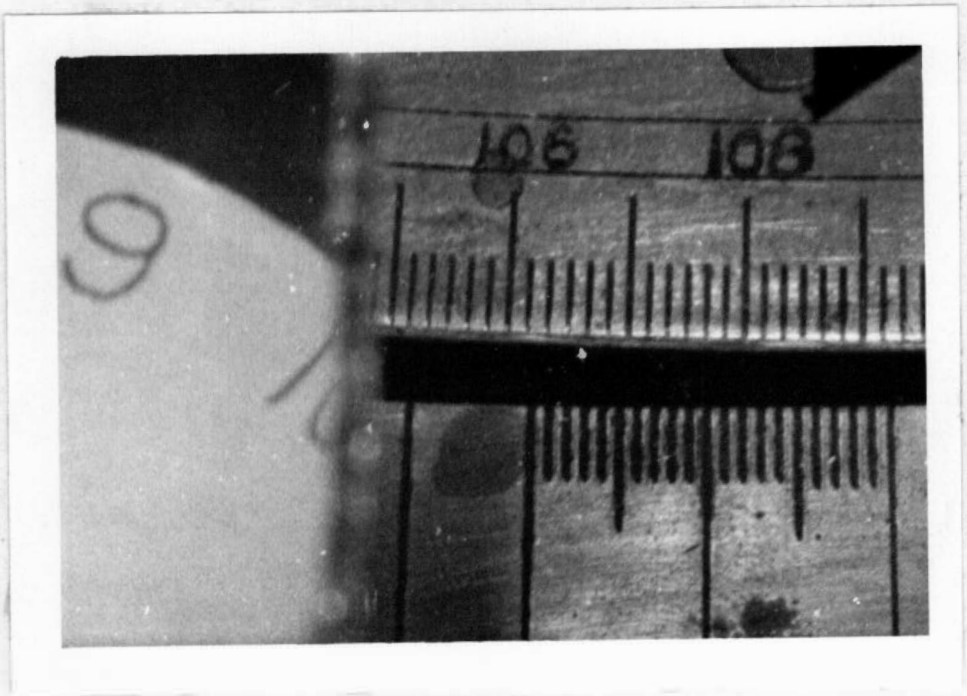

FIGURE 39

AN ENLARGEMENT OF AN 8mm X 16mm
NEGATIVE OF ONE FRAME OF DATA

CHAPTER VII

SPECIFIC MEASUREMENTS AND ANALYSIS OF DATA

Different sections of the apparatus required specific techniques and measurements peculiar to them. The major measurements are discussed in this chapter. Minor or routine measurements such as those made concerning power supplies are omitted, for the results have been presented in graphical form in Chapter VI.

I. ELECTRICAL MEASUREMENTS

The Slotted Line

A slotted line is a length of air-dielectric coaxial cable with a slot in the outer conductor so that a probe may be placed between the two conductors to sample the electric field. It is desirable that there be very little energy loss in this slotted line.

Figure 40 on page 100 shows a cross-section of a probe in between the two conductors. This represents the simplest situation. Actual instruments usually have more elaborate coupling arrangements.

The probe capacitively couples a small amount of energy from the region in which it is located to a circuit external to the slotted line. If the energy coupled with

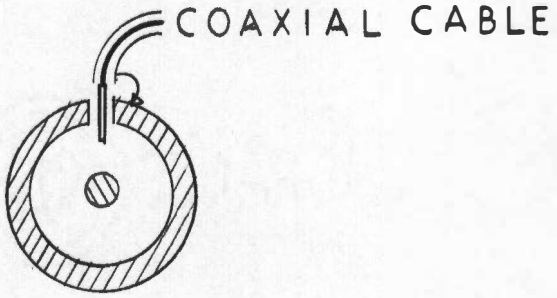

FIGURE 40

A PROBE BETWEEN THE CONDUCTORS
OF A COAXIAL CABLE

sufficient detection for a given measurement is small, the disturbance of the fields due to the presence of the probe is small.

The potential of the probe is proportional to the electric field intensity existing between the two conductors of the line at the probe position. This probe voltage was applied to an external circuit which consisted of a built-in crystal detector and a microammeter. Figure 41 on page 102 shows the General Radio Type 874-LBA slotted line which was used in making radio frequency measurements.

If one connects a source to one end of the lossless slotted line and a resistive load to the other such that all the energy is absorbed, then the root-mean-square of the voltage along the line is a constant. This is represented schematically in Figure 42 on page 103.

If, however, there is an impedance connected to the output of such a line which does not absorb all of the incident energy, waves will be reflected back up to the line. The incident and reflected waves will add so that the voltage along the line varies as shown in Figure 43 on page 104.

This voltage pattern is constant in position along the line. The voltage standing wave ratio is defined as

$$VSWR = \frac{E_{max}}{E_{min}} . \qquad \text{(VII.I.1)}$$

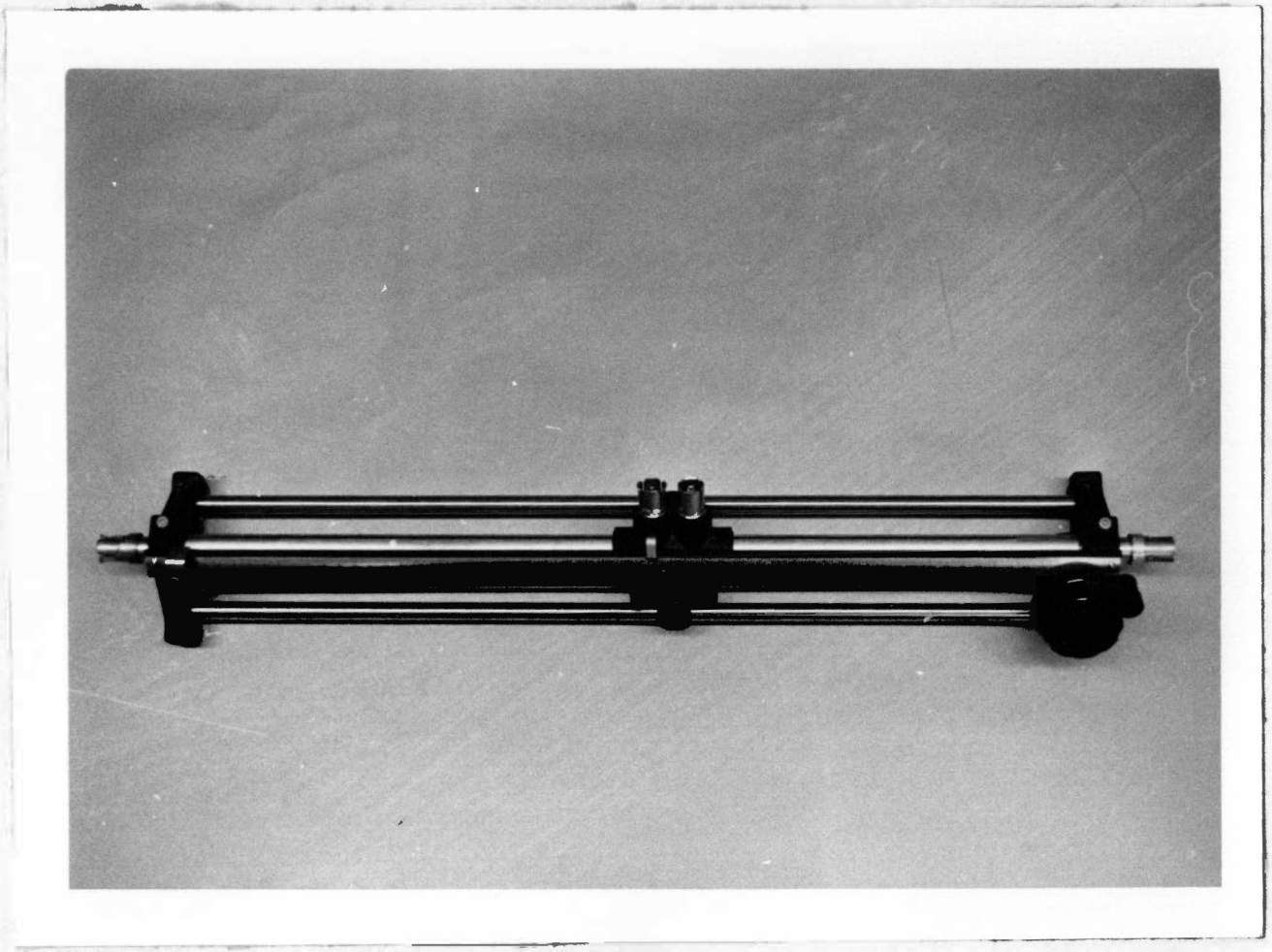

FIGURE 41

THE SLOTTED LINE

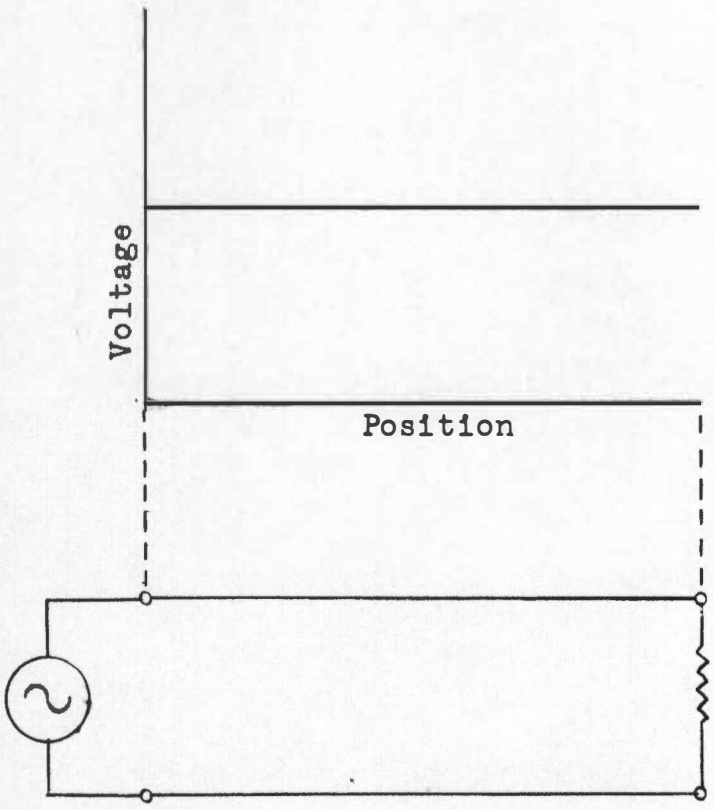

FIGURE 42

THE VOLTAGE ALONG A LOSSLESS LINE WITH NO ENERGY REFLECTED FROM THE LOAD

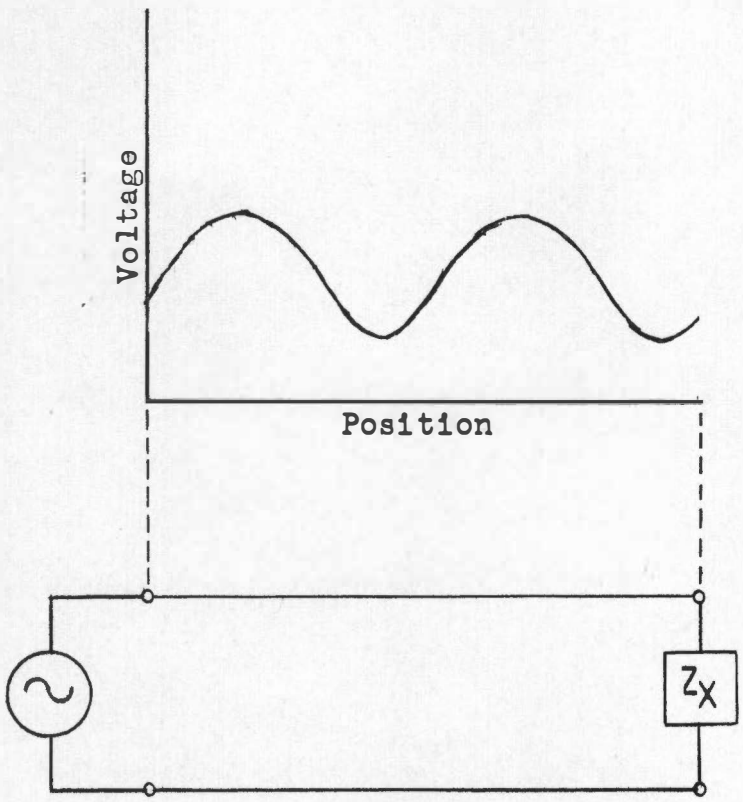

FIGURE 43

A VOLTAGE STANDING WAVE ALONG
A SLOTTED LINE

For the case previously described, when there is no energy reflected from the load, the voltage standing wave ratio is one.

Other special cases are those with an infinite impedance and a short-circuit as loads. For the case of an infinite impedance the voltage at the load-end of the line is a maximum as shown in Figure 44 on page 106. For the case of a short-circuited line the voltage at the load-end of the line is zero as shown in Figure 45 on page 107.

In all cases the maxima appear one-half wavelength apart, and the minima appear one-half wavelength apart.

The preceding discussion is a limited one compared to the available theory of the slotted line, but it is all that is needed for the measurement of wavelength and for an indication of how well a device connected to the end of the line absorbs the incident energy. For a more general theory one can consult the instruction book for the General Radio Type 874-LBA slotted line.

The Response of the Crystal Detector in the Slotted Line

The induced voltage in the probe circuit was alternating and was rectified by the crystal detector to produce an output of direct current. It was necessary to know the relationship between the output current and the input voltage. The manufacturer claims that the crystal operates as

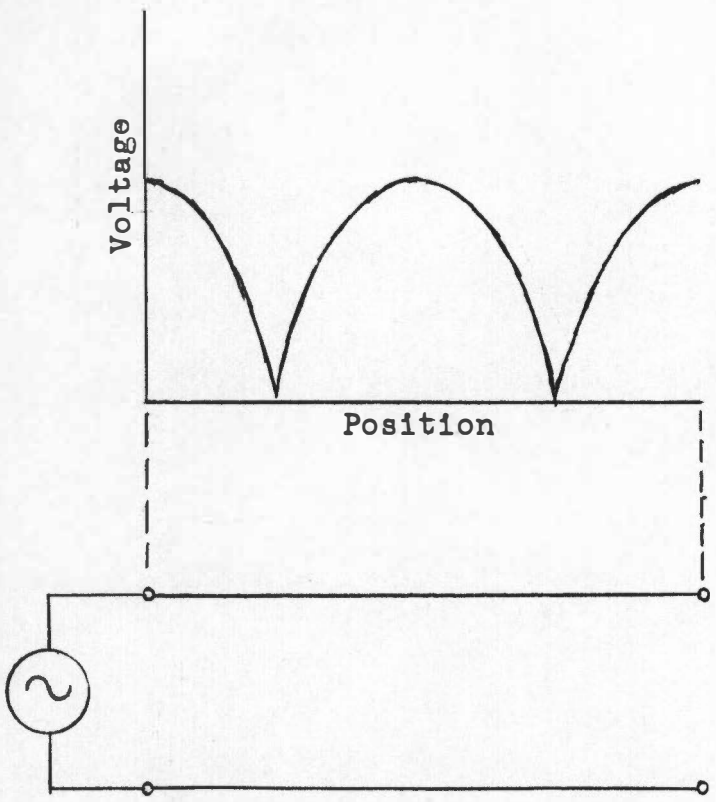

FIGURE 44

A VOLTAGE STANDING WAVE ALONG A SLOTTED LINE WITH AN OPEN END

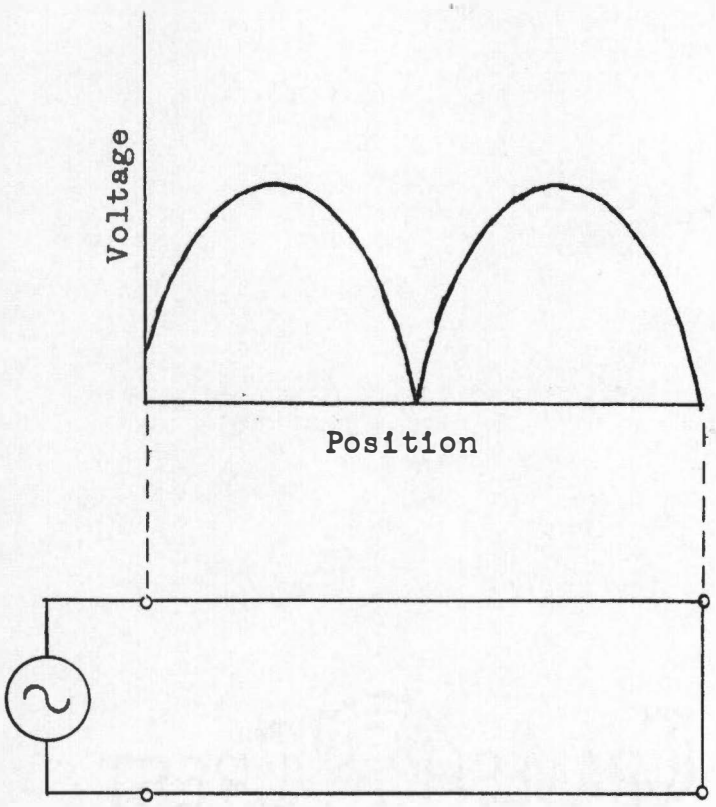

FIGURE 45

A VOLTAGE STANDING WAVE ALONG A SLOTTED LINE WITH A SHORT-CIRCUITED END

a square-law device at very low levels and as a linear device at high levels.

Figure 47 on page 110 shows the response of the detector as the probe was moved along the slotted line. The slotted line was connected as shown in Figure 46 on page 109. The klystron was connected through an attenuator to one end of the slotted line, and the other end was not terminated, so that standing waves would be set up. The variation of the electric field inside the line from node to node was sinusoidal. For a linear detector the meter reading would have varied as the absolute value of a sine function. Figure 47 on page 110 shows the detector current as a function of probe position over a distance of approximately one wavelength. Figure 48 on page 111 shows the detector current plotted against some constant times the theoretical sinusoidal electric intensity inside the line. Data was obtained as the probe was moved over a distance equal to three and one-half wavelengths along the slotted line. From Figure 48 it may be seen that the crystal detector is operating in a linear manner for currents above twenty microamperes.

Measurement of Wavelength

From the data used to check the response of the crystal detector, it is possible to determine the wavelength

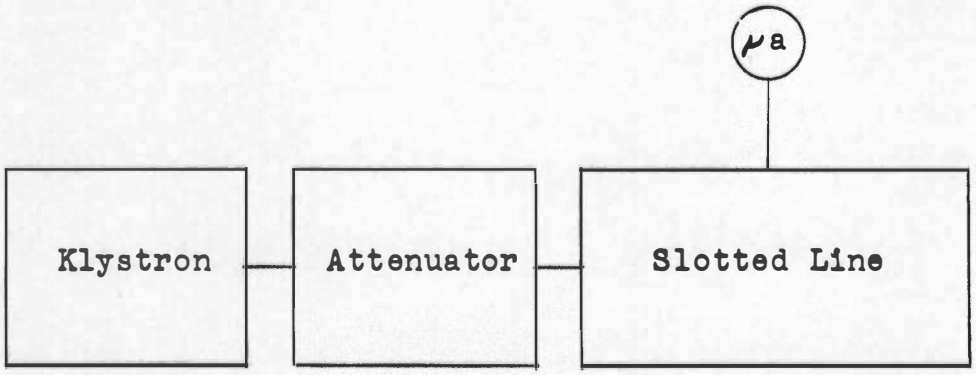

FIGURE 46

THE CONNECTIONS TO THE SLOTTED LINE FOR MAKING THE DETECTOR TESTS

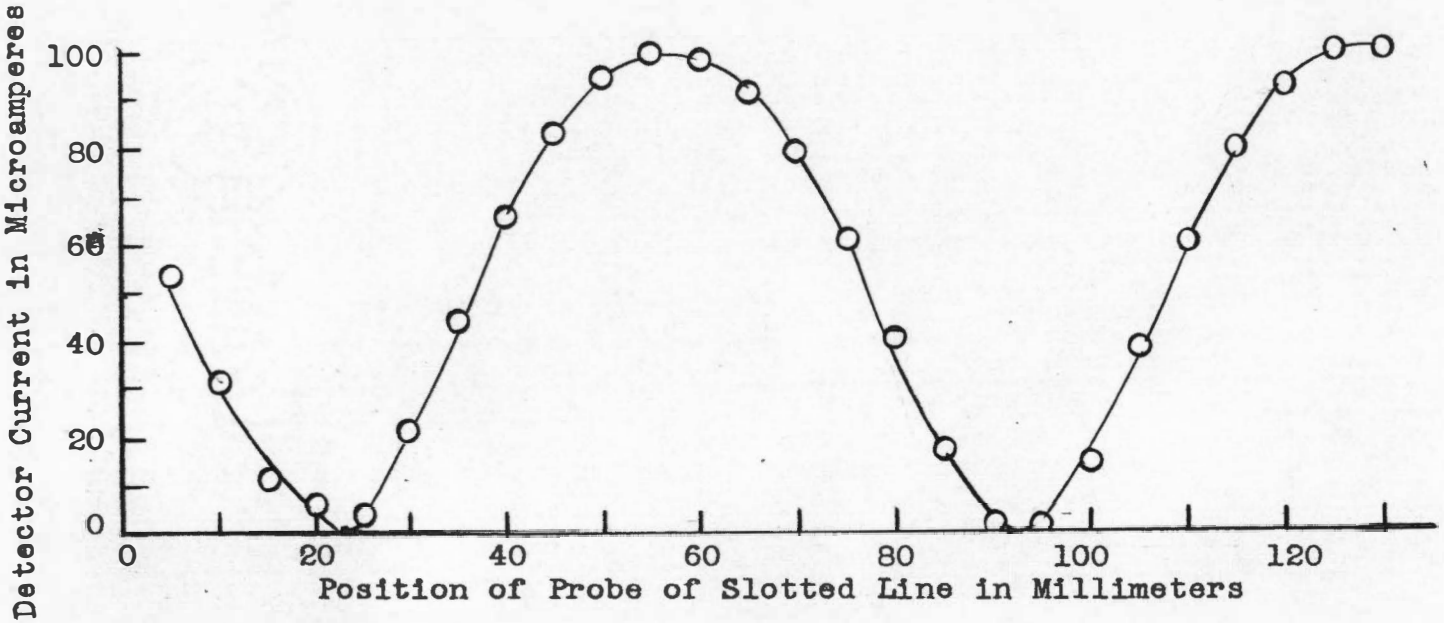

FIGURE 47

THE DETECTOR CURRENT ALONG THE SLOTTED LINE

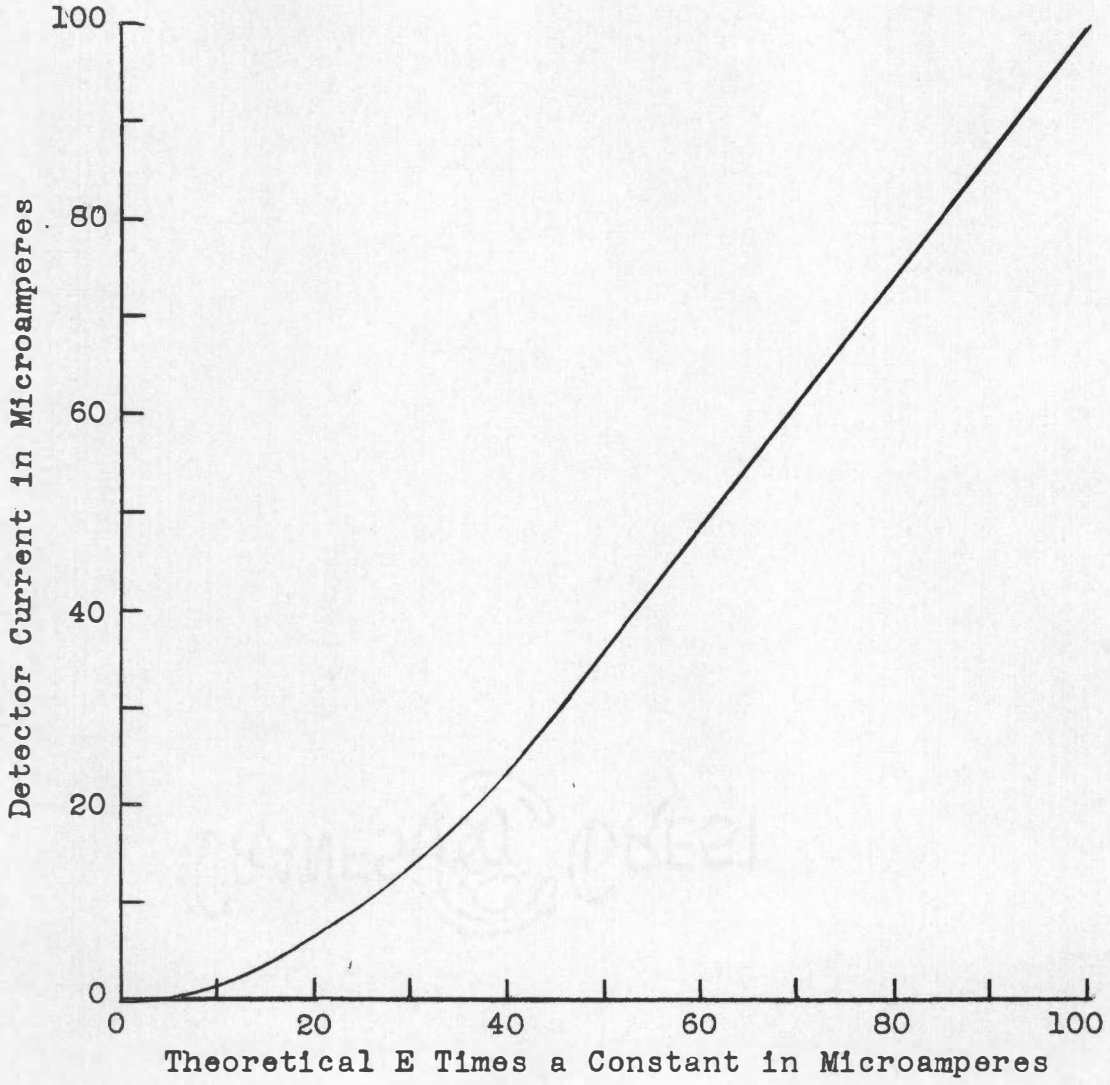

FIGURE 48

THE DETECTOR CURRENT AS A FUNCTION OF THE ELECTRIC INTENSITY BETWEEN THE CONDUCTORS OF THE SLOTTED LINE

in air of the klystron output and to calculate its operating frequency. The wavelength in air from this data was 14.3 centimeters.

Klystron Stability

Since the klystron voltages were set to the same values each time it was used, there were no other adjustments made which should have altered its frequency. The slotted line was used at different times to make measurements of wavelength. For five sets of data at different times, average wavelengths of 14.33, 14.33, 14.32, 14.30 and 14.30 centimeters were found. Six distances between voltage minima were used in each set of data.

Matching Lengths of Cable

It was desirable to have corresponding parts of the transmission lines identical except those used for phase shifters. This meant making cables of equal electrical length in most cases.

This was done by cutting two lengths of cable as nearly the same length as possible with a hacksaw and grinding them little by little on a power grinder to their final lengths. When the same standing wave pattern for each cable was obtained, the two were considered approximately equal in length.

The same procedure could be used for making one length of cable a fraction of a wavelength shorter or longer than another except that in this case, the two standing wave patterns were shifted by the desired fraction of a wavelength.

Matching the Two Dipoles

The two dipoles were matched as closely as possible by using the slotted line. A minimum voltage standing wave ratio with corresponding maxima and minima occurring at identical positions on the slotted line was necessary. The success of this process was indicated by the measurements of incident and reflected power indicated by the power meters.

The Measurement of Power

The power to each dipole was measured as close to the antenna as possible. Both incident and reflected powers were measured. The only cable between each power meter and each dipole was a short piece of RG 58U coaxial cable. A coaxial fitting which fastened to the power meter also contributed to the losses. A separate measurement indicated that the loss in each of these cables was one-fifth the power entering the cable from the power meter. The forward powers to the two dipoles from the power meters were 3.9 watts each, and the reflected powers were 0.3 watts each.

The actual total power into the dipoles was 5.8 watts. The fact that the reflected powers were so low meant that there was a good impedance match between the dipole and the rest of its transmission line.

The Measurement of the Phase Difference Between the Dipole Moments

The polarization was checked by rotating a single dipole under the array while the transmitter was on and by observing the current in the crystal detector in the slotted line. Figure 49 on page 115 shows the arrangement for making the measurement. Consider the two dipoles shown in Figure 50 on page 116. Let the dotted line indicate the dipole which is sampling the fields due to the dipoles connected to the transmitter. The voltage induced in the test dipole is assumed to be proportional to the electric intensity at its location. The electric intensity at the location of the test dipole is

$$E = E_1 \cos\theta \sin(\omega t - \phi) + E_2 \sin\omega t \sin\theta,$$

where E_1 is the magnitude of the electric field intensity due to dipole one, θ is the angle between the test dipole and dipole one, ϕ is the phase angle of dipole moment one with respect to dipole moment two, ω is 2π times the operating frequency of the transmitter, and E_2 is the magnitude of the electric intensity due to dipole two.

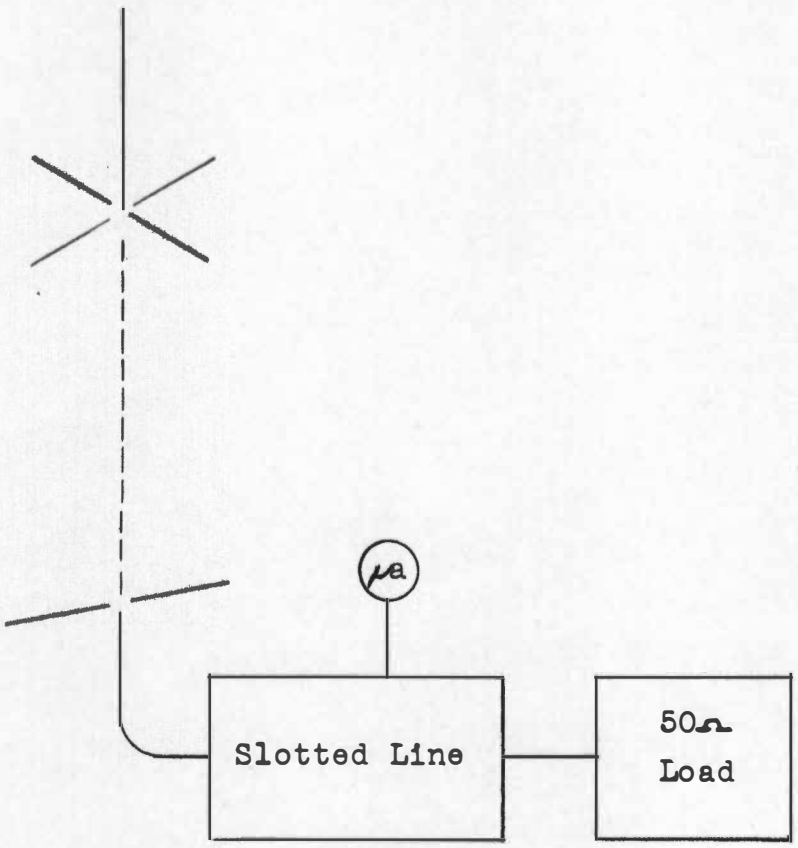

FIGURE 49

APPARATUS FOR MEASURING THE PHASE DIFFERENCE
BETWEEN THE TWO DIPOLE MOMENTS

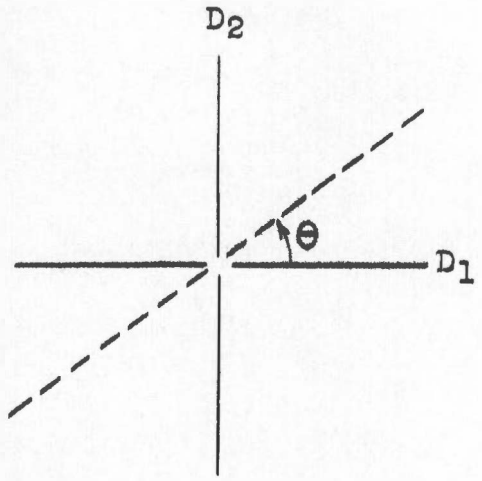

FIGURE 50

THE GEOMETRY OF THE POLARIZATION MEASUREMENT

For equal powers into the dipoles $E_1 = E_2$, and

$$E = E_1 \sqrt{1 + 2 \cos\theta \sin\theta \cos\phi} \quad \sin(\omega t + \beta). \quad \text{(VII.I.2)}$$

Since the crystal rectifies the induced current, the time average recorded by the microammeter will not be zero but will be proportional to the electric intensity,

$$\text{Meter Reading} = \text{Constant} \cdot \sqrt{1 + 2 \cos\theta \sin\theta \cos\phi}\,. \quad \text{(VII.I.3)}$$

Thus, as one rotates the test dipole under the array, the current will be a function of the angular position of the test dipole and of the phase angle. This assumes a linear relationship between E and the crystal current. As has been previously discussed, the response of the crystal is not linear for small currents. Hence, one must use the graph in Figure 48 on page 111 to make corrections for this effect.

Figure 51 on page 118 shows the corrected data for the case in which the two dipoles were supposed to be in phase and the theoretical curve for this case.

It was desired to have a ninety-degree phase difference between the two dipoles when detecting the angular momentum. Figure 52 on page 119 shows the corrected data for the case in which the dipoles were not in phase. The theoretical curves show that the phase angle was about 115 degrees.

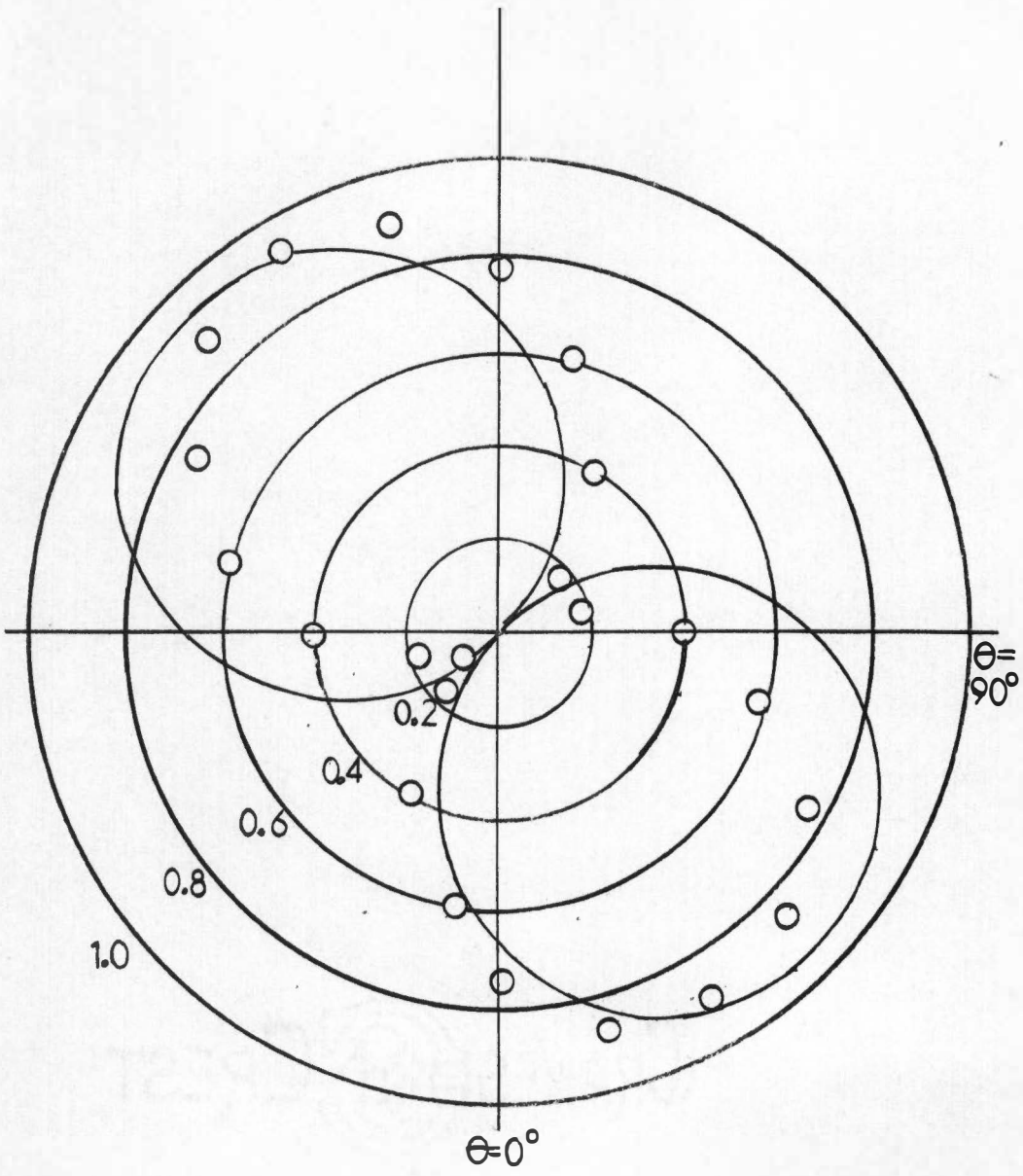

FIGURE 51

THE ELECTRIC INTENSITY AS A FUNCTION OF ANGLE FOR A SMALL PHASE DIFFERENCE BETWEEN THE DIPOLE MOMENTS

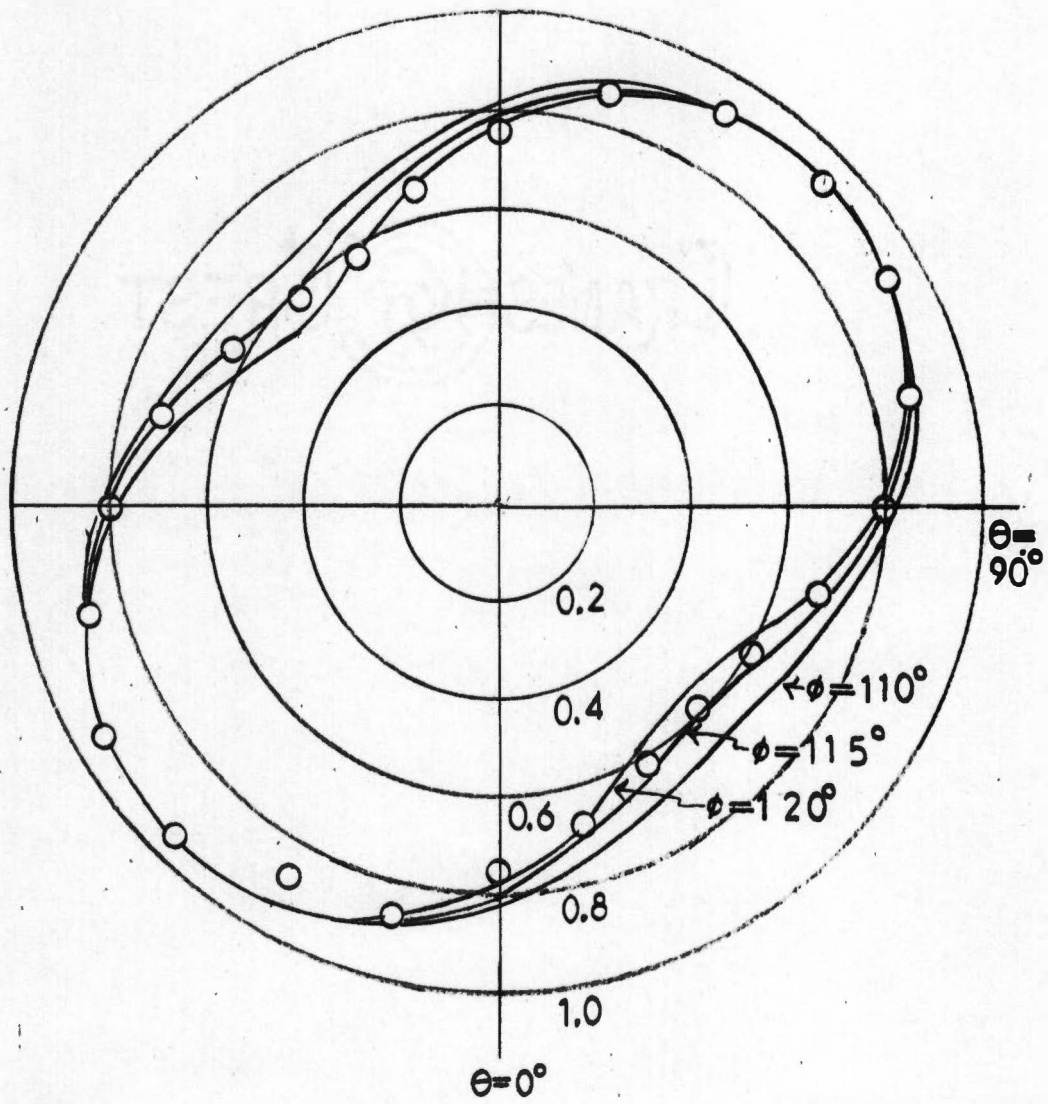

FIGURE 52

THE ELECTRIC INTENSITY AS A FUNCTION OF ANGLE FOR ABOUT 115° PHASE DIFFERENCE BETWEEN THE DIPOLE MOMENTS

II. MECHANICAL MEASUREMENTS

The Measurement of the Moment of Inertia of the Rotator

A torsional pendulum was used to measure the moment of inertia of the individual parts of the rotating apparatus. A brass cylinder was used as a standard moment of inertia, and a steel wire was used as a fiber. Using the same fiber, periods of oscillation of the different parts were observed while suspended by the fiber. When the same fiber is used,

$$\frac{T_{\text{of unknown}}}{T_{\text{of standard}}} = \sqrt{\frac{I_{\text{unknown}}}{I_{\text{standard}}}} \quad . \qquad \text{(VII.II.1)}$$

The moment of inertia of the entire rotator was found by adding the moments of inertia of the individual parts. This total was found to be 0.68 kg m^2.

Measurements of γ

Two trials were made with a gold galvanometer suspension with a torque constant of 1.54×10^{-7} n m/radian. In the first measurement, the floating apparatus was started from rest, and the top of the fiber was twisted at a constant angular velocity by a motor and gear assembly. This has been referred to as the fiber drive mechanism. The dynamics of this case was treated in Section III of Chapter IV. The data are plotted in Figure 53 on page 121 along

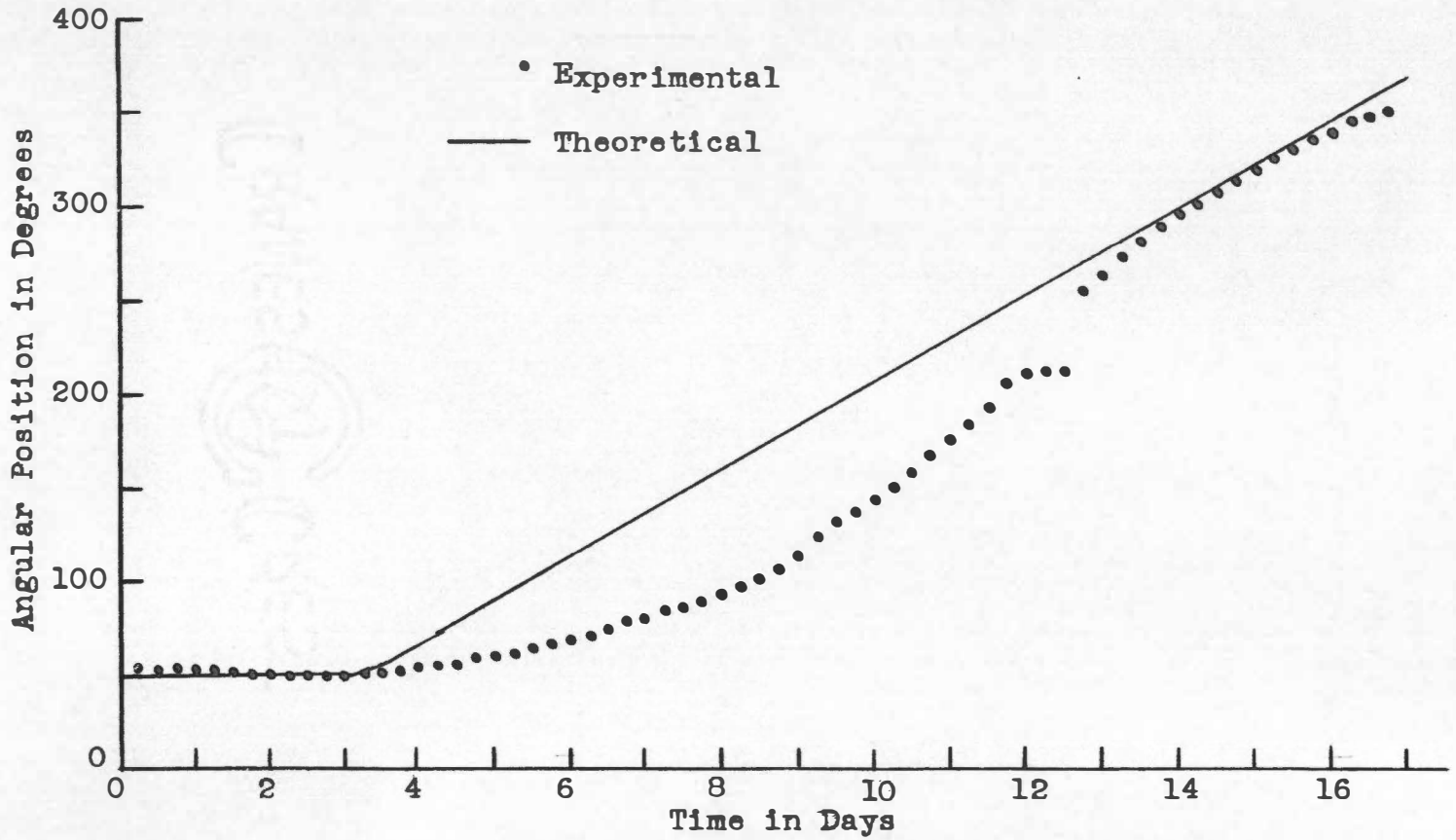

FIGURE 53

THE MOTION OF THE FLOATING APPARATUS DUE TO A FIBER WITH A ROTATING UPPER END

with a theoretical curve using the predicted value of $\gamma = 8.6 \times 10^{-5}$ n m sec.

In the second measurement the floating apparatus was twisted through an angle of 360° and released from rest. The dynamics of this case was treated in Section II of Chapter IV. The data are plotted in Figure 54 on page 123. Also plotted is a theoretical curve using the predicted value of γ.

Noise

With no fiber to supply a restoring torque, the rotator moved without any externally applied torque. These rotations are termed "noise" in the system used in the experiment.

Figure 55 on page 124 shows the motion of the floating apparatus without any applied external torque.

McCombie[1] has pointed out that from fluctuation theory that one can expect changes in the angle of the system on the order

$$\overline{\Delta\theta^2} = \frac{2k'T}{\gamma}\left[S - \frac{I}{\gamma}\left(1 - e^{-\frac{\gamma}{I}S}\right)\right] , \qquad \text{(VII.II.2)}$$

where $\overline{\Delta\theta^2}$ is the mean square change in angular position in time S, k' is Boltzman's constant, T is the absolute

---

[1] C. W. McCombie, Reports on Progress in Physics XVI, 289 (1953).

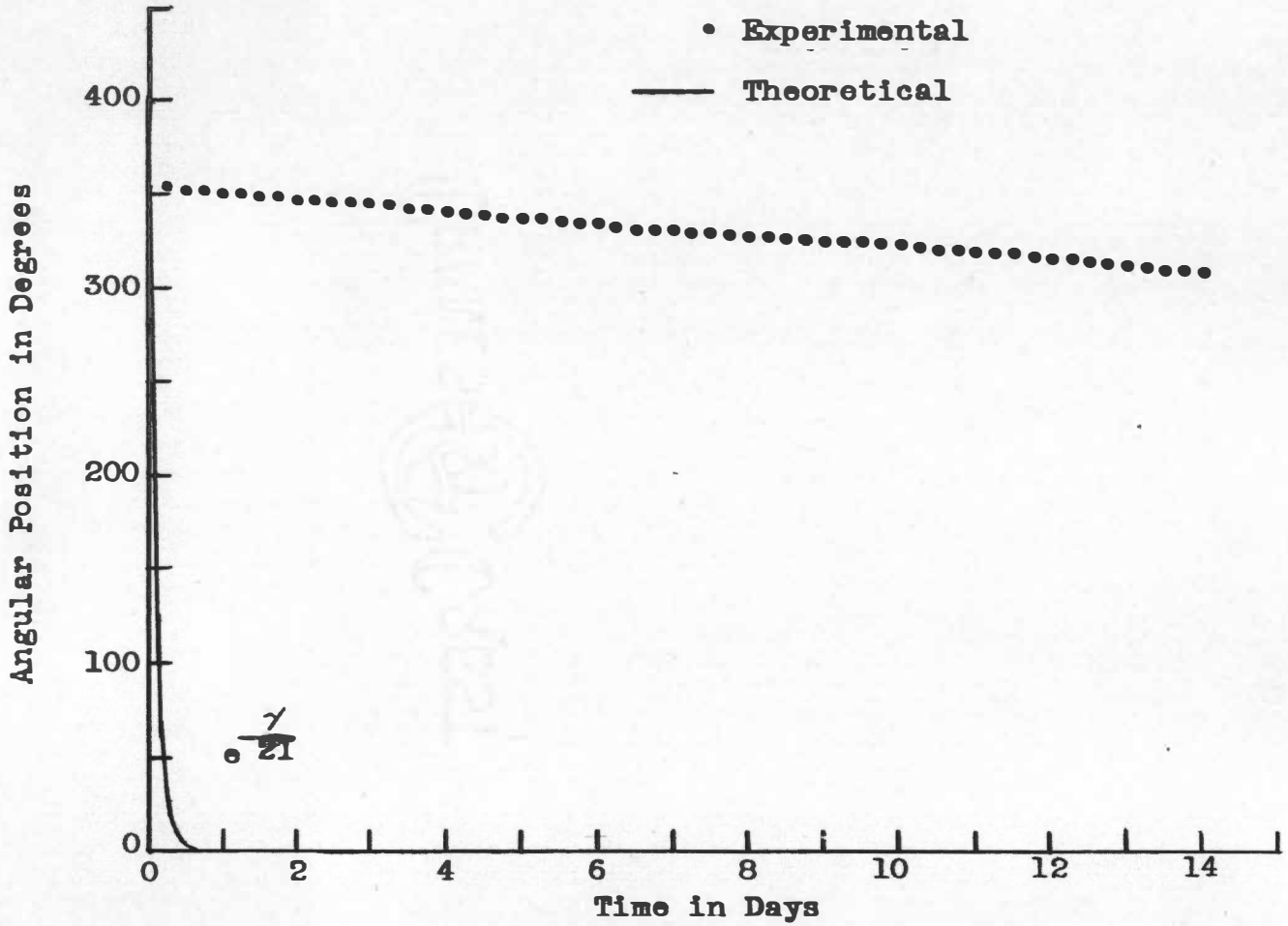

FIGURE 54

THE MOTION OF THE FLOATING APPARATUS WITH A FIBER AND AN INITIAL ANGULAR DISPLACEMENT

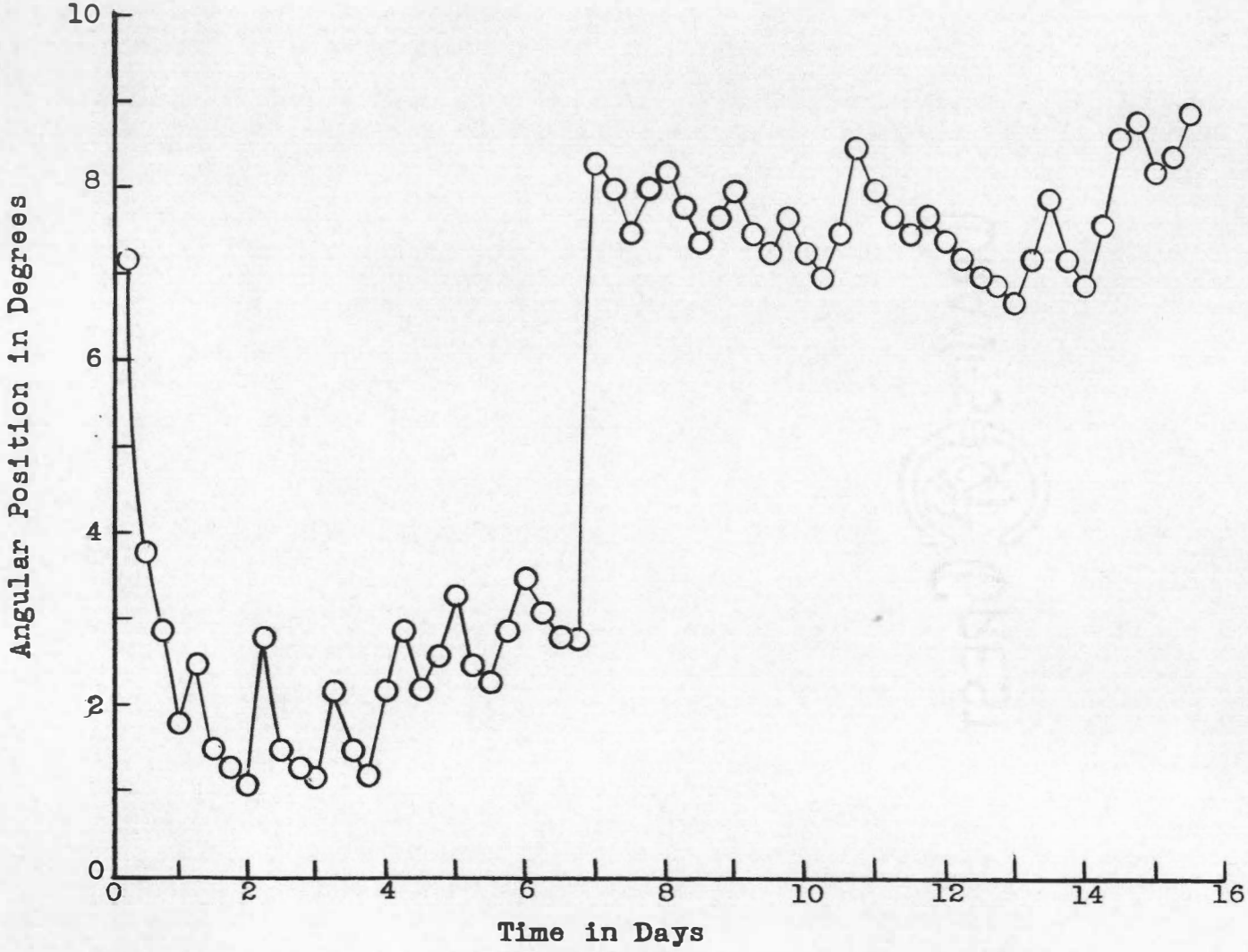

FIGURE 55

MOTION OF THE FLOATING APPARATUS WITHOUT EXTERNALLY APPLIED TORQUE

temperature, I is the moment of inertia, and γ is the coefficient of the torque per unit angular velocity.

For $T = 300^{\circ}$ K, the calculated value of $\gamma = 8.6 \times 10^{-5}$ n m sec, and S = 6 hrs one obtains

$$\overline{\Delta\theta^2} = 6.7 \times 10^{-5} \text{ degree of angle.}$$

From the data graphed in Figure 55 on page 124, a value of $\overline{\Delta\theta^2} = 0.32^{\circ}$. Thus, the noise is not close to a theoretical minimum value, and there were disturbances producing the comparatively large changes in angle.

Difficulties

From the results shown in Figure 53 on page 121 and Figure 54 on page 123, one sees that if he assumes an opposing torque exerted by the water on the floating apparatus which is directly proportional to its angular velocity he is faced with contradictory data. For, if the actual value of γ is greater than the predicted value, then the transient envelope in Figure 54 on page 123 would vanish even more rapidly; if the value of γ is less than the predicted value, then the oscillations in Figure 53 on page 121 would have had a period much less than that observed. Thus, from these data one would conclude that the torque exerted by the water and perhaps some contaminates is not simply a constant times the angular velocity.

If this is the case, it may make more sense to speak of "the torque exerted by the water," rather than "the torque due to the viscosity of the water."

CHAPTER VIII

EXPERIMENTS WHICH APPEAR FEASIBLE

Theoretical consideration has been given to systems suspended by a fiber in Chapter IV. In this chapter practical consideration is given to two cases.

I. SINUSOIDAL FORCING AT THE RESONANCE FREQUENCY

If one has a system in a vacuum such as that in Figure 56 on page 128, the damping will be due mainly to the viscosity in the suspending fiber.

Since quartz has a very low internal viscosity for its tensile strength, one can estimate an expected magnitude of Θ_{max} from

$$\Theta_{max} = \frac{E_0}{\gamma}\sqrt{\frac{I}{k}} \quad . \tag{IV.IV.6}$$

In the sinusoidal forcing, E_0 would be the amplitude of the torque. For a total of five watts into two dipoles with a phase difference of ninety degrees at a frequency of two thousand megacycles, one could expect

$$E_0 = \frac{p}{2\pi f} = \frac{5 \text{ watts}}{2\pi \times 2 \times 10^9 \ \frac{1}{\text{sec}}}$$

$$= 3.98 \times 10^{-10} \text{n m} \quad . \tag{VIII.I.1}$$

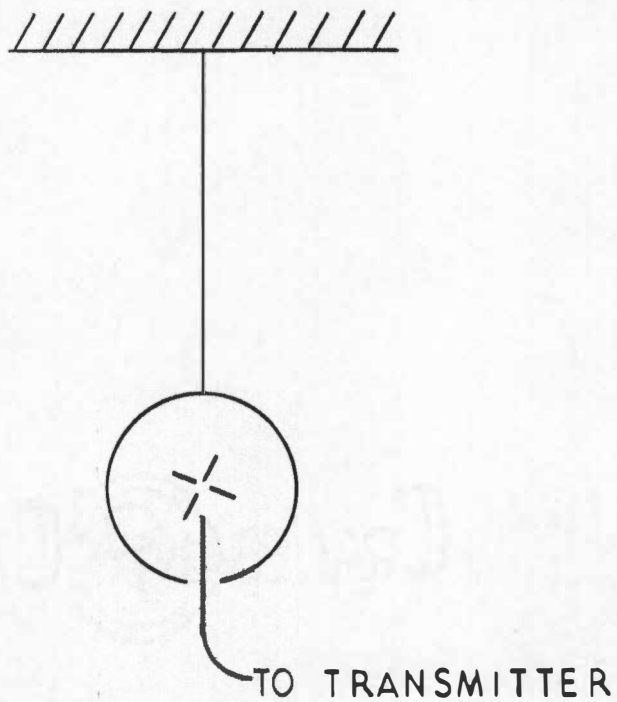

FIGURE 56

A SUSPENDED SYSTEM

The sphere which was used in the experiment already performed has a weight of 11.1 newtons. The tensile strength of quartz is approximately 10^9 dynes per square centimeter.[1] To support the sphere one would need a fiber to withstand a tension of 11.1×10^5 dynes, so its cross-sectional area would have to be $11.1 \times 10^{-4} cm^2$. The radius of the fiber would be $1.88 \times 10^{-2} cm$.

The shearing stress is given by

$$S_z = \frac{Z\theta r}{2\ell} + \frac{\eta r}{2\ell} \frac{d\theta}{dt}, \qquad \text{(VIII.I.2)}$$

where Z is the modulus of rigidity of the fiber material, θ is the angle through which the fiber is twisted, r is the radius, ℓ is its length, and η is the coefficient of viscosity of the fiber material.[2]

The torque at an end of the fiber may be found by integrating the shearing stress over the cross-section of the fiber:

$$dL = r \cdot dF = r \cdot 2\pi r \cdot S_z \, dr, \qquad \text{(VIII.I.3)}$$

$$L = \frac{\pi r^4 Z \theta}{4\ell} + \frac{\pi r^4 \eta}{4\ell} \frac{d\theta}{dt}, \qquad \text{(VIII.I.4)}$$

---

[1]This approximate value was taken from page eighteen of catalogue number Q-3 of the General Electric Company.

[2]John Strong et al, Procedures in Experimental Physics (New York: Prentice-Hall, Inc., 1939), pp. 191-193.

$$L = k\theta + \gamma \frac{d\theta}{dt} \quad . \qquad \text{(VIII.I.5)}$$

For values of

$$Z = 3 \times 10^{11} \ \frac{\text{dynes}}{\text{cm}^2} ,$$

$$\eta = 10^6 \text{ poises},$$

the fiber above with a length of one meter would have values of

$$k = 2.9 \times 10^{-5} \ \frac{\text{nm}}{\text{rad}} ,$$

$$\gamma = 9.8 \times 10^{-11} \text{nm sec.}$$

From (IV.IV.6) one obtains a maximum amplitude for θ,

$$\theta_{max} = \frac{E_0}{\gamma}\sqrt{\frac{I}{k}} = 75.5 \text{ radians} \quad . \qquad \text{(VIII.I.6)}$$

II. PULSING THE SYSTEM

Suppose one applies a constant torque T during part of a cycle of the oscillation of a rotator so that it makes the amplitude of the oscillation grow in magnitude. The maximum amplitude would come when the energy furnished by the torque T acting through an angle would just replenish the losses in the system. The motion would approximate simple harmonic motion, so that the graph of the angle versus time might appear as in Figure 57 on page 131. The second half cycle would have an amplitude not quite equal

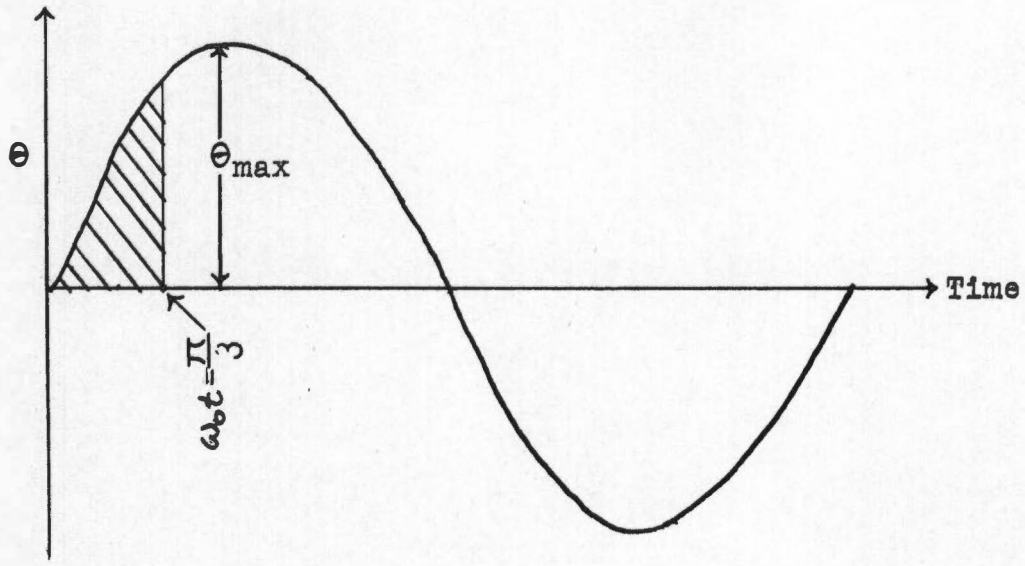

FIGURE 57

THE APPROXIMATE MOTION OF A
PULSED SUSPENDED SYSTEM

to θ_{max} due mainly to losses in the fiber if the system is in a vacuum. If the system has been pulsed long enough, the angular velocity at $\omega_o t = 0$ will essentially equal the angular velocity at $\omega_o t = 2\pi$. Then

$$\begin{array}{l}\text{Work done by}\\ \text{applied torque}\end{array} = \begin{array}{l}\text{Work done by}\\ \text{torque of viscous}\\ \text{origin in the fiber.}\end{array} \qquad \text{(VIII.II.1)}$$

Let the torque which is to be applied by the electromagnetic radiation be applied for a length of time,

$$\tau = \frac{\pi}{3\omega_o},$$

One should get a rough estimate of the maximum amplitude by assuming sinusoidal motion,

$$\theta = \theta_{max} \sin \omega_o t \ . \qquad \text{(VIII.II.2)}$$

Then

$$\frac{d\theta}{dt} = \omega_o \theta_{max} \cos \omega_o t \ . \qquad \text{(VIII.II.3)}$$

From (VIII.II.1),

$$L\theta_{\omega_o t = \frac{\pi}{3}} = 4 \int_0^{\frac{\pi}{2}} \gamma \frac{d\theta}{dt} \, d\theta \ , \qquad \text{(VIII.II.4)}$$

$$L \frac{\sqrt{3}}{2} \theta_{max} = 4 \int_0^{\frac{\pi}{2\omega_o}} \gamma (\theta_{max} \omega_o \cos \omega_o t)^2 dt \qquad \text{(VIII.II.5)}$$

$$= 4\gamma \theta^2_{max} \omega_o \int_0^{\frac{\pi}{2}} \cos^2 \omega_o t \, d(\omega_o t), \qquad \text{(VIII.II.6)}$$

$$L\frac{\sqrt{3}}{2} = 4\gamma\theta_{max}\omega_o\left[\frac{\omega_o t}{2} + \frac{\sin 2(\omega_o t)}{4}\right]_0^{\frac{\pi}{2}}, \qquad \text{(VIII.II.7)}$$

$$L\frac{\sqrt{3}}{2} = \gamma\theta_{max}\omega_o\pi \ . \qquad \text{(VIII.II.8)}$$

From this result,

$$\theta_{max} = \frac{L\sqrt{3}}{2\pi\omega_o\gamma} \qquad \text{(VIII.II.9)}$$

$$= 0.275\ \frac{E_o}{\gamma}\sqrt{\frac{I}{k}} \ . \qquad \text{(VIII.II.10)}$$

This may be compared with (IV.IV.6),

$$\theta_{max} = \frac{E_o}{\gamma}\sqrt{\frac{I}{k}} \ .$$

Thus, one would not expect as great a maximum amplitude, but there would still be a large angle of rotation,

$$\theta_{max} = 20.7 \text{ radians.} \qquad \text{(VIII.II.11)}$$

Experimentally the pulsing would be much easier to perform. The production of such large angles of rotation would hinge upon the low viscosity of the quartz used. Also, one would have to wait for some time for these large angles to be produced if the system started from rest. The transient term to the response solution contains a factor $e^{-\frac{\gamma}{2I}t}$,

so that for this to become negligibly small, t must be much larger than $\frac{2I}{\gamma}$. As a practical value let $t = 10\,\frac{2I}{\gamma}$. For the system just described

$$t = \frac{(10)\ (2)\ (1.47 \times 10^{-2})\ \text{kg m}^2}{9.8 \times 10^{-11}\ \text{n m sec}};$$

$$t = 3.0 \times 10^{9}\ \text{sec}.$$

So, one must use some procedure other than waiting around for the maximum amplitude to be approached in order to measure the torque.

CHAPTER IX

SUMMARY AND CONCLUSIONS

I. SUMMARY

Theoretically, certain types of electromagnetic waves in the microwave region should carry angular momentum. Experiments performed by others indicate that they do carry angular momentum.

An absorption experiment using half-wave electric dipoles was performed, but no angular momentum was detected. Using a measured value of the moment of inertia and a calculated value of torque due to the viscosity of water resulted in the prediction of a large angle of rotation of an absorbing sphere during the time of the experiment. But, none comparable to the predicted value was observed. These results are shown in Figure 16 on page 59.

Experiments which attempted to measure the torque on the floating apparatus due to the water indicated that the torque was not that predicted by the product of a constant times the angular velocity. These results are shown in Figure 53 on page 121 and Figure 54 on page 123.

Experiments which show promise of detecting the angular momentum due to the half-wave dipoles, if it exists and has the expected value, were discussed theoretically.

These involved suspending the absorbing sphere by a quartz fiber. The success of these experiments would be dependent upon the low viscosity of quartz. Once again, one would be involved with an experiment with a transient component of motion that lasts an extremely long time. He would have the advantage, however, of having a natural frequency of the system, and this should improve the signal-to-noise situation.

After precautions were taken to eliminate rotational disturbances in the system, there still occurred sudden angular impulses. A typical one is shown in Figure 55 on page 124.

II. CONCLUSIONS

Valid conclusions from the data of the experimental work are: (1) no evidence for the existence of angular momentum of the microwaves was found, (2) the fact that the microwaves did not possess angular momentum was not conclusively demonstrated, (3) if one uses the usually quoted values of the coefficient of viscosity of water, the system used is not described by the differential equation

$$I \frac{d\omega}{dt} + \gamma\omega = F(t), \qquad \text{(IX.II.1)}$$

and (4) the ratic of $\frac{\gamma'}{I}$ was not a constant at the very low angular velocities at which the floating apparatus turned.

BIBLIOGRAPHY

BIBLIOGRAPHY

Abraham, Max. "Der Drehimpuls des Lichtes." Physikalische Zeitschrift, XV (1914), pp. 914-918.

Beth, Richard A. "Mechanical Detection and Measurement of the Angular Momentum of Light," The Physical Review, 50 (July, 1936), pp. 115-125.

Carrara, N. "Torque and Angular Momentum of Centimeter Electromagnetic Waves," Nature, 164 (November, 1949), pp. 883-884.

McCombie, C. W. "Fluctuation Theory in Physical Measurements." Reports in Progress in Physics, XVI (1953), pp. 266-319.

O'Rahilly, Alfred. Electromagnetics, A Discussion of Fundamentals. London: Longmans, Green and Company, 1938.

Page, Leigh. Introduction to Theoretical Physics. New York: D. Van Nostrand Company, Inc., 1949.

Poynting, J. H. "The Wave Motion of a Revolving Shaft, and a Suggestion as to the Angular Momentum in a Beam of Circularly Polarised Light," Proceedings of the Royal Society, 82 (June, 1909), pp. 560-567.

Richtmyer, F. K., and E. H. Kennard. Introduction to Modern Physics. New York: McGraw-Hill Book Company, Inc., 1947.

Smythe, William R. Static and Dynamic Electricity. New York: McGraw-Hill Book Company, Inc., 1939.

Sommerfeld, Arnold. Atomic Structures and Spectral Lines. London: Methuen and Company, Ltd., 1923.

Stratton, Julius Adams. Electromagnetic Theory. New York: McGraw-Hill Book Company, Inc., 1941.

Strong, John, et al. Procedures in Experimental Physics. New York: Prentice-Hall, Inc., 1939.

APPENDIXES

APPENDIX A

THE ANGULAR MOMENTUM DUE TO A SINGLE DIPOLE

$$rG_\theta = \left[\frac{2p\cos\theta}{r^2 c}\cos\omega\left(t - \frac{r}{c}\right)\right.$$

$$\left. - \frac{2pk\cos\theta}{rc}\sin\omega\left(t - \frac{r}{c}\right)\right]$$

$$\left[-\frac{pk^2}{r}\sin\theta\cos\omega\left(t - \frac{r}{c}\right)\right.$$

$$\left. - p\frac{k}{r^2}\sin\theta\sin\omega\left(t - \frac{r}{c}\right)\right] . \qquad \text{(A.1)}$$

Now terms of the form

$$\left[\cos\left(\omega t - \frac{\omega r}{c}\right)\right]\left[\sin\left(\omega t - \frac{\omega r}{c}\right)\right]$$

averaged over time are equal to zero; so that when taking the time average of the above quantity, one can omit writing them down. Thus

$$\overline{rG_\theta} = \frac{2p^2k^2\sin\theta\cos\theta}{r^3 c}\overline{\cos^2\omega\left(t - \frac{r}{c}\right)}$$

$$- \frac{2p^2k^2}{r^3 c}\sin\theta\cos\theta\,\overline{\sin^2\omega\left(t - \frac{r}{c}\right)} \qquad \text{(A.2)}$$

$$\overline{rG_\theta} = \frac{2p^2k^2 \sin\theta\cos\theta}{r^3c}\left[\overline{1 - 2\sin^2\omega(t - \tfrac{r}{c})}\right] \qquad (A.3)$$

$$= \frac{2p^2k^2 \sin\theta\cos\theta}{r^3c}\Big[1 - 2\,(\overline{\sin^2\omega t}\cos^2\tfrac{\omega r}{c} + \overline{\cos^2\omega t}\sin^2\tfrac{\omega r}{c} - 2\,\overline{\sin\omega t\ \cos\omega t}\sin\omega\tfrac{r}{c}\cos\omega\tfrac{r}{c})\Big] \qquad (A.4)$$

$$= \frac{2p^2k^2 \sin\theta\cos\theta}{r^3c}\left[1 - (\sin^2\omega\tfrac{r}{c} + \cos^2\omega\tfrac{r}{c})\right] \qquad (A.5)$$

$$= 0\,. \qquad (A.6)$$

ENERGY CONTAINED IN A SPHERICAL SHELL
DUE TO A SINGLE DIPOLE

$$E_\Theta = \left[- \frac{pk^2 \sin\Theta}{r} + \frac{p \sin\Theta}{r^3} \right] \cos\psi$$

$$- \left[\frac{pk \sin\Theta}{r^2} \right] \sin\psi \; ; \qquad \text{(III.II.2)}$$

$$H_\phi = - \left[\frac{pk^2 \sin\Theta}{r} \right] \cos\psi$$

$$- \left[\frac{pk \sin\Theta}{r^2} \right] \sin\psi \; ; \qquad \text{(III.II.6)}$$

$$\overline{E_\Theta H_\phi} = \left[\frac{p^2k^4 \sin\Theta}{r^2} \right.$$

$$\left. - \frac{p^2k^2 \sin^2\Theta}{r^4} \right] \cos^2\psi$$

$$+ \left[\frac{p^2k^2 \sin^2\Theta}{r^4} \right] \sin^2\psi \; ; \qquad \text{(A.7)}$$

$$\overline{G_r} = \frac{\overline{E_\Theta H_\phi}}{4\pi c} = \frac{1}{8\pi c} \frac{p^2 \sin^2\Theta \, k^2}{r^4} \; ; \qquad \text{(A.8)}$$

$$\int_V \overline{G_r} dV = \frac{1}{8\pi c} p^2 k^4 \int_0^{\pi} \sin^3\Theta \, d\Theta \int_{R_1}^{R_2} dr \int_0^{2\pi} d\phi \quad ; \qquad (A.9)$$

$$= \frac{1}{8\pi c} p^2 k^4 \left(\frac{4}{3}\right) (R_2 - R_1) (2\pi) \; ; \qquad (A.10)$$

$$= \frac{8}{24\pi c} p^2 k^4 (R_2 - R_1) \; ; \qquad (A.11)$$

$$= \frac{1}{3c} p^2 k^4 (R_2 - R_1) \; ; \qquad (A.12)$$

$$\overline{W} = c \int_V \overline{G_r} \, dV = \tfrac{1}{3} p^2 k^4 (R_2 - R_1) \; . \qquad (A.13)$$

APPENDIX B

TABLE I

SPECIFICATIONS OF THE KLYSTRON

Specific characteristic or feature	Specifications
Type	Sperry Rand Corporation SRL-7C reflex oscillator
Applications	Local oscillator or bench oscillator
Frequency range	1,850 to 2,100 MC
Temperature coefficient	50 Kc/°C
Tuning	Integral cavity and tuner
Power output	5 to 10 watts
RF output fitting	Type N for use with 50-ohm plug UG-21B/U or equivalent
Weight	2 lb
Mounting position	Any
Base	Shortened medium shell, octal, 8-pin
Repeller cap	Small C1-1
Heater voltage	6.3v, ac or dc
Heater current	2.0 amp
Maximum beam voltage	1,000 v
Maximum beam current	220 ma
Maximum beam power	220 w
Reflector voltage	-350 v to -1,000 vdc

TABLE I (continued)

Specific characteristic or feature	Specifications
Maximum operating temperature of base	75°C
Maximum operating temperature of shell	100°C
Cooling required	Forced air, 50 cubic feet per minute minimum
Base and other connections	1. Internal connection 2. Heater 3. Internal connection 4. Internal connection 5. Control electrode 6. Internal connection 7. Heater and cathode 8. Heater and cathode Top cap-reflector Envelope-resonator Side terminal-output

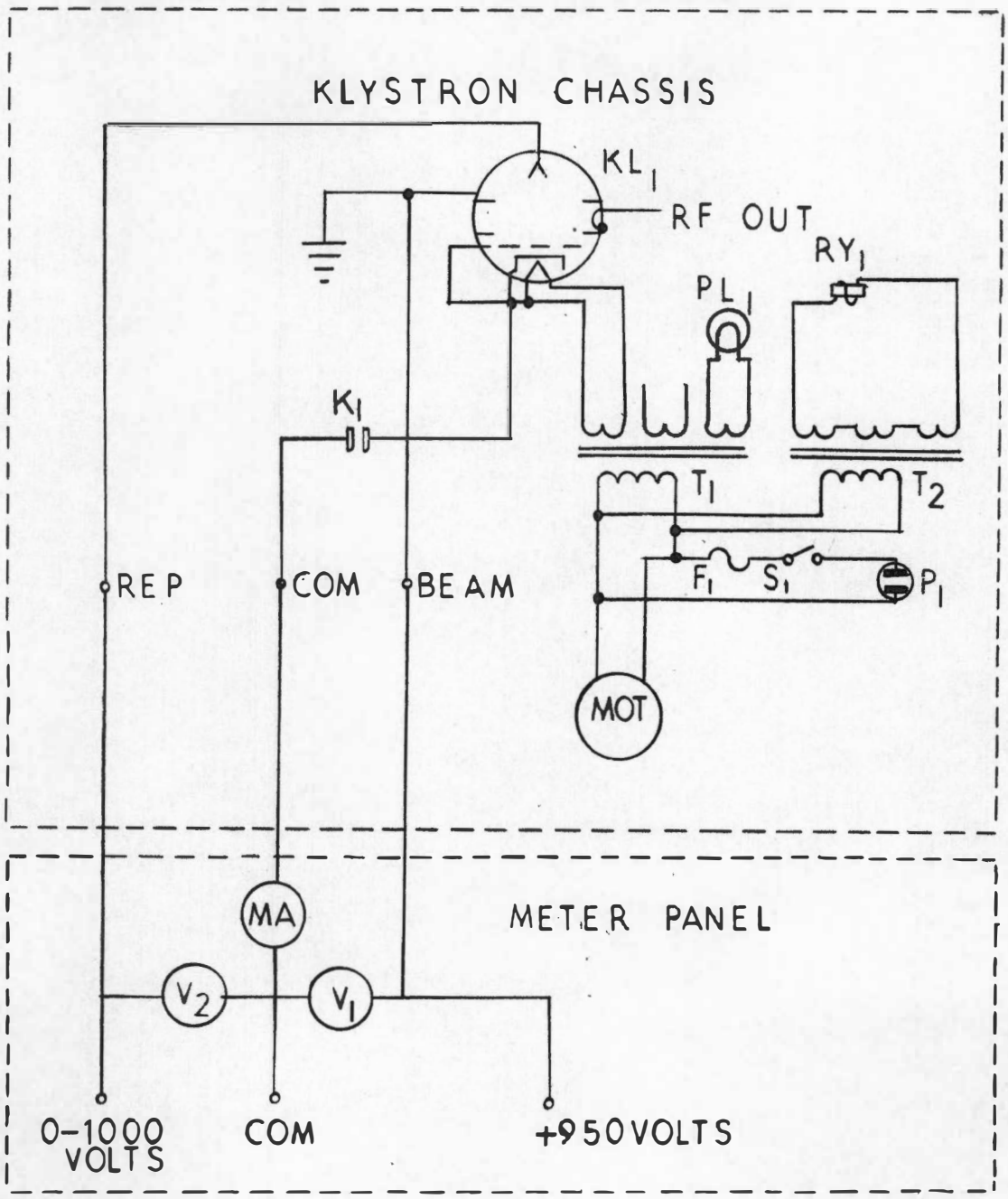

FIGURE 58

THE KLYSTRON CHASSIS AND METER PANEL

TABLE II

SPECIFICATIONS OF THE COMPONENTS ON THE KLYSTRON CHASSIS AND THE METER PANEL

Symbol	Component	Specifications
F_1	Fuse	3AG 3 amp
K_1	Contacts on RY_1	Open when relay is not energized
KL_1	Klystron	Sperry Rand Corporation SRL-7C
MA	Milliammeter	0-500 ma
MOT	Blower	115 vac motor 50 cfm blower
P_1	Plug	Standard 115 vac
PL_1	Pilot lamp	6.3 v, 0.15 amp
RY_1	Relay	18 vac coil
S_1	Toggle switch	SPST
T_1, T_2	Filament transformer	Secondary Windings: 1. 6.3 v, 9 amp 2. 6.3 v, 0.6 amp 3. 6.3 v, 0.6 amp
V_1	Voltmeter	0-1,000 vdc
V_2	Voltmeter	0-1,500 vdc

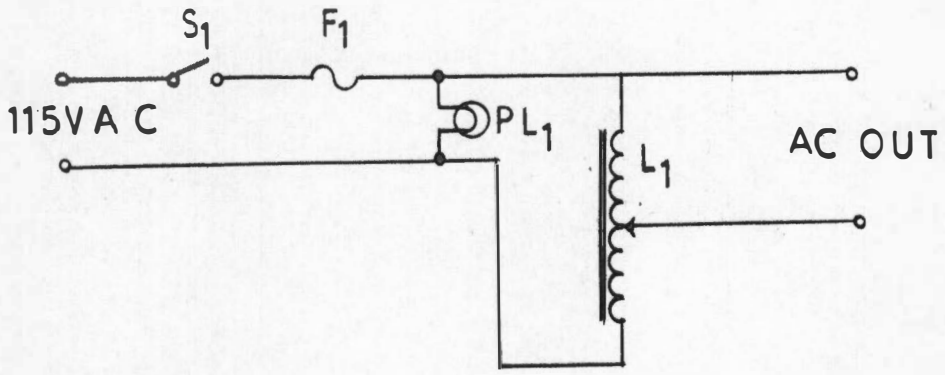

FIGURE 59

THE VARIAC CIRCUIT

TABLE III

SPECIFICATIONS OF THE COMPONENTS
OF THE VARIAC CIRCUIT

Symbol	Component	Specifications
F_1	Fuse	3AG, 7½ amp
L_1	Variac	115 v, 5 amp
PL_1	Pilot lamp	115 v, screw base
S_1	Switch	SPST

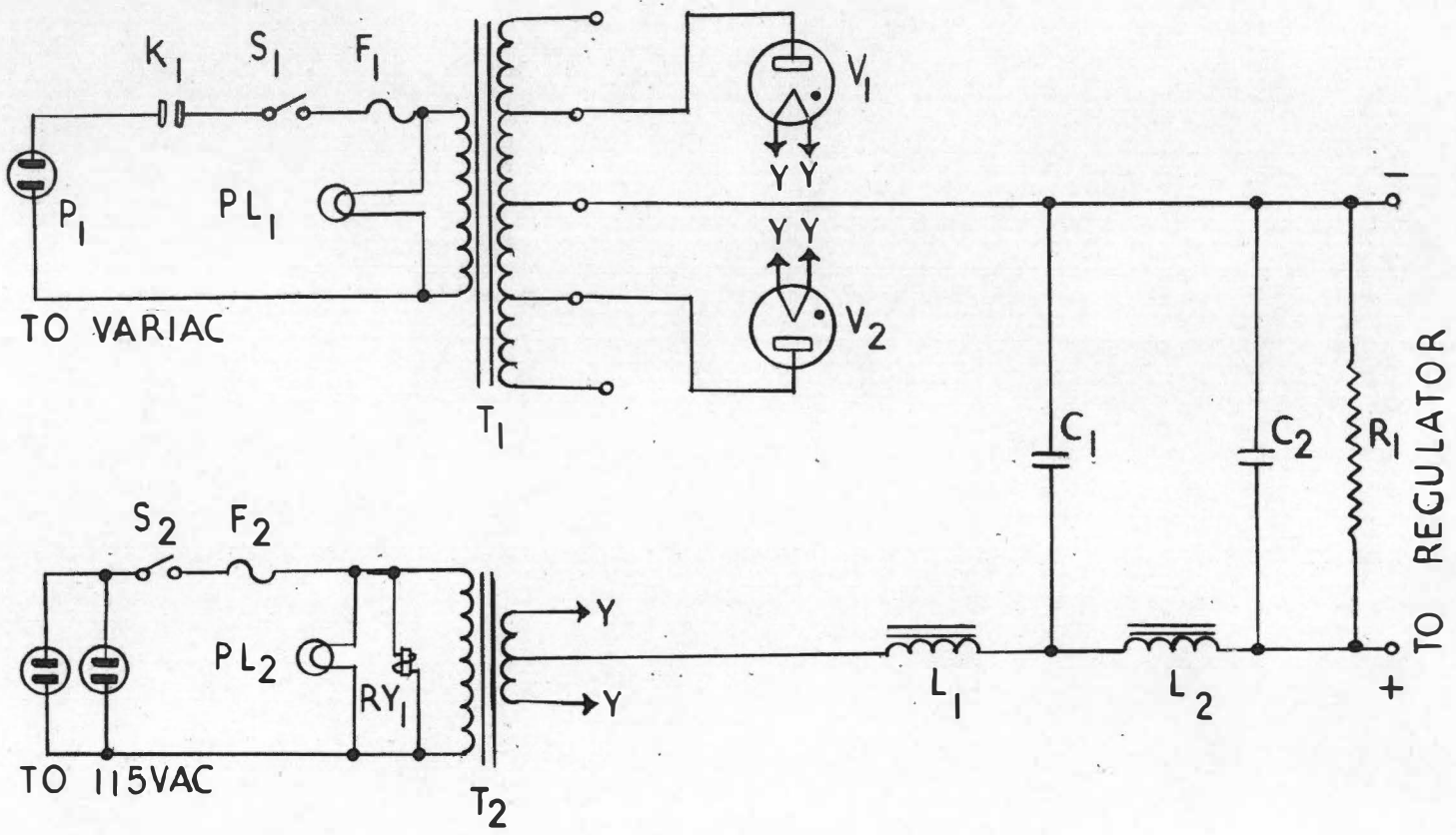

FIGURE 60

THE UNREGULATED SUPPLY OF THE KLYSTRON BEAM SUPPLY

TABLE IV

SPECIFICATIONS OF THE COMPONENTS OF THE UNREGULATED SUPPLY OF THE KLYSTRON BEAM POWER SUPPLY

Symbol	Component	Specifications
C_1, C_2	Filter capacitor	2 mfd, 3,000 wvdc, oil-filled, paper dielectric
F_1	Fuse	3AG 4 amp
F_2	Fuse	3AG 10 amp
K_1	Relay contacts on RY_1	Open when relay is not energized, 20 amp contact rating
L_1, L_2	Filter inductance	UTC CG 102, 12 h, 250 ma, 3,000 vdc insulation
P_1, P_2, P_3	Plug	115 vdc male recessed into chassis
PL_1, PL_2	Pilot lamp	115 v screw base
R_1	Resistor	100,000 ohm, 100 w
RY_1	Relay	Potter and Brumfield Type PR3AY
S_1, S_2	Toggle switch	SPST
T_1	Plate transformer	Secondary winding 3,000-2,500-0-2,00-3,000 vac
T_2	Filament transformer	UTC S-57, Secondary winding 2.5 v, C.T., 10 amp, 10,000 vdc insulation
V_1, V_2	Mercury vapor rectifier	Type 866A

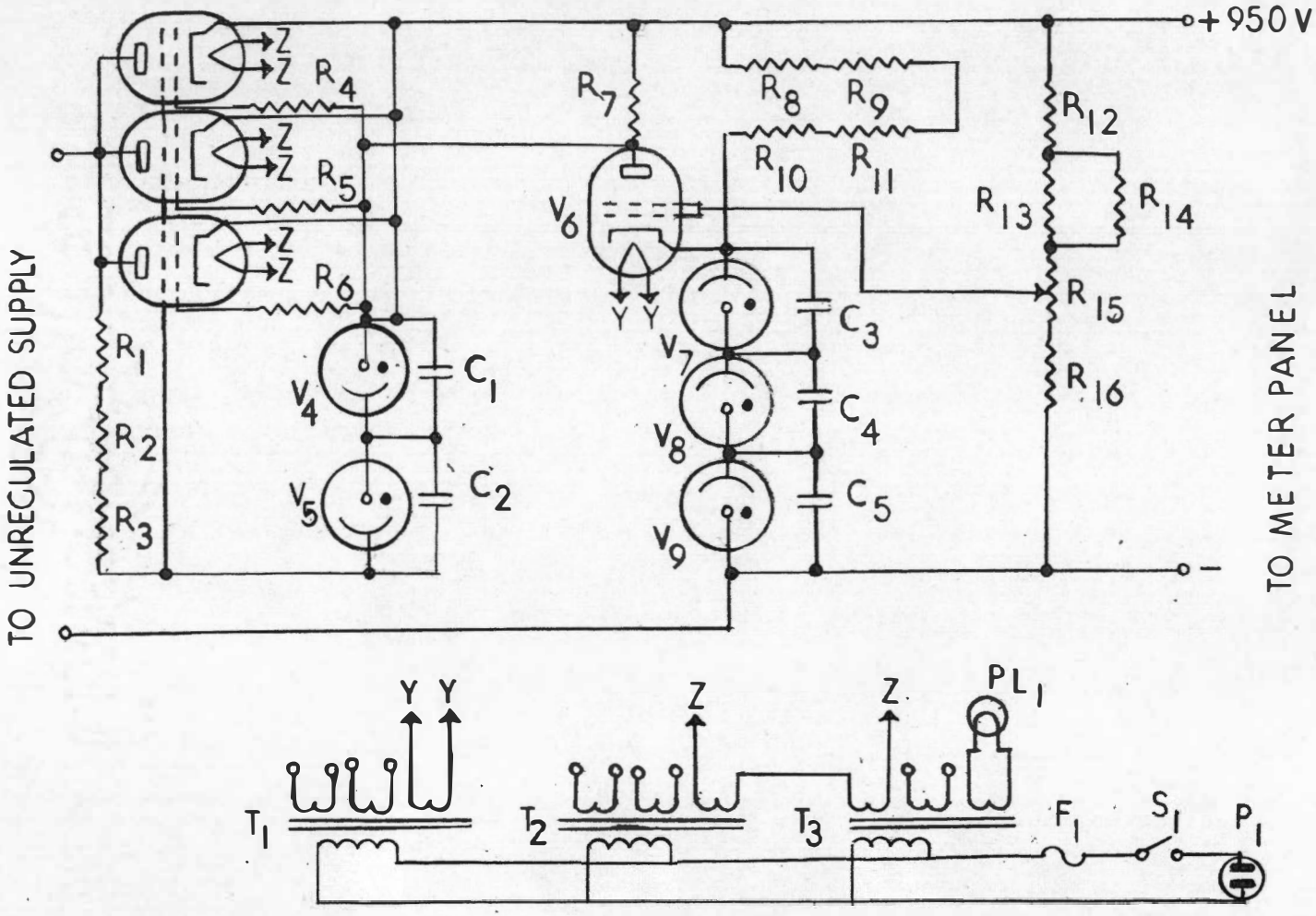

FIGURE 61

THE REGULATOR OF THE KLYSTRON BEAM SUPPLY

TABLE V

SPECIFICATIONS OF COMPONENTS OF REGULATOR FOR KLYSTRON BEAM POWER SUPPLY

Symbol	Component	Specifications
C_1, C_2	Capacitor	0.02 mfd, 600 wvdc, paper dielectric
C_3, C_4, C_5	Capacitor	0.05 mfd, 600 wvdc, paper dielectric
F_1	Fuse	3AG 3 amp
P_1	Plug	Standard 115 vac male
PL_1	Pilot lamp	6.3 v, 0.15 amp
R_1, R_2, R_3	Resistor	1,000 ohm, 10 w, wirewound
R_4, R_5, R_6	Resistor	100 ohm, 1 w, carbon
R_7	Resistor	100,000 ohm, 1 w, carbon
R_8, R_9, R_{10}, R_{11}	Resistor	15,000 ohm, 2 w carbon
R_{12}	Resistor	500,000 ohm, 2 w, carbon
R_{13}, R_{14}	Resistor	1 megohm, 1 w, carbon
R_{15}	Variable resistor	500,000 ohm, wirewound
R_{16}	Resistor	680,000 ohm, 2 w, carbon
S_1	Toggle Switch	SPST
T_1, T_2, T_3	Filament transformer	Secondary windings: (1) 6.3 v, 9.0 amp (2) 6.3 v, 0.6 amp (3) 6.3 v, 0.6 amp

TABLE V (continued)

Symbol	Component	Specifications
V_1, V_2, V_3	Vacuum tube	Type 1625
V_4	Voltage regulator tube	Type VR-105
V_5	Voltage regulator tube	Type VR-150
V_6	Vacuum tube	Type 807
V_7, V_8, V_9	Voltage regulator tube	Type VR-150

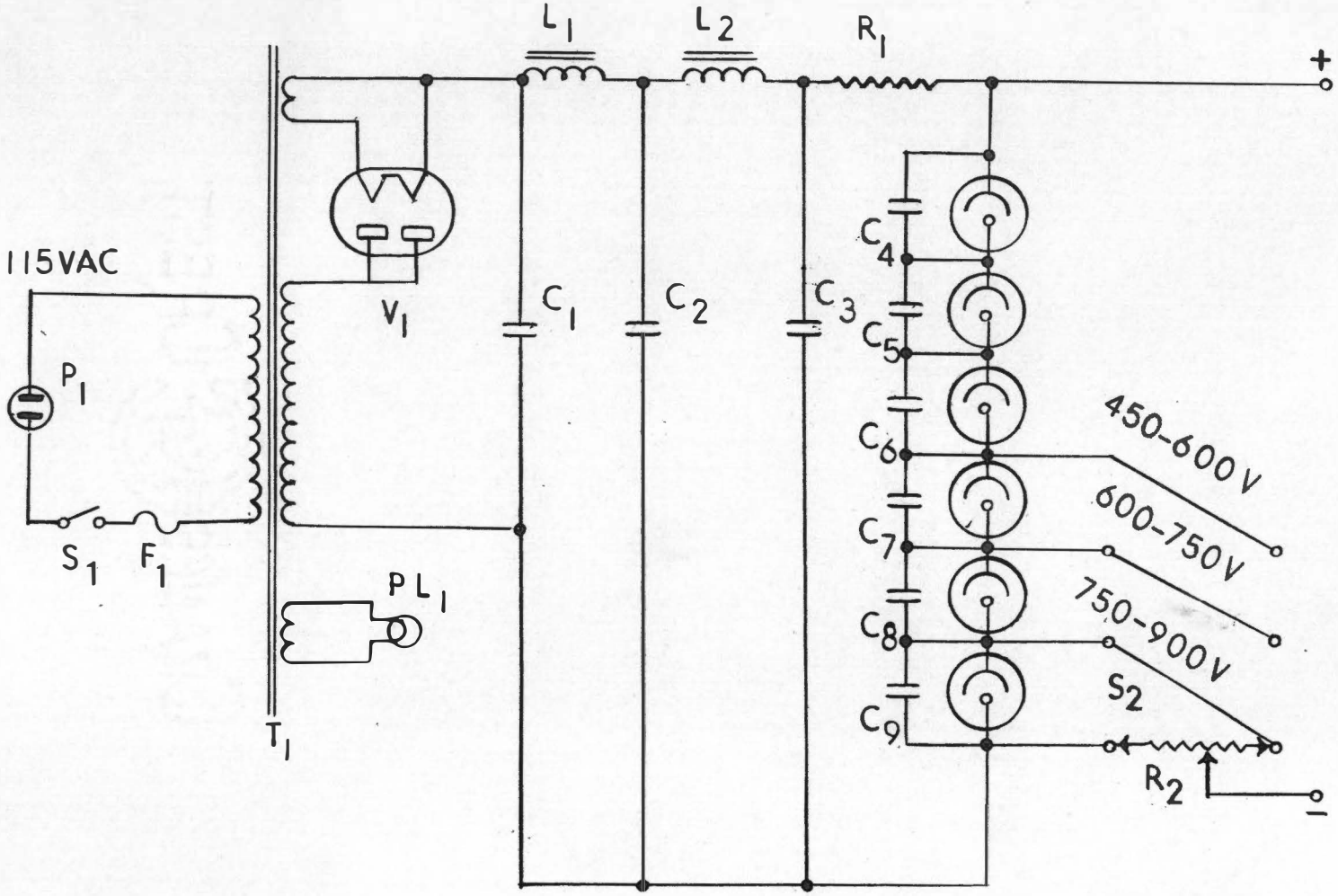

FIGURE 62

THE KLYSTRON REPELLER SUPPLY

TABLE VI

SPECIFICATIONS OF COMPONENTS OF
KLYSTRON REPELLER SUPPLY

Symbol	Component	Specifications
C_1	Filter capacitor	5 mfd, 2,000 wvdc, oil-filled paper dielectric
C_2	Filter capacitor	2 mfd, 2,000 wvdc, oil-filled paper dielectric
C_4, C_5, C_6, C_7, C_8, C_9	Capacitor	0.02 mfd, 600 wvdc, paper dielectric
F_1	Fuse	3AG 3 amp
L_1, L_2	Filter inductance	UTC HC 117
P_1	Plug	Standard 115 vac male
PL_1	Pilot lamp	6.3 v, 0.15 amp
R_1	Resistor	20,000 ohm, 20 w, wirewound
R_2	Potentiometer	Mallory E150 MP
S_1	Toggle switch	SPST
S_2	Rotary switch	Two pole, six position
T_1	Power transformer	Secondary windings: (1) 750 vac CT, 0.110 amp (2) 5 vac, 3.0 amp (3) 6.3 vac, 3.0 amp
V_1	Vacuum tube	Type 5R4GY
V_2, V_3, V_4, V_5, V_6, V_7	Voltage regulator tube	Type VR-150

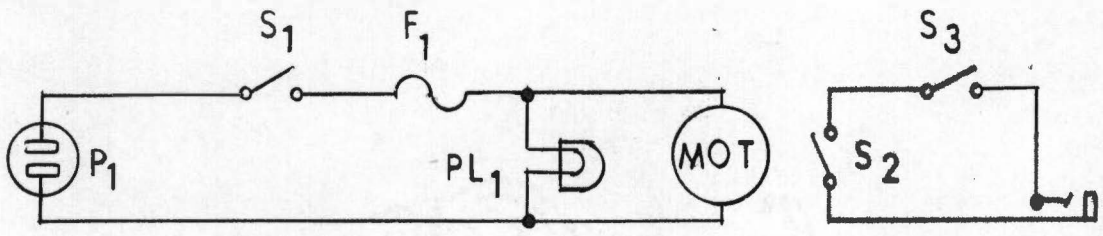

FIGURE 63

ELECTRICAL CIRCUIT OF THE TIMER

TABLE VII

SPECIFICATIONS OF THE TIMER COMPONENTS

Symbol	Component	Specifications
F_1	Fuse	3AG 1/2 amp
J_1	Microphone jack	Open circuit
MOT	Motor	110 vac, 1/3 RPH
P_1	Plug	110 vac
PL_1	Pilot lamp	110 v, screw base
S_1	Toggle switch	SPST
S_2	Microswitch	SPST
S_3	Toggle switch	SPST

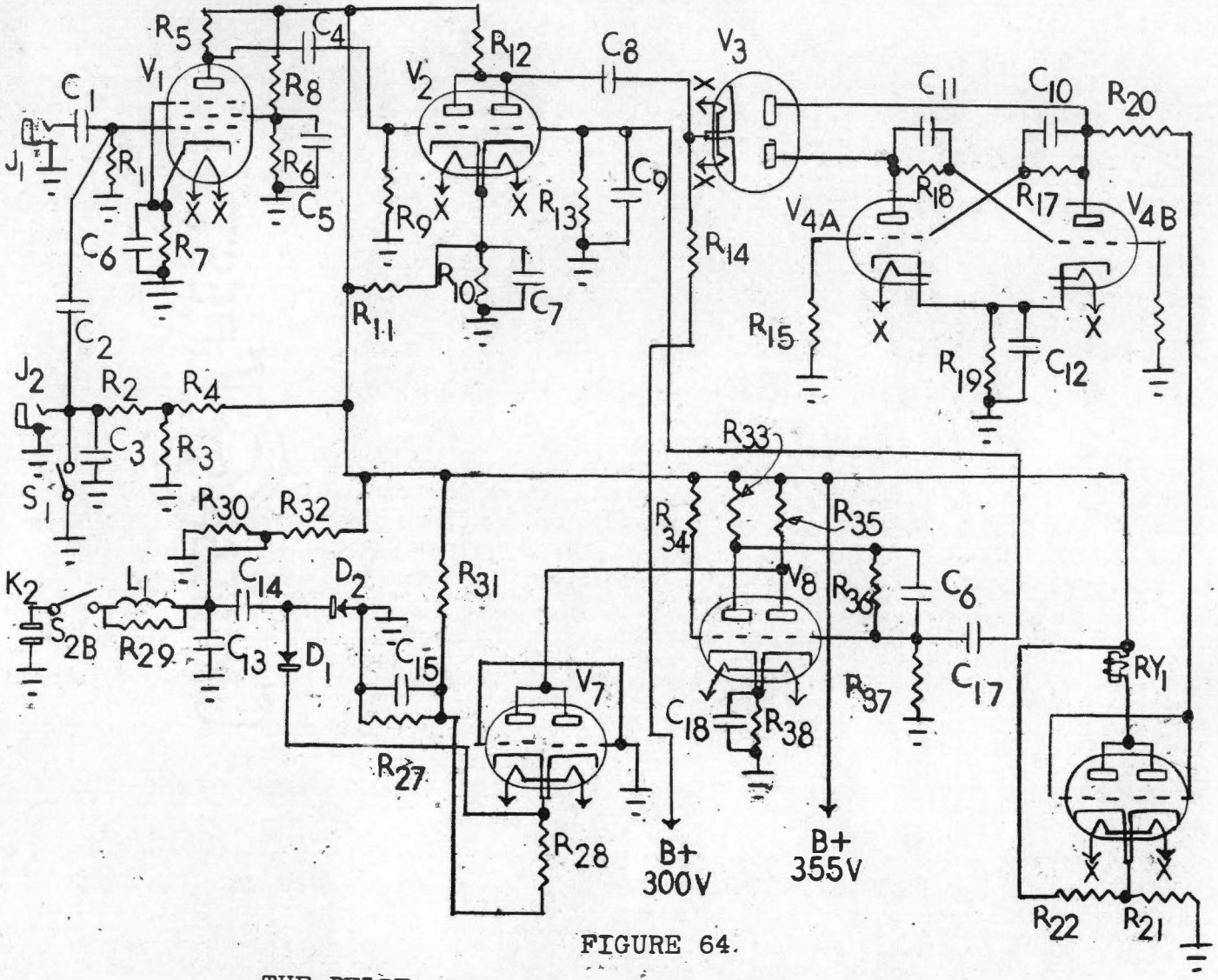

FIGURE 64.

THE PULSE CIRCUITRY OF THE CAMERA POWER SUPPLY

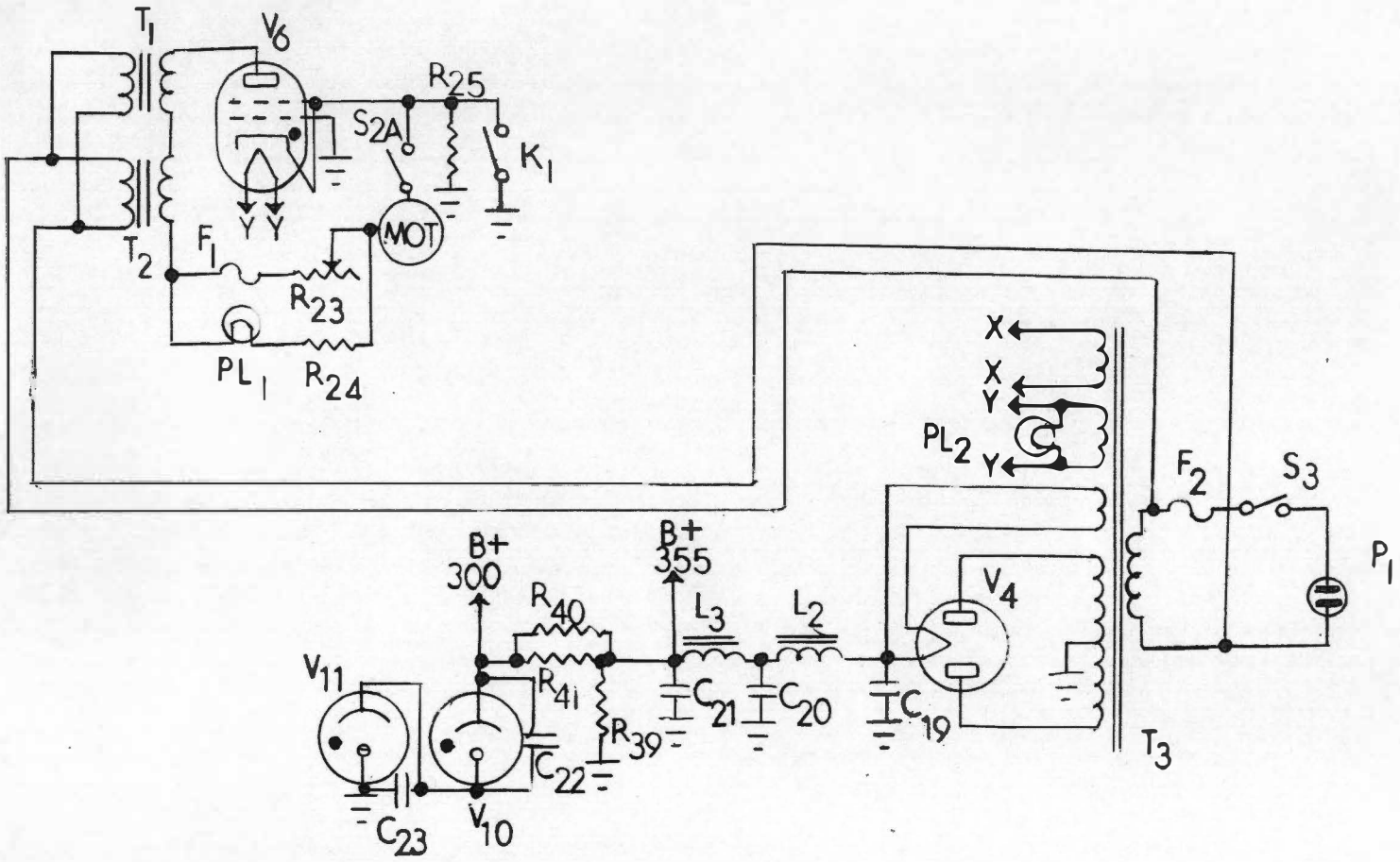

FIGURE 65

THE POWER SUPPLIES OF THE
CAMERA POWER SUPPLY

TABLE VIII

SPECIFICATIONS OF COMPONENTS OF CAMERA POWER SUPPLY

Symbol	Component	Specifications
C_1, C_2	Capacitor	0.00075 mfd, 400 wvdc, mica dielectric
C_3	Capacitor	0.1 mfd, 600 wvdc, paper dielectric
C_4	Capacitor	0.00007 mfd, 400 wvdc, mica dielectric
C_5	Capacitor	0.1 mfd, 600 wvdc, paper dielectric
C_6	Capacitor	0.03 mfd, 600 wvdc, paper dielectric
C_7	Capacitor	4.0 mfd, 250 wvdc, electrolytic
C_8	Capacitor	0.001 mfd, 1,000 wvdc, paper dielectric
C_9	Capacitor	0.000047 mfd, 400 wvdc, mica dielectric
C_{10}, C_{11}	Capacitor	0.00007 mfd, 400 wvdc, mica dielectric
C_{12}	Capacitor	0.01 mfd, 600 wvdc, paper dielectric
C_{13}	Capacitor	4.0 mfd, 250 wvdc, electrolytic
C_{14}	Capacitor	0.1 mfd, 600 wvdc, paper dielectric
C_{15}	Capacitor	30.0 mfd, 450 wvdc, electrolytic

TABLE VIII (continued)

Symbol	Component	Specifications
C_{16}	Capacitor	0.000039 mfd, 400 wvdc, mica dielectric
C_{17}	Capacitor	0.000047 mfd, 400 wvdc, mica dielectric
C_{18}	Capacitor	0.01 mfd, 400 wvdc, paper dielectric
C_{19}	Capacitor	30.0 mfd, 450 wvdc, electrolytic
C_{20}, C_{21}	Capacitor	8.0 mfd, 475 wvdc, electrolytic
C_{22}, C_{23}	Capacitor	0.01 mfd, 600 wvdc, paper dielectric
D_1, D_2	Rectifier	1N34 Germanium diode
F_1	Fuse	3AG 1½ amp
F_2	Fuse	3AG 3 amp
J_1, J_2	Microphone jack	Closed circuit used as open circuit
K_1	Relay contacts	Contacts on relay RY_1, normally open
K_2	Contacts	Custom made, placed on shaft of motor armature
L_1	Noise filter inductance	100 turns of #30 wire wound on resistor with resistance of 100 ohm
L_2, L_3	Filter choke	10 hy. 150 ma

TABLE VIII (continued)

Symbol	Component	Specifications
MOT	Motor	24 volt dc motor in gunsight camera
P_1	Connector	115 vac standard male plug
PL_1, PL_2	Pilot lamp	6.3 v, 0.15 amp
R_1	Resistor	3 megohm, 1 w, carbon
R_2	Resistor	10 megohm, 1 w, carbon
R_3	Resistor	330,000 ohm, 1 w, carbon
R_4	Resistor	100,000 ohm, 1 w, carbon
R_5	Resistor	180,000 ohm, 2 w, carbon
R_6	Resistor	68,000 ohm, 2 w, carbon
R_7	Resistor	1,800 ohm, 1 w, carbon
R_8	Resistor	33,000 ohm, 2 w, carbon
R_9	Resistor	1 megohm, 1 w, carbon
R_{10}	Resistor	18,000 ohm, 2 w, carbon
R_{11}	Resistor	330,000 ohm, 2 w, carbon
R_{12}	Resistor	150,000 ohm, 2 w, carbon
R_{13}	Resistor	1 megohm, 1 w, carbon
R_{14}	Resistor	1 megohm, 1 w, carbon
R_{15}, R_{16}	Resistor	100,000 ohm, 1 w, carbon
R_{17}, R_{18}	Resistor	330,000 ohm, 1 w, carbon
R_{19}	Resistor	10,000 ohm, 2 w, carbon

TABLE VIII (continued)

Symbol	Component	Specifications
R_{20}	Resistor	10 megohm, 1 w, carbon
R_{21}	Resistor	7,500 ohm, 10 w, wirewound
R_{22}	Resistor	20,000 ohm, 5 w, wirewound
R_{23}	Potentiometer	20 ohm, General Radio Model 301
R_{24}	Resistor	56 ohm, 1 w, carbon
R_{25}	Resistor	15,000 ohm, 1 w, carbon
R_{26}	Resistor	330,000 ohm, 2 w, carbon
R_{27}	Resistor	15,000 ohm, 2 w, carbon
R_{28}	Resistor	1,000 ohm, 1 w, carbon
R_{29}	Resistor	10 megohm, 2 w, carbon
R_{30}	Resistor	56,000 ohm, 2 w, carbon
R_{31}	Resistor	50,000 ohm, 10 w, wirewound
R_{32}	Resistor	330,000 ohm, 1 w, carbon
R_{33}	Resistor	10,000 ohm, 2 w, carbon
R_{34}	Resistor	1 meg, 1 w, carbon
R_{35}	Resistor	10,000 ohm, 2 w, carbon
R_{36}	Resistor	220,000 ohm, 1 w, carbon
R_{37}	Resistor	180,000 ohm, 1 w, carbon
R_{38}	Resistor	10,000 ohm, 2 w, carbon
R_{39}	Resistor	10,000 ohm, 20 w, wirewound

TABLE VIII (continued)

Symbol	Component	Specifications
R_{40}, R_{41}	Resistor	5,000 ohm, 5 w, wirewound
RY_1	Relay	Claire relay, 10,000 ohm resistance
S_1	Momentary-contact switch	Push button type, one section of a switch with several sections
S_2	Toggle switch of which S_{2A} and S_{2B} are sections	DPST
S_3	Toggle switch	SPST
T_1	Transformer	
T_2	Transformer	
T_3	Power transformer with windings listed	p - Primary, 115 v, 1.05 amp, 60 cps W_1 - 750 vac center-tapped, 0.110 amp W_2 - 5 vac 3.0 amp W_3 - 6.3 vac 3.0 amp W_4 - 6.3 vac 0.7 amp
T_4	Filament transformer	6.3 vac 6.0 amp
V_1	Vacuum tube	Type 1852
V_2	Vacuum tube	Type 6SL7
V_3	Vacuum tube	Type 6H6
V_4	Vacuum tube	Type 6SN7
V_5	Vacuum tube	Type 6SL7

TABLE VIII (continued)

Symbol	Component	Specifications
V_6	Gas-filled Thyratron	Type 2050
V_7	Vacuum tube	Type 6SL7
V_8	Vacuum tube	Type 6SN7
V_9	Vacuum tube	Type 5R4GY
V_{10}, V_{11}	Gas-filled voltage regulator	Type VR-150

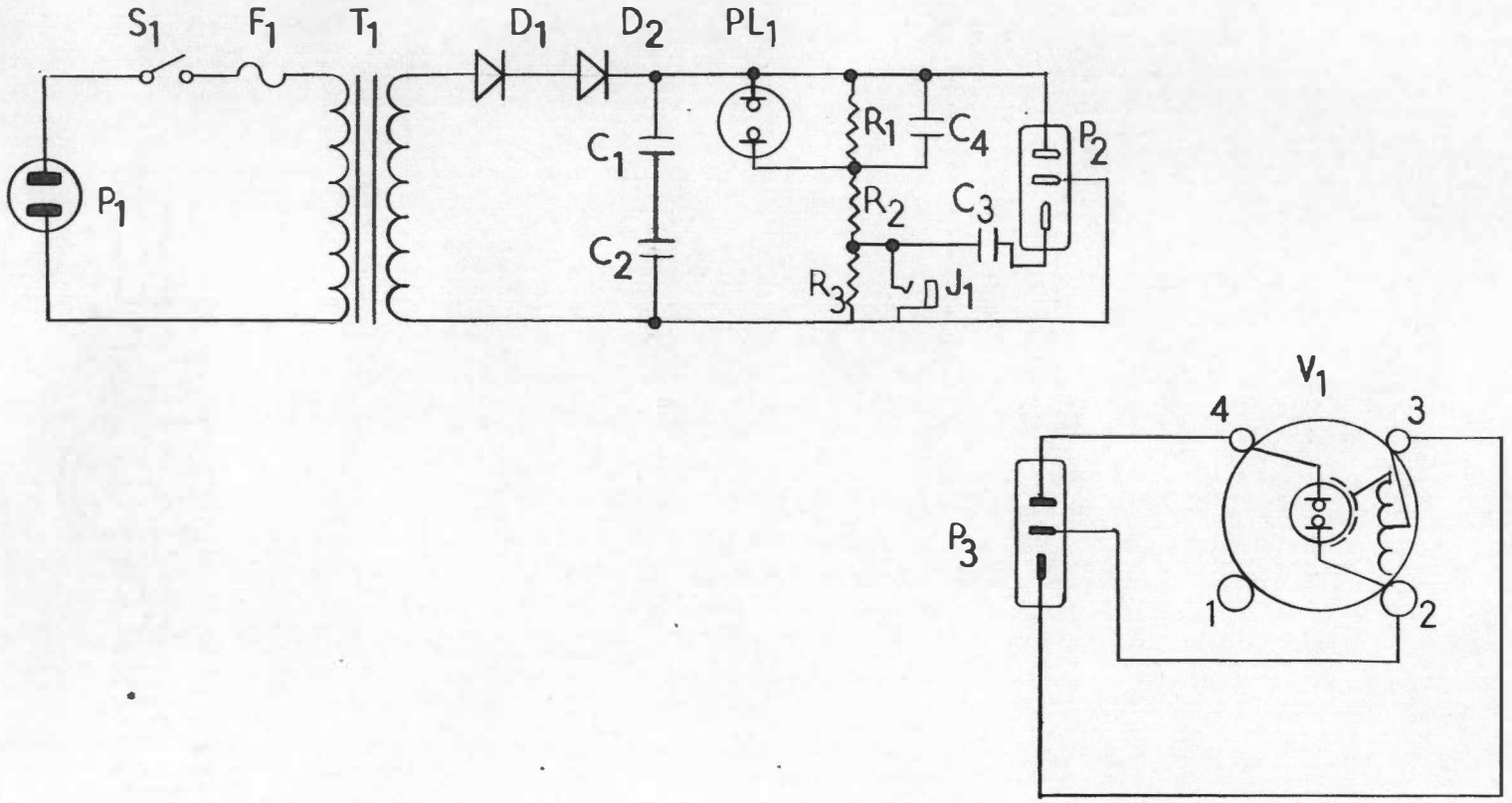

FIGURE 66

THE ELECTRONIC FLASH UNIT

TABLE IX

SPECIFICATIONS OF COMPONENTS OF THE ELECTRONIC FLASH UNIT

Symbol	Component	Specifications
C_1, C_2	Capacitor	Sprague Type FF-1 525 mfd, 450 wvdc, electrolytic
C_3	Capacitor	0.25 mfd, 600 wvdc, paper dielectric
C_4	Capacitor	0.05 mfd, 400 wvdc, paper dielectric
D_1, D_2	Rectifier	Radio Receptor Co., Inc. Type 16Y1, 20 ma, 260 vac, selenium
F_1	Fuse	3AG 2 amp
J_1	Phone Jack	Open-circuit
P_1	Plug	115 vac standard male
P_2	Connector	Jones type, 3 prong female
P_3	Connector	Jones type, 3 prong male
PL_1	Pilot lamp	Neon bulb type NE51
R_1	Resistor	2,200 ohm, 1 w, carbon
R_2, R_3	Resistor	3.3 megohm, 1 w, carbon
S_1	Toggle switch	SPST
T_1	Transformer	Stancor Model P-6425
V_1	Photoflash tube	Kemlite Laboratories Type DX with internal trigger coil